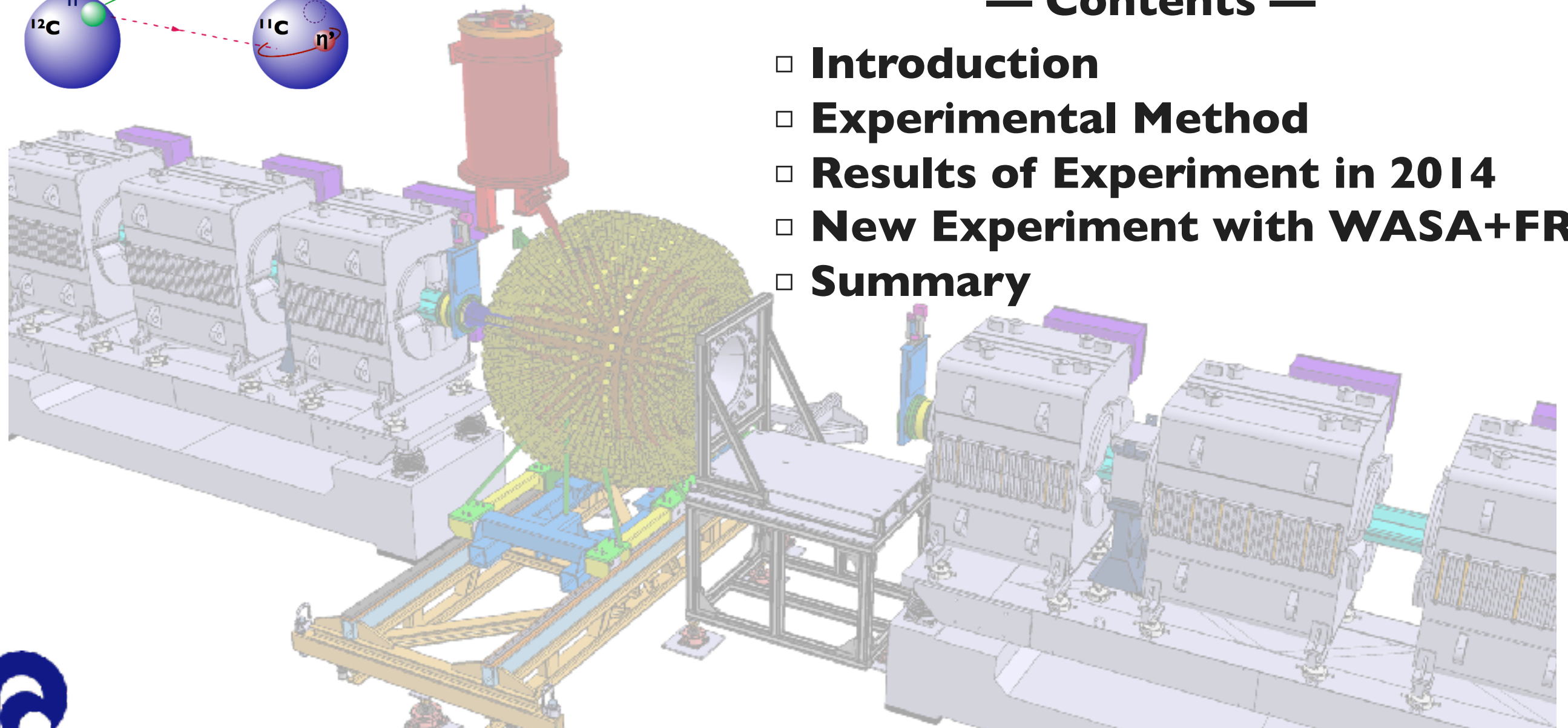
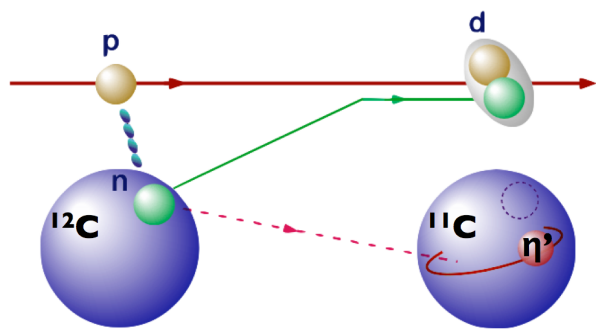


Search for η' -meson nucleus bound states at GSI/FAIR

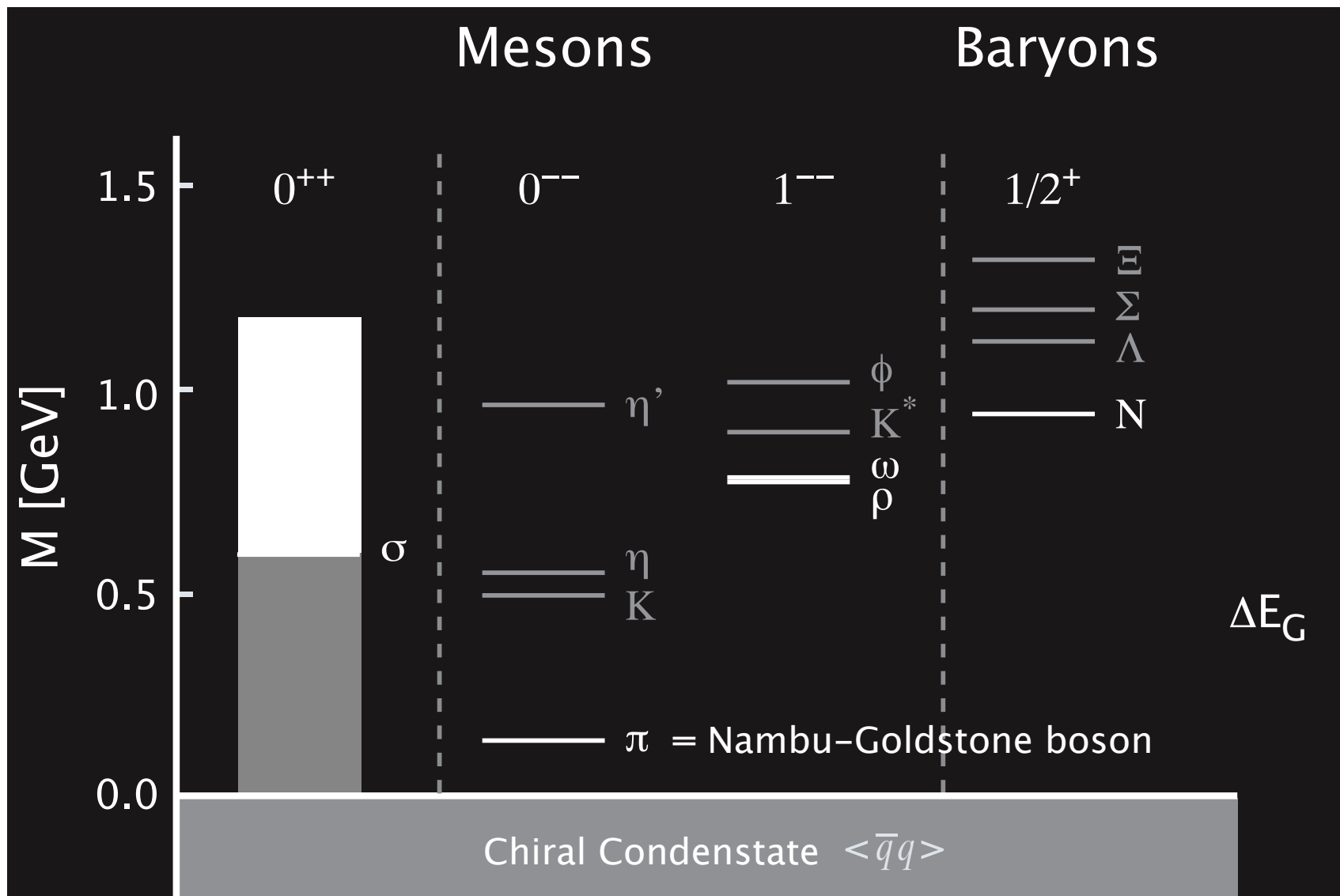
Yoshiaki Tanaka (RIKEN)

— Contents —

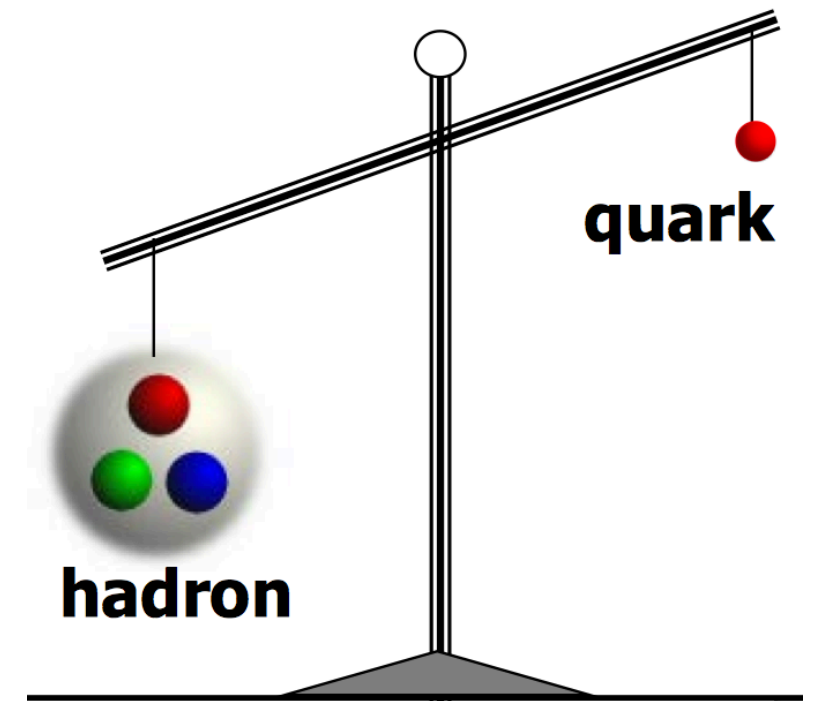
- Introduction
- Experimental Method
- Results of Experiment in 2014
- New Experiment with WASA+FRS
- Summary



Hadron mass



Hayano



$$m_q \simeq 3 \text{ MeV}$$

$$m_N \simeq 1000 \text{ MeV}$$

"Chiral" condensate

Nambu (1960)

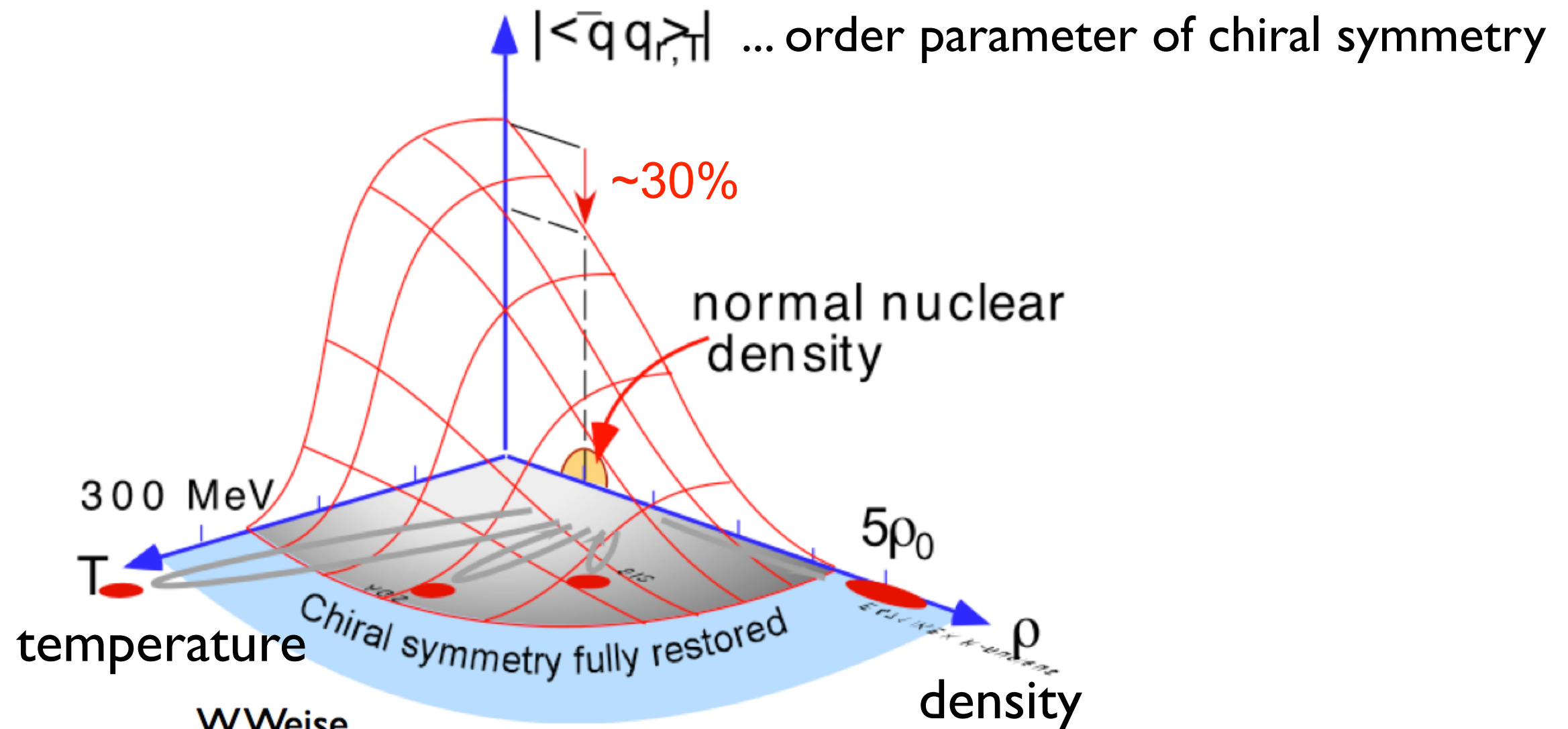
Hatsuda

QCD vacuum : spontaneous breaking of chiral symmetry

- Hadron masses are dynamically generated
- $\pi, K, \eta \sim$ Nambu-Goldstone boson

Restoration of chiral symmetry

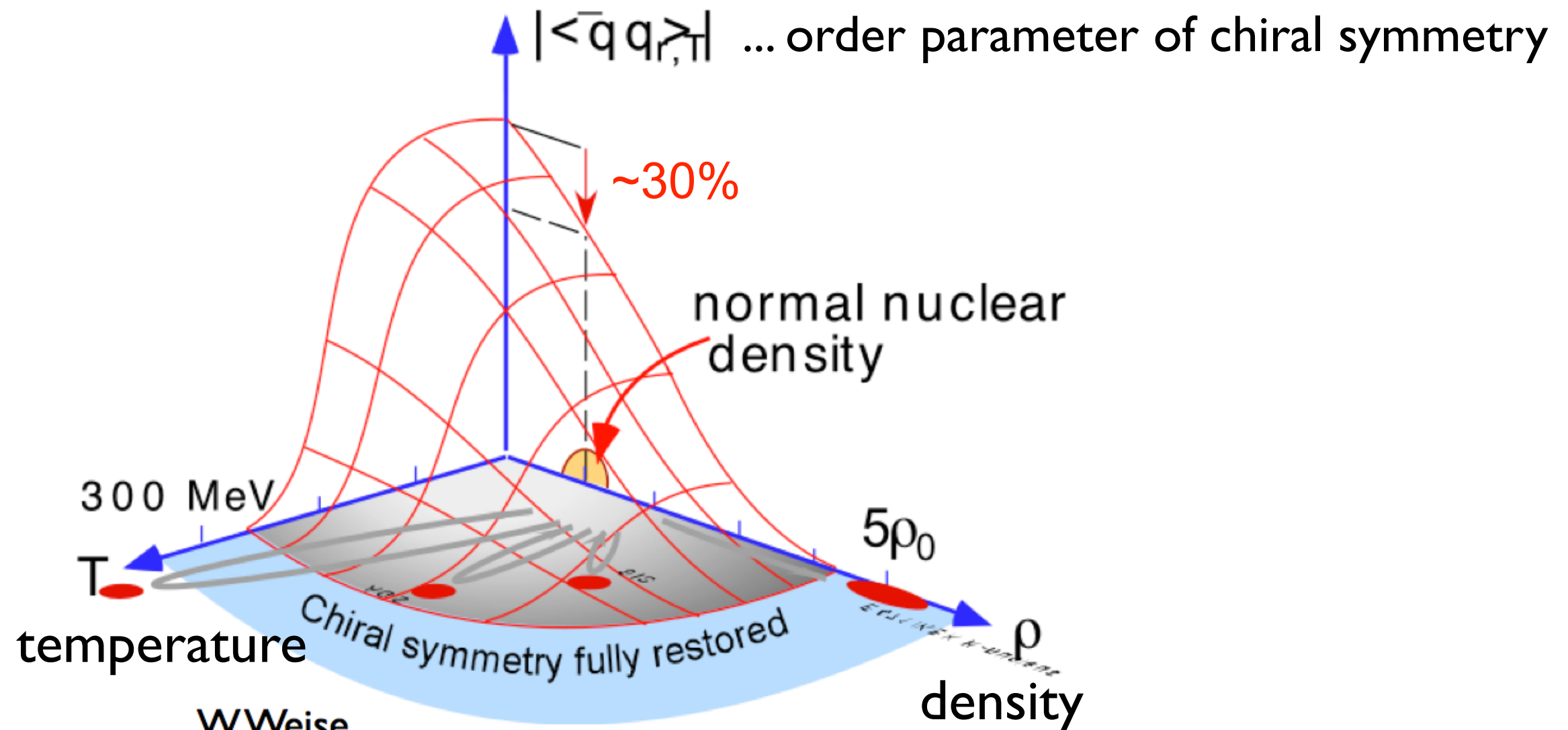
- Chiral symmetry could be partially restored in finite T and/or ρ



W.Weise,
NPA553(93)59.

Restoration of chiral symmetry

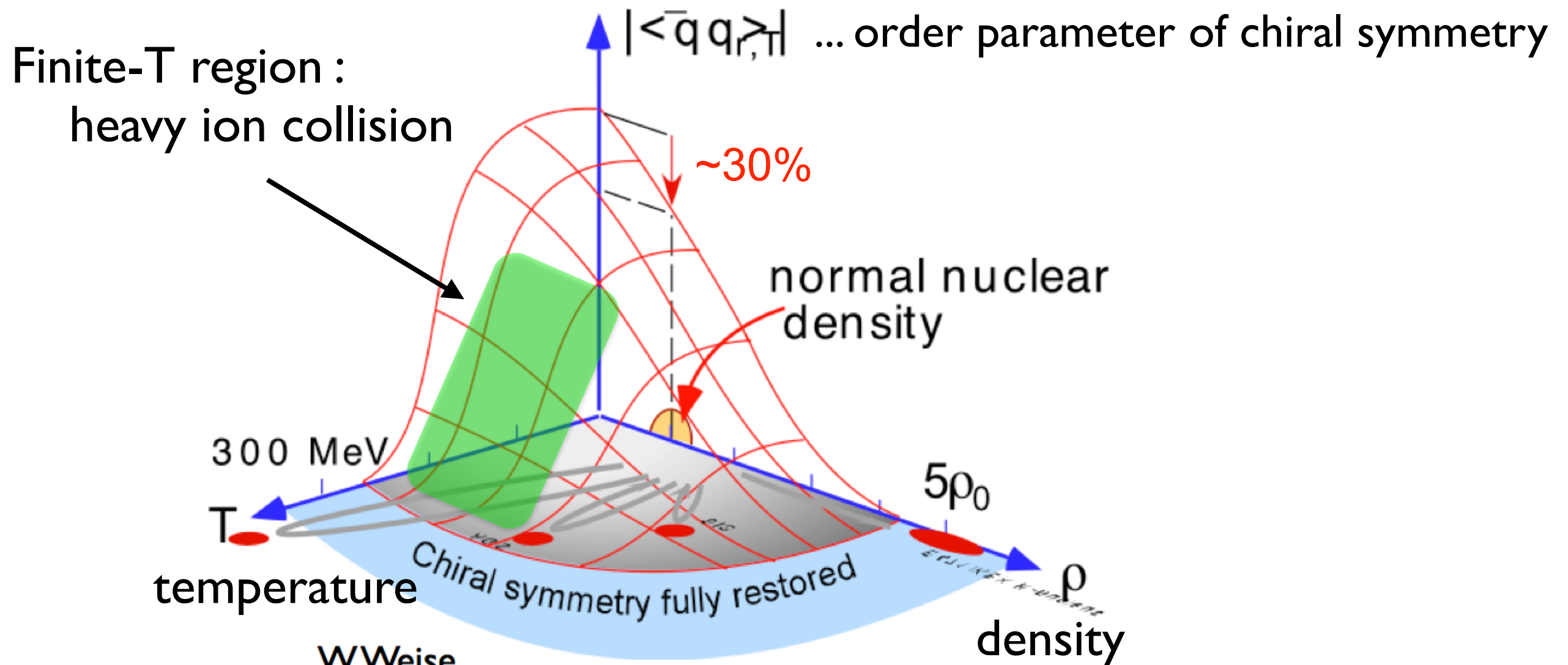
- Chiral symmetry could be partially restored in finite T and/or ρ
- Hadron properties (e.g., mass, width) under restoration of chiral symmetry



W.Weise,
NPA553(93)59.

Restoration of chiral symmetry

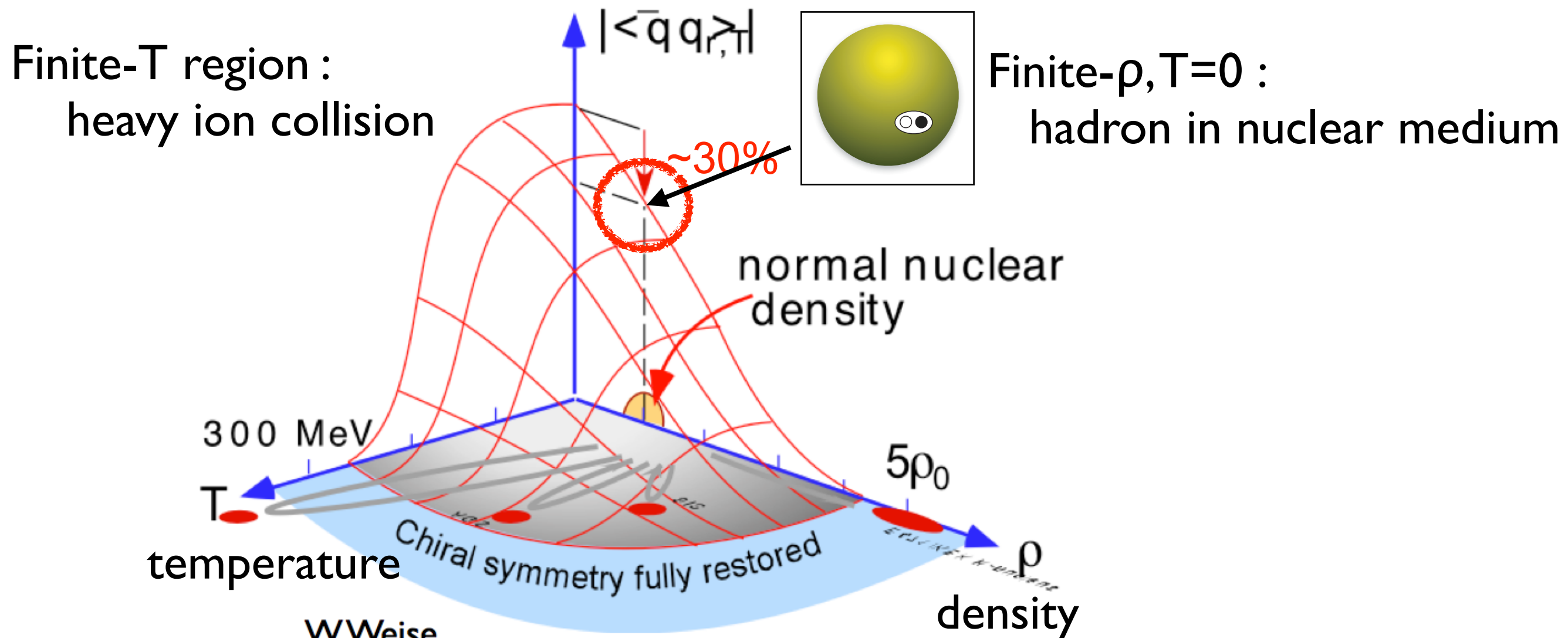
- Chiral symmetry could be partially restored in finite T and/or ρ
- Hadron properties (e.g., mass, width) under restoration of chiral symmetry



W.Weise,
NPA553(93)59.

Restoration of chiral symmetry

- Chiral symmetry could be partially restored in finite T and/or ρ
- Hadron properties (e.g., mass, width) under restoration of chiral symmetry

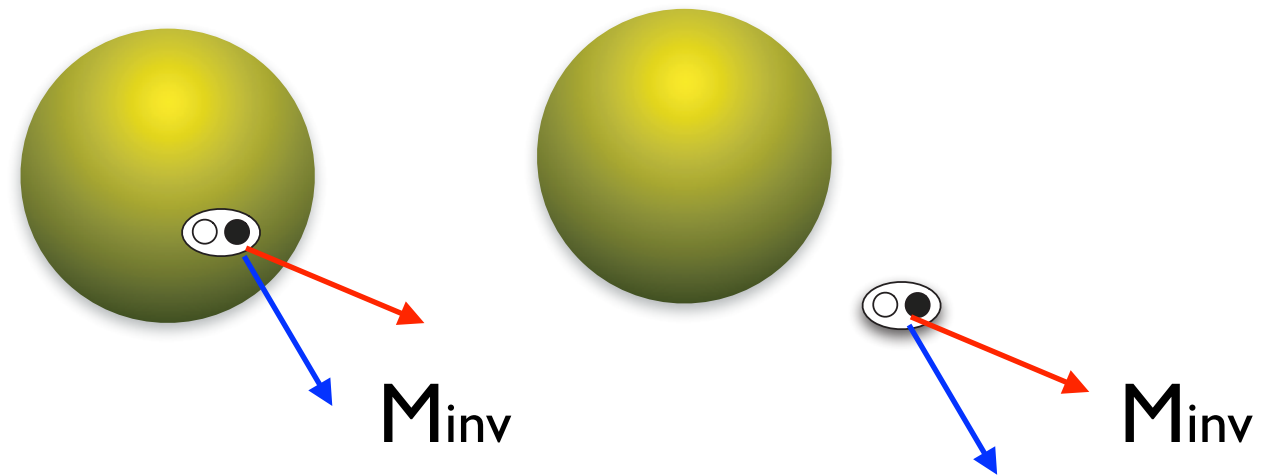


W.Weise,
NPA553(93)59.

Experimental approach

Invariant mass spectroscopy

- produce mesons in nucleus, some may decay in nucleus
- reconstruct invariant-mass from e^+e^- decay etc.



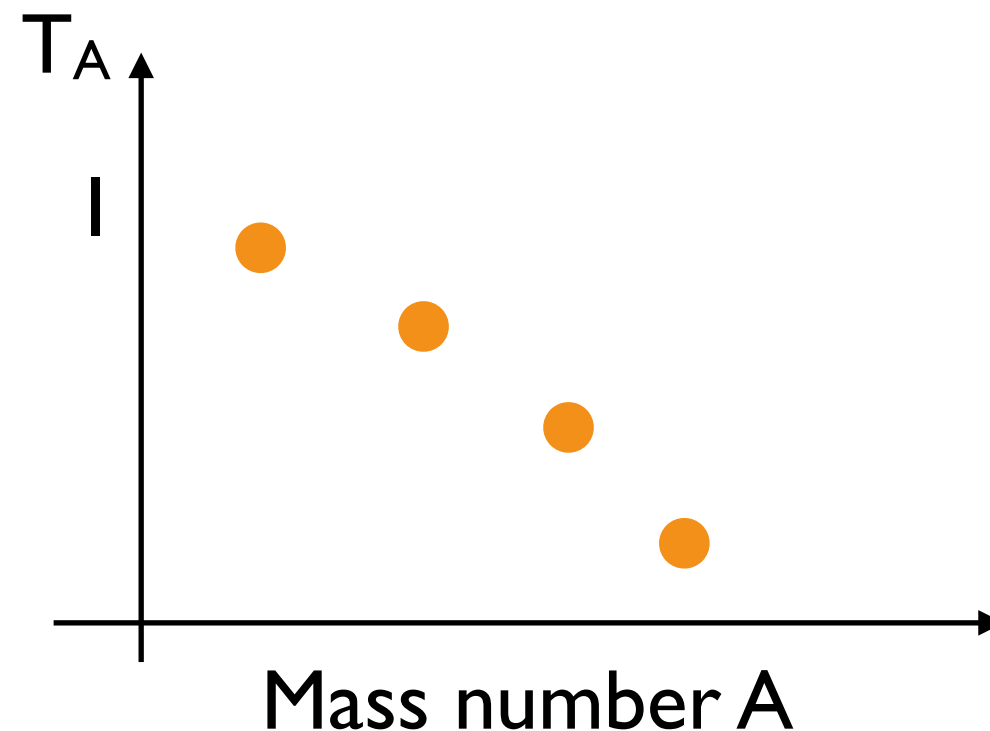
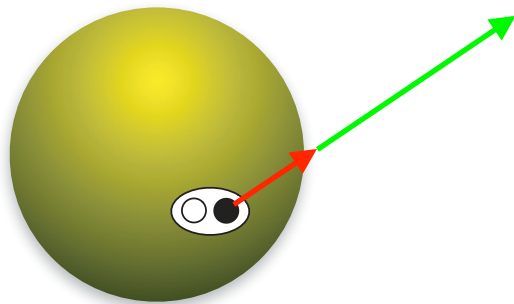
Experimental approach

Invariant mass spectroscopy

- produce mesons in nucleus, some may decay in nucleus
- reconstruct invariant-mass from e^+e^- decay etc.

Transparency ratio

- $T_A = \sigma(\gamma A \rightarrow XA') / A \times \sigma(\gamma N \rightarrow XN)$
- information on in-medium width



Experimental approach

Invariant mass spectroscopy

- produce mesons in nucleus, some may decay in nucleus
- reconstruct invariant-mass from e^+e^- decay etc.

Transparency ratio

- $T_A = \sigma(\gamma A \rightarrow XA') / A \times \sigma(\gamma N \rightarrow XN)$
- information on in-medium width

Excitation function, Momentum distribution

- enhancement in production cross section
- shift in momentum distribution of meson

Experimental approach

Invariant mass spectroscopy

- produce mesons in nucleus, some may decay in nucleus
- reconstruct invariant-mass from e^+e^- decay etc.

Transparency ratio

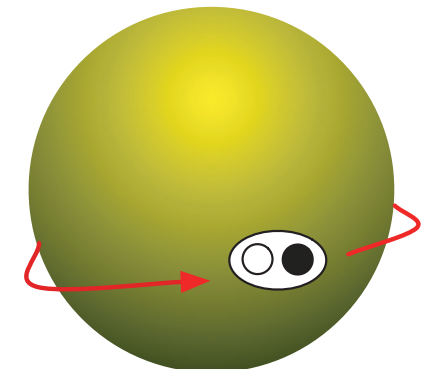
- $T_A = \sigma(\gamma A \rightarrow XA') / A \times \sigma(\gamma N \rightarrow XN)$
- information on in-medium width

Excitation function, Momentum distribution

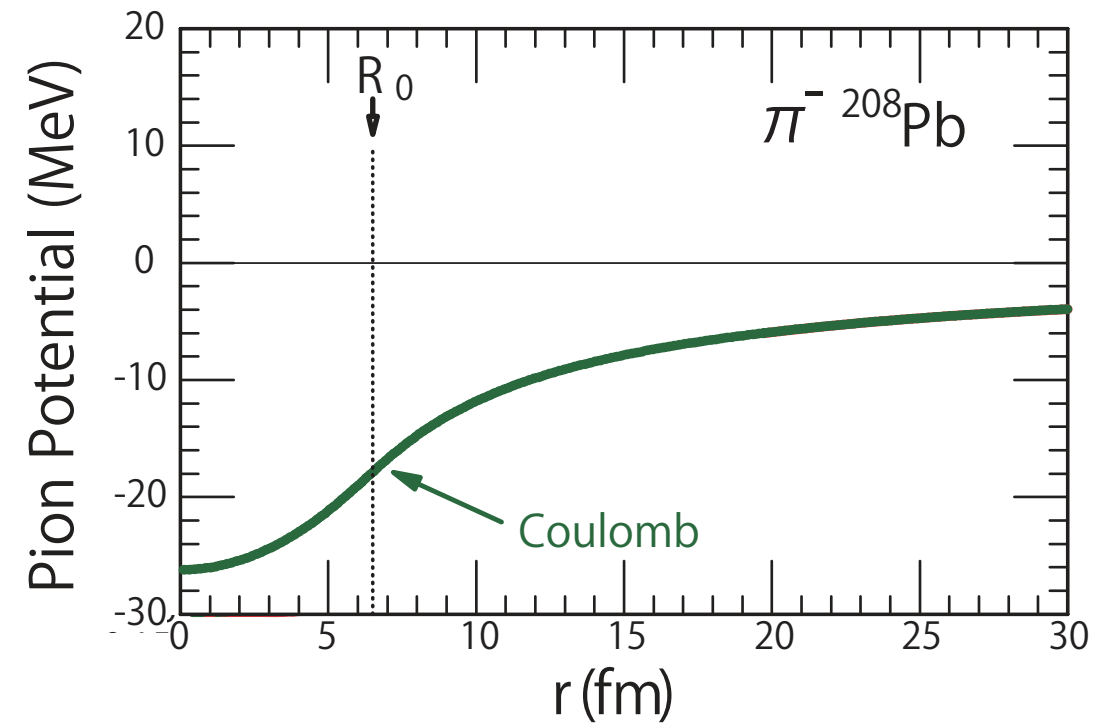
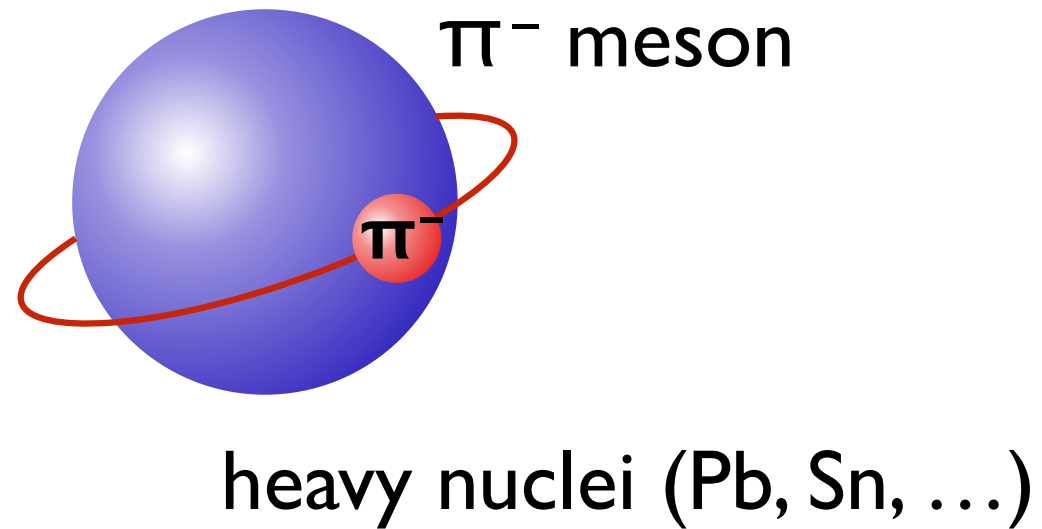
- enhancement in production cross section
- shift in momentum distribution of meson

Spectroscopy of bound states in nuclei

- well defined quantum states (nucleus x meson)
- overlap with nucleus \rightarrow probe for finite density

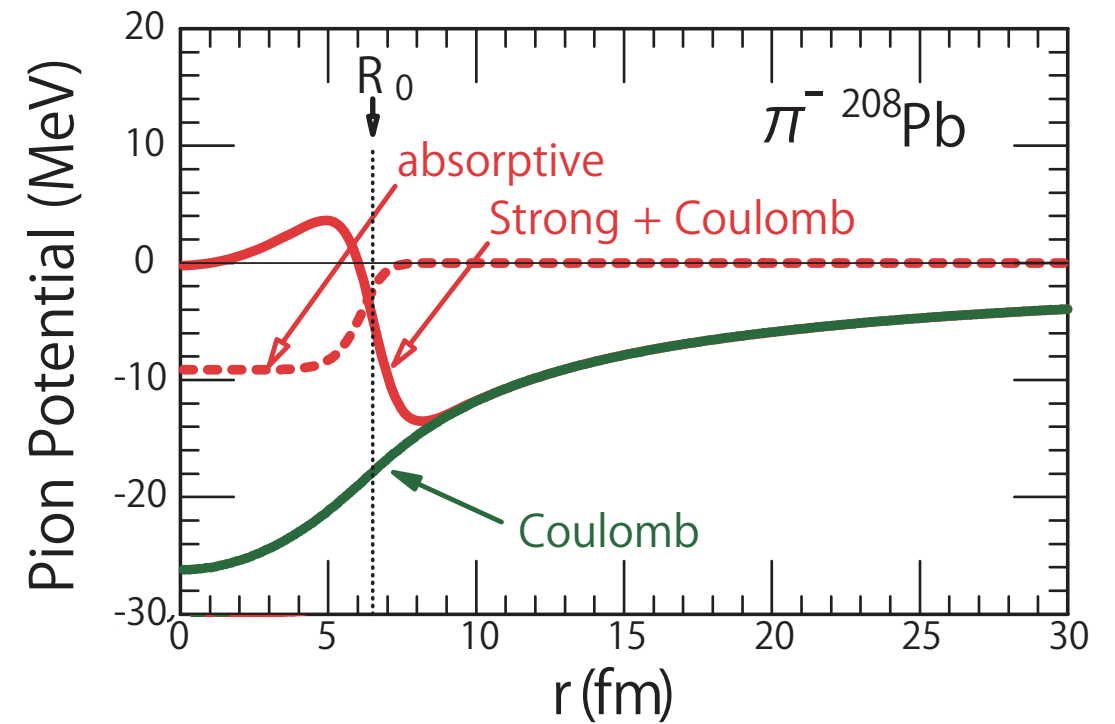
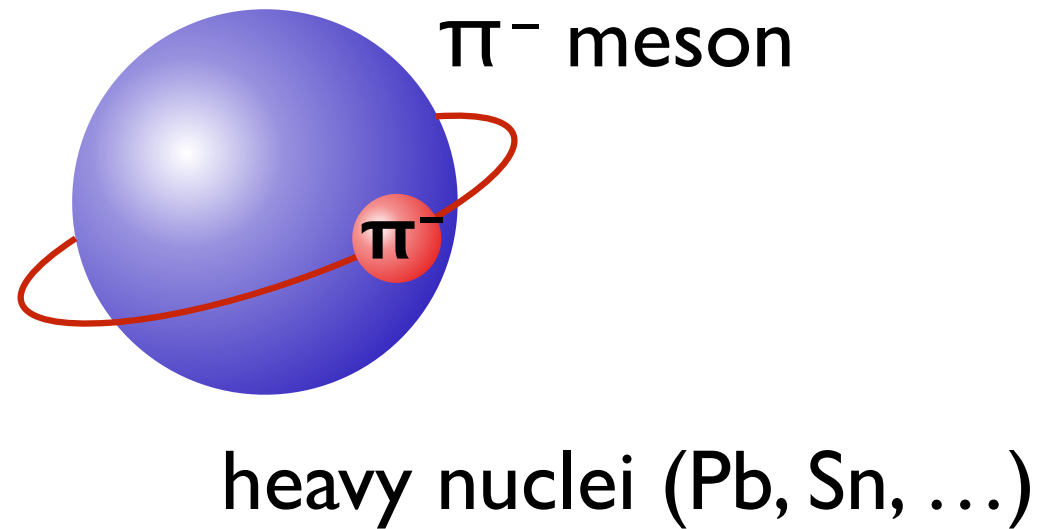


Deeply bound π^- states in nuclei



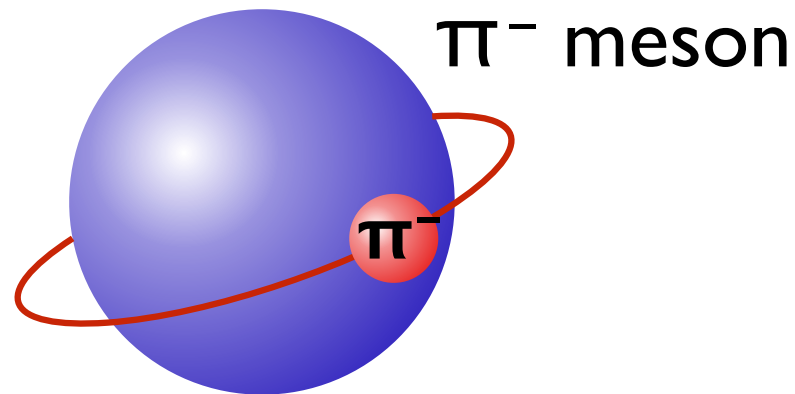
- Coulomb + strong interaction

Deeply bound π^- states in nuclei



- Coulomb + strong interaction

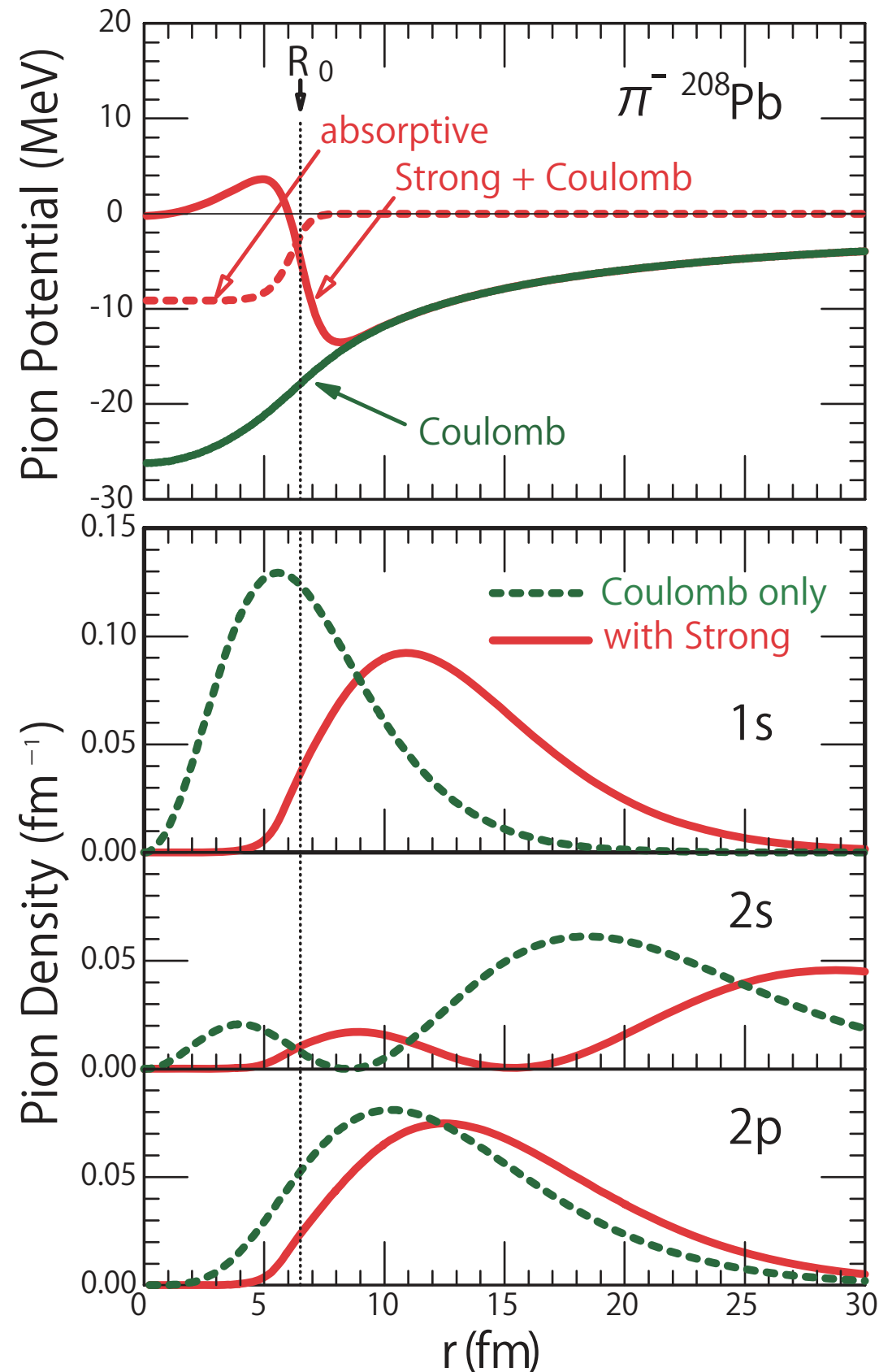
Deeply bound π^- states in nuclei



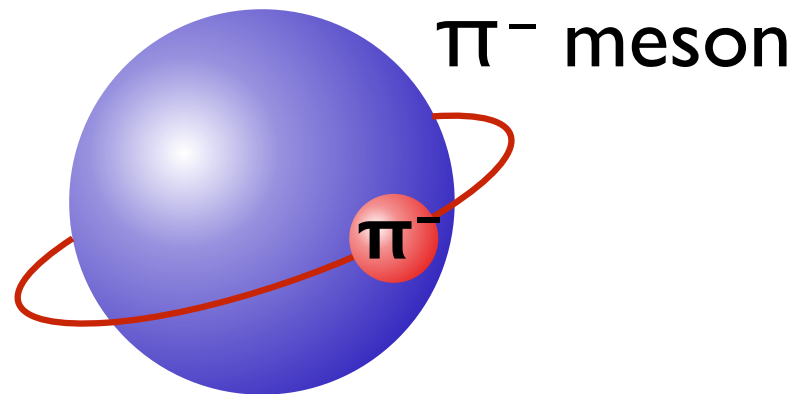
heavy nuclei (Pb, Sn, ...)

- Coulomb + strong interaction
- deeply bound states (1s, 2p, ...)
- near nuclear surface
- probe for finite density

H. Toki, T. Yamazaki, Phys. Lett. B (1988).
E. Friedman, G. Soff, J. Phys. G11, L37 (1985).



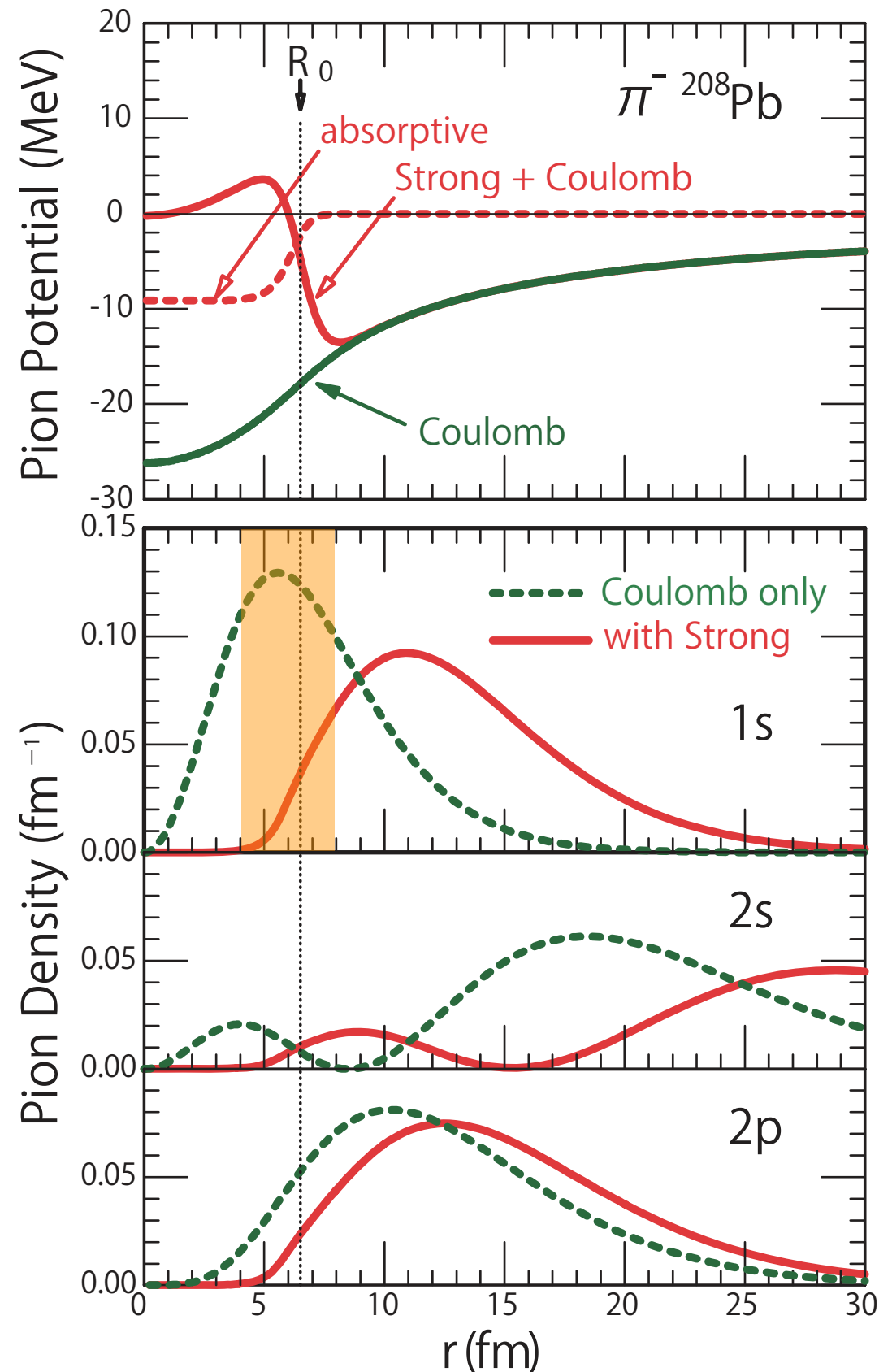
Deeply bound π^- states in nuclei



heavy nuclei (Pb, Sn, ...)

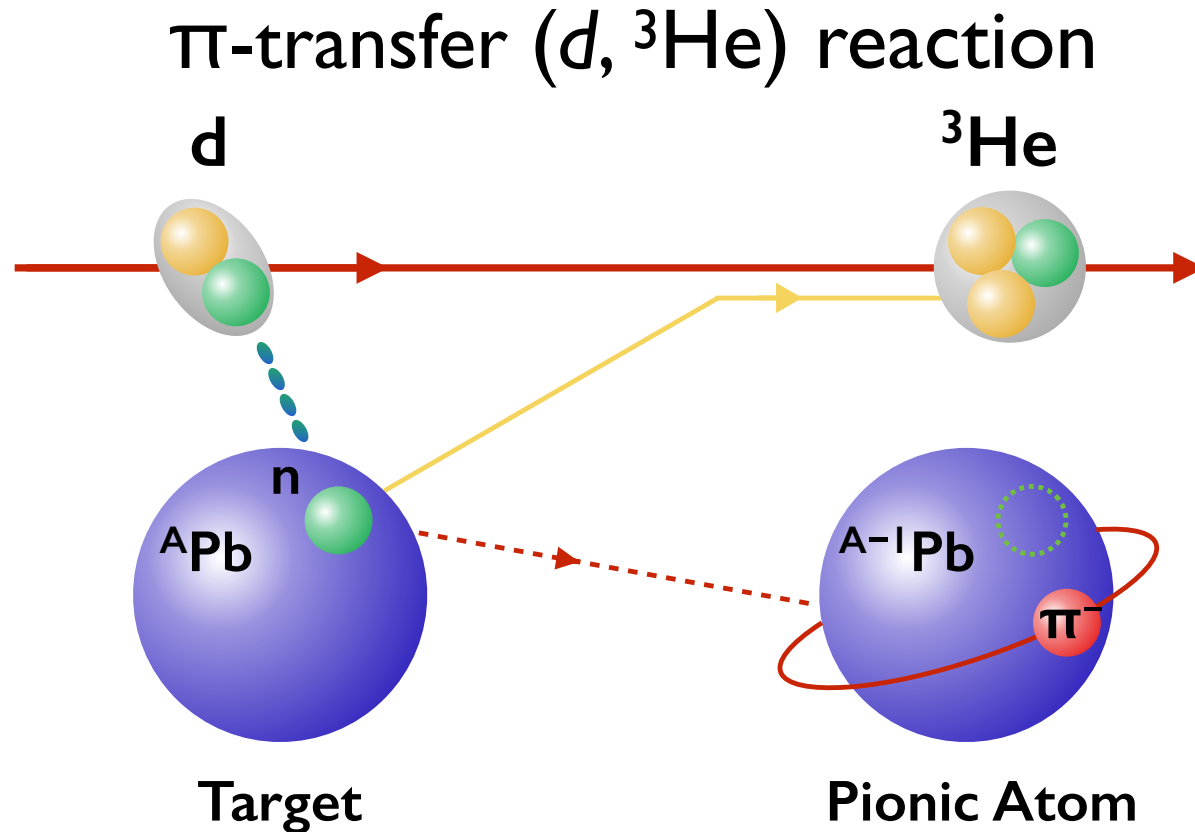
- Coulomb + strong interaction
- deeply bound states (1s, 2p, ...)
- near nuclear surface
- probe for finite density

H. Toki, T. Yamazaki, Phys. Lett. B (1988).
E. Friedman, G. Soff, J. Phys. G11, L37 (1985).

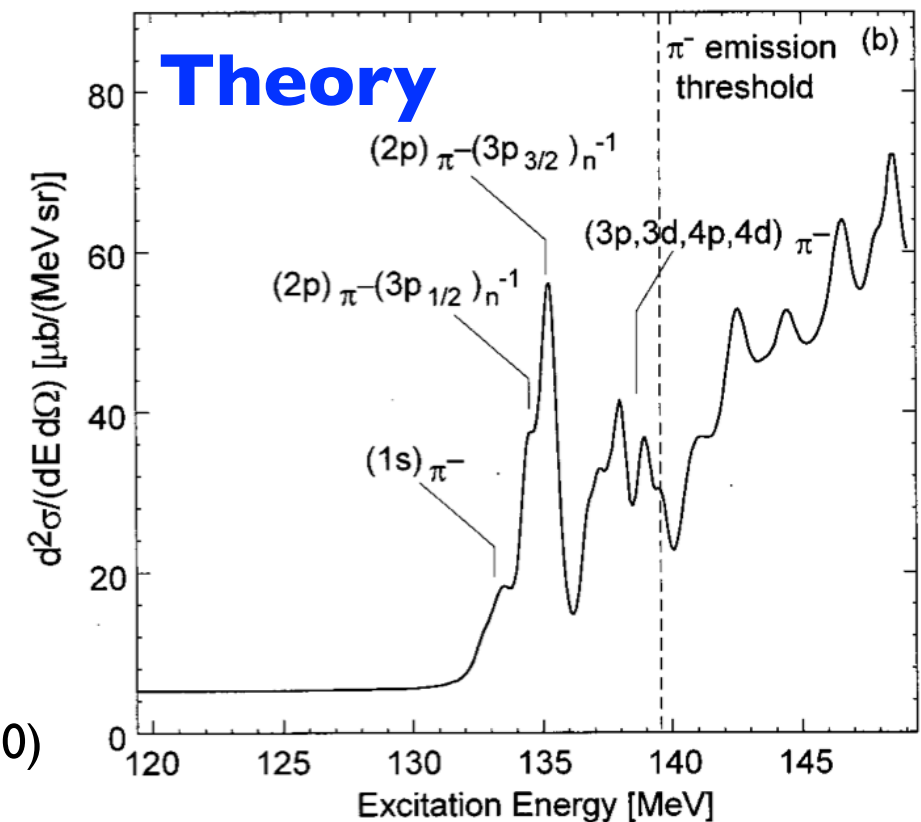
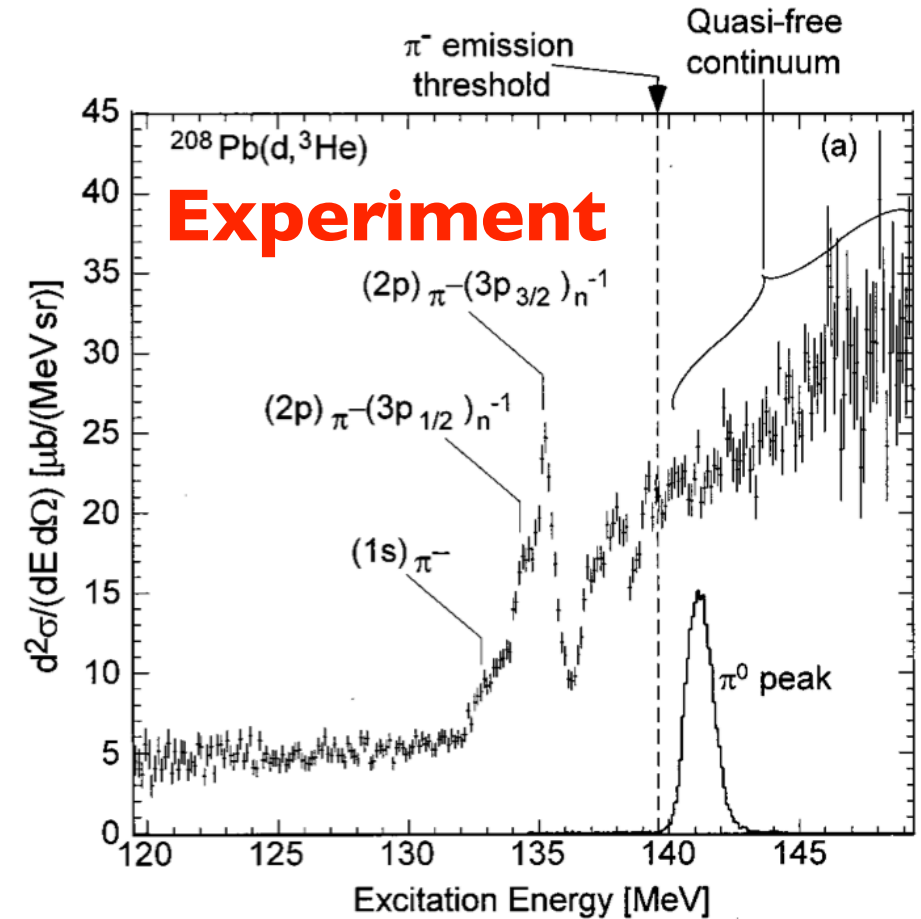


Deeply bound π^- states in nuclei

Discovery at FRS, GSI (1996)



- recoil-free kinematics to directly populate deeply-bound states
- [π bound states] \times [neutron hole states]



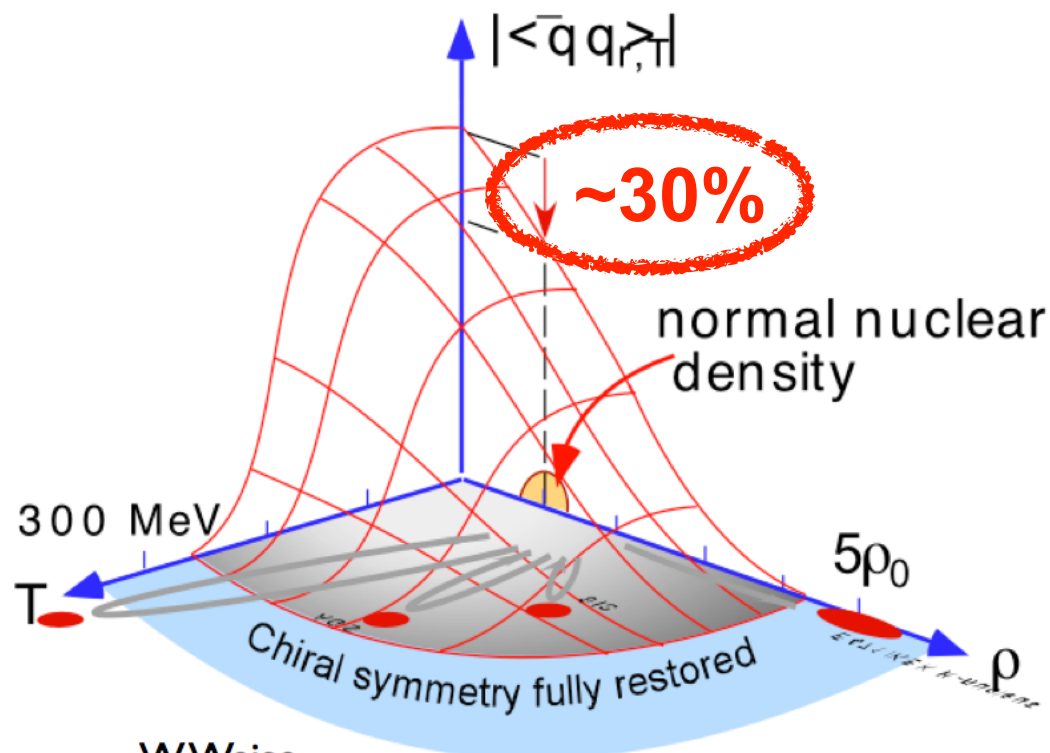
Deeply bound π^- states in nuclei

Pionic states in Sn isotopes

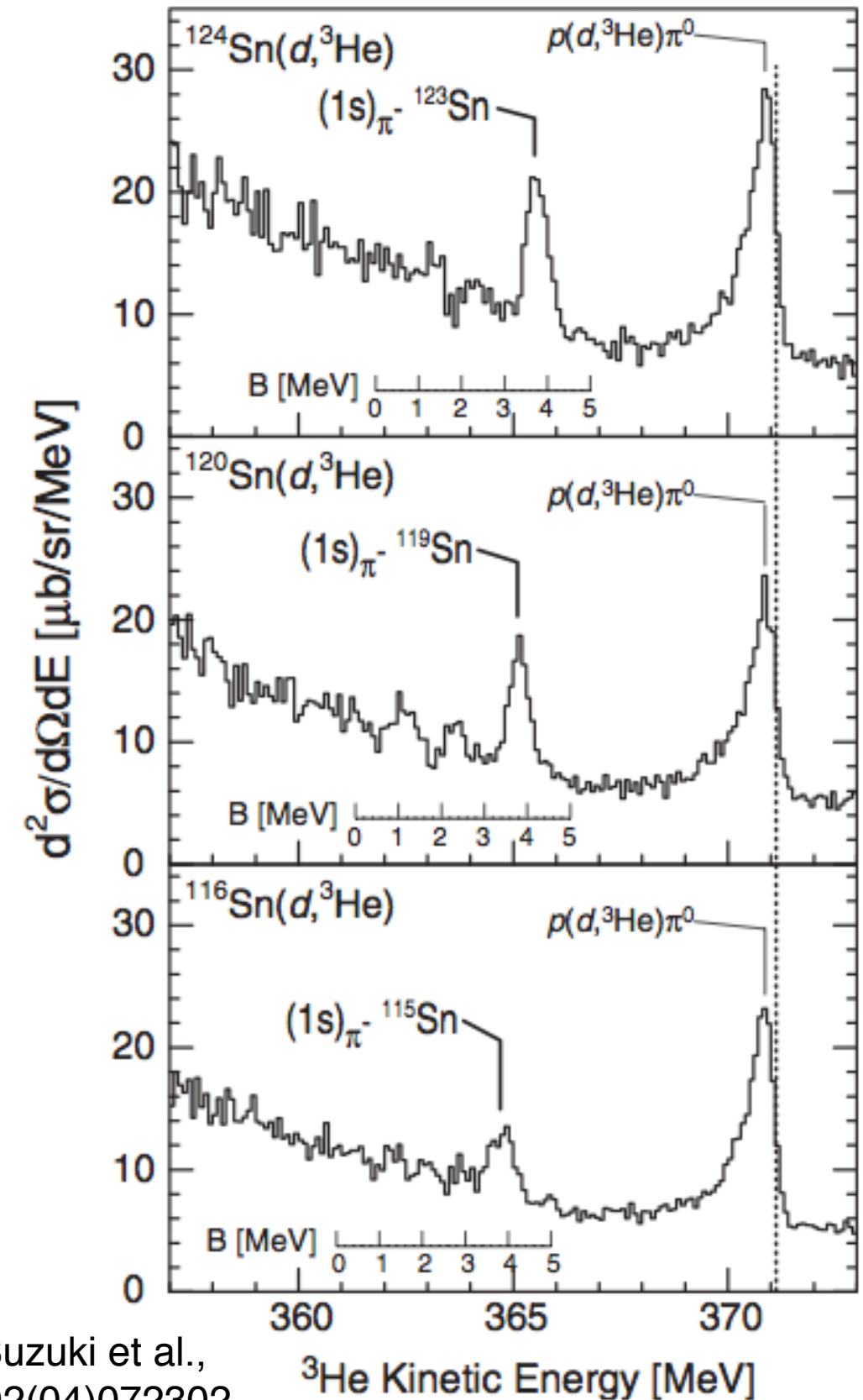
- Is states in $^{115}, ^{119}, ^{123}\text{Sn}$ observed
- in-medium s-wave isovector scattering amplitude

$$V_s(r) = -\frac{2\pi}{\mu} [\epsilon_1 \{b_0\rho(r) + b_1\delta\rho(r)\} + \epsilon_2 B_0\rho(r)^2]$$

- comparison with free b_I
 $\rightarrow \langle \bar{q}q \rangle_{\rho_0} / \langle \bar{q}q \rangle_0 \approx 0.67$



W.Weise,
NPA553(93)59.

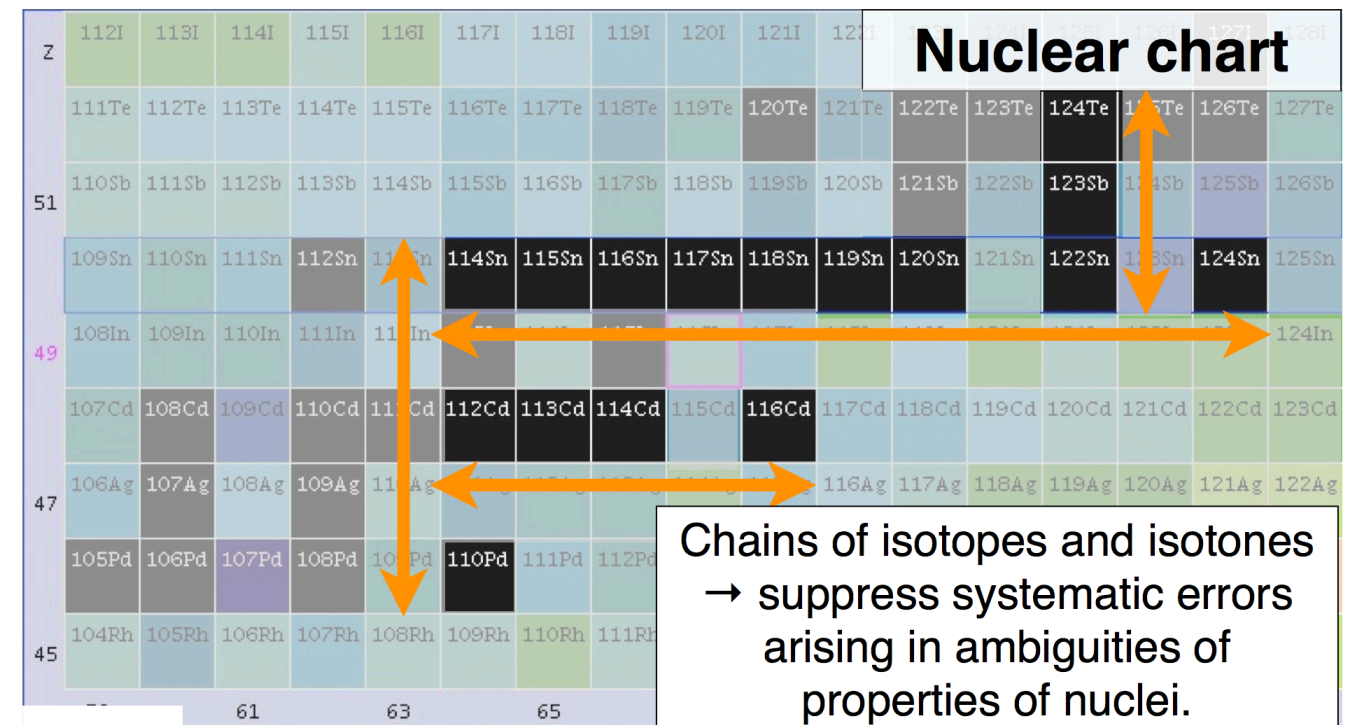
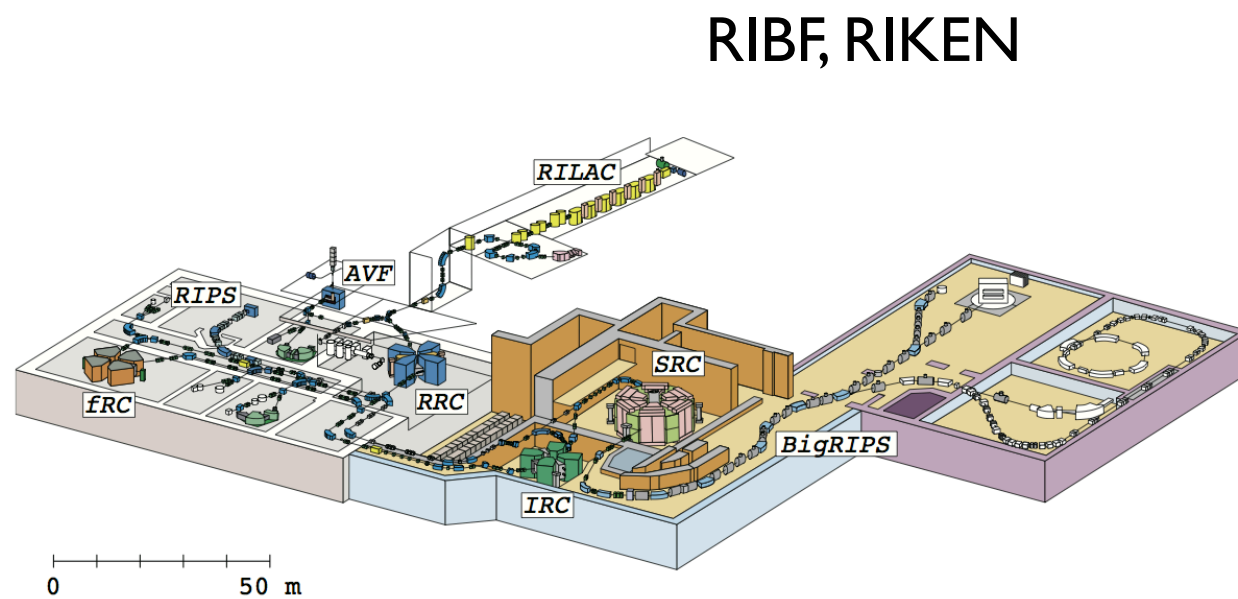


K. Suzuki et al.,
PRL92(04)072302

Deeply bound π^- states in nuclei

Pionic-atom factory experiments at RIKEN (2010–)

- intense d beam from SRC
 - + large-acceptance BigRIPS spectrometer
- systematic study in a wide region along Sn isotopes along Sn isotopes



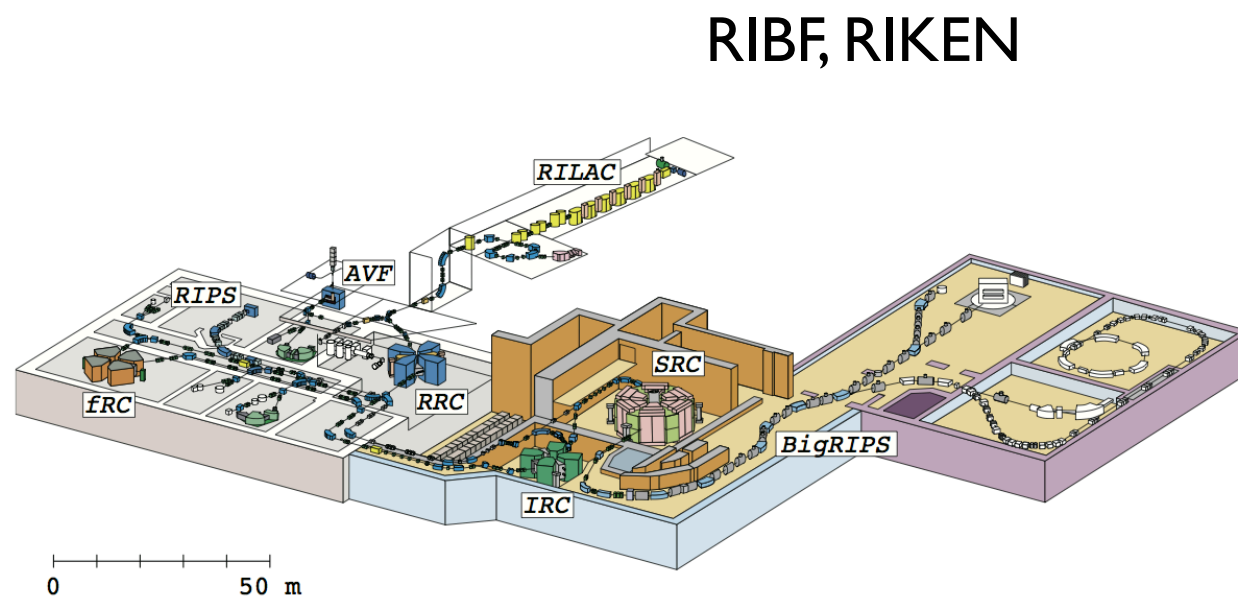
T. Nishi

NNDC, BNL

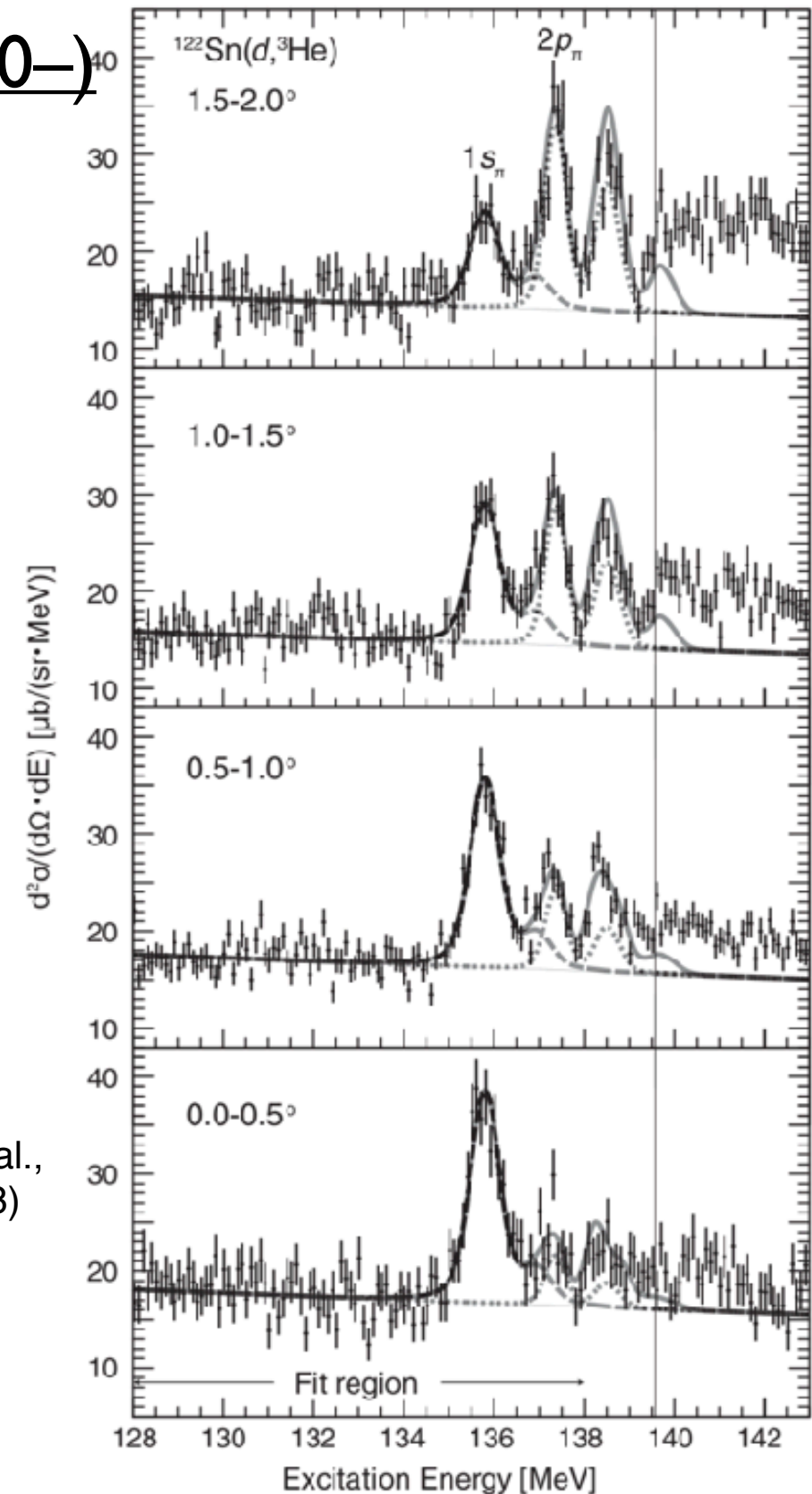
Deeply bound π^- states in nuclei

Pionic-atom factory experiments at RIKEN (2010–)

- intense d beam from SRC
 - + large-acceptance BigRIPS spectrometer
- systematic study in a wide region along Sn isotopes



T. Nishi, K. Itahashi et al.,
PRL120, 152505 (2018)



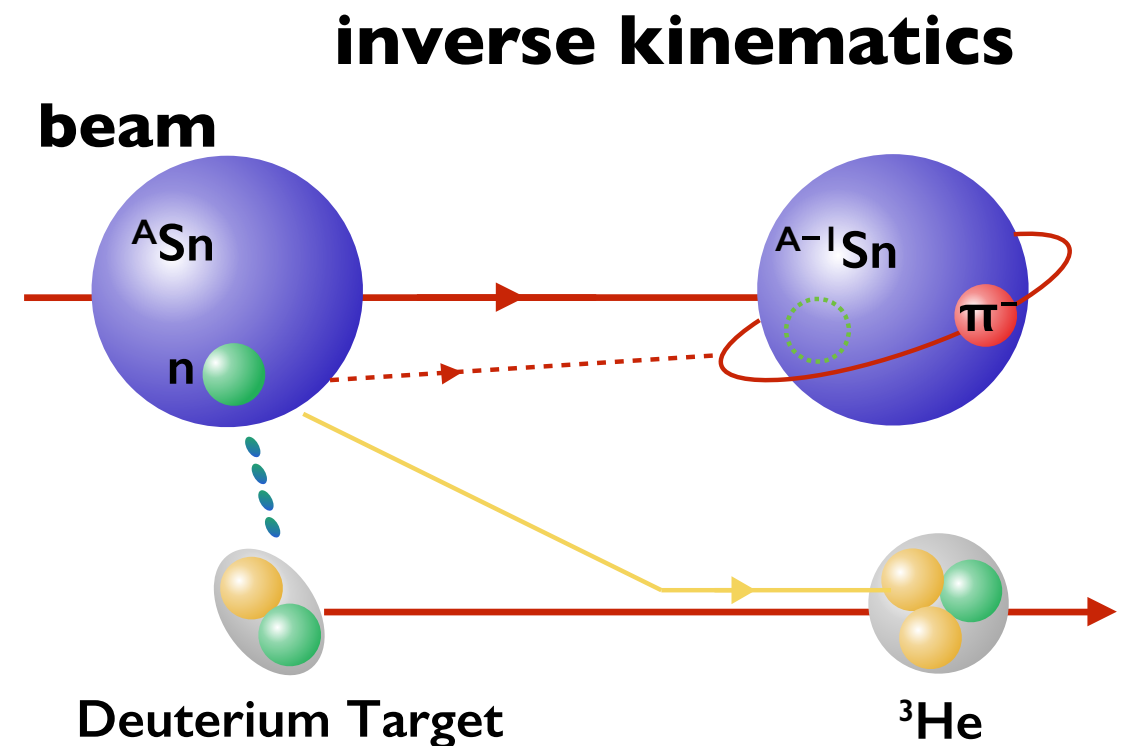
Deeply bound π^- states in nuclei

Pionic-atom factory experiments at RIKEN (2010–)

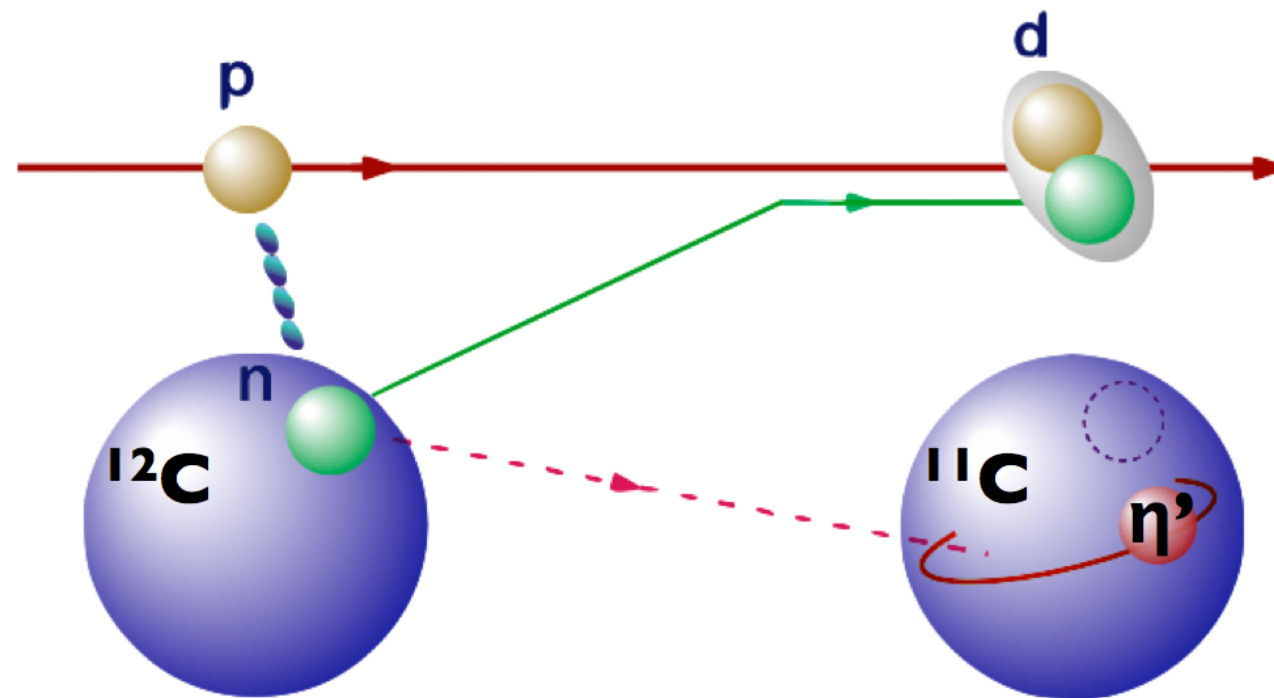
- intense d beam from SRC
 - + large-acceptance BigRIPS spectrometer
- systematic study in a wide region along Sn isotopes

D(HI, ^3He) reaction

- high resolution owing to its kinematics
- π atom is formed in projectile nucleus (Xe, U, or unstable nuclei?)
- ρ dependence of quark condensate



Search for η' -nucleus bound states



η -PRiME/Super-FRS collaboration

S437 experiment at GSI (2014)

Y. Ayyad, J. Benlliure, K.-T. Brinkmann, S. Friedrich, H. Fujioka, H. Geissel, J. Gellanki, C. Guo, E. Gutz, E. Haettner, M. N. Harakeh, R. S. Hayano, Y. Higashi, S. Hirenzaki, C. Hornung, Y. Igarashi, N. Ikeno, K. Itahashi, M. Iwasaki, D. Jido, N. Kalantar-Nayestanaki, R. Kanungo, R. Knöbel, N. Kurz, V. Metag, I. Mukha, T. Nagae, H. Nagahiro, M. Nanova, T. Nishi, H. J. Ong, S. Pietri, A. Prochazka, C. Rappold, M. P. Reiter, J.L. Rodríguez-Sánchez, C. Scheidenberger, H. Simon, B. Sitar, P. Strmen, B. Sun, K. Suzuki, I. Szarka, M. Takechi, Y. K. Tanaka, I. Tanihata, S. Terashima, Y. N. Watanabe, H. Weick, E. Widmann, J. S. Winfield, X. Xu, H. Yamakami, J. Zhao

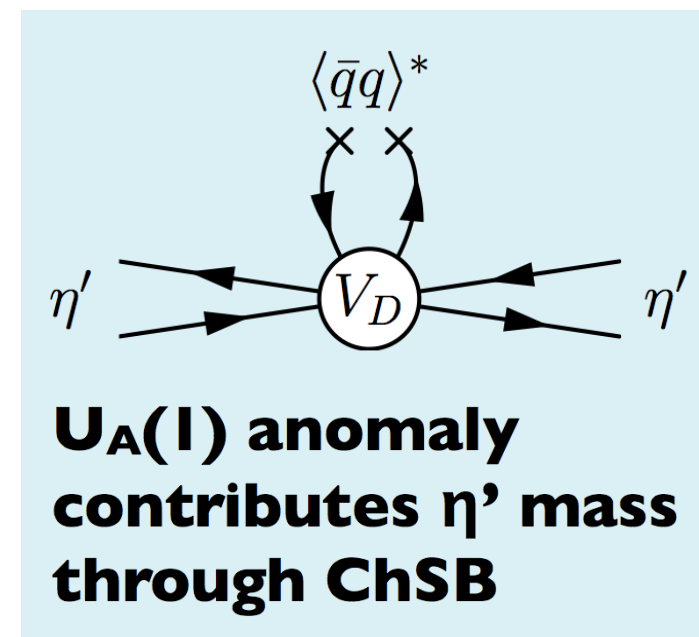
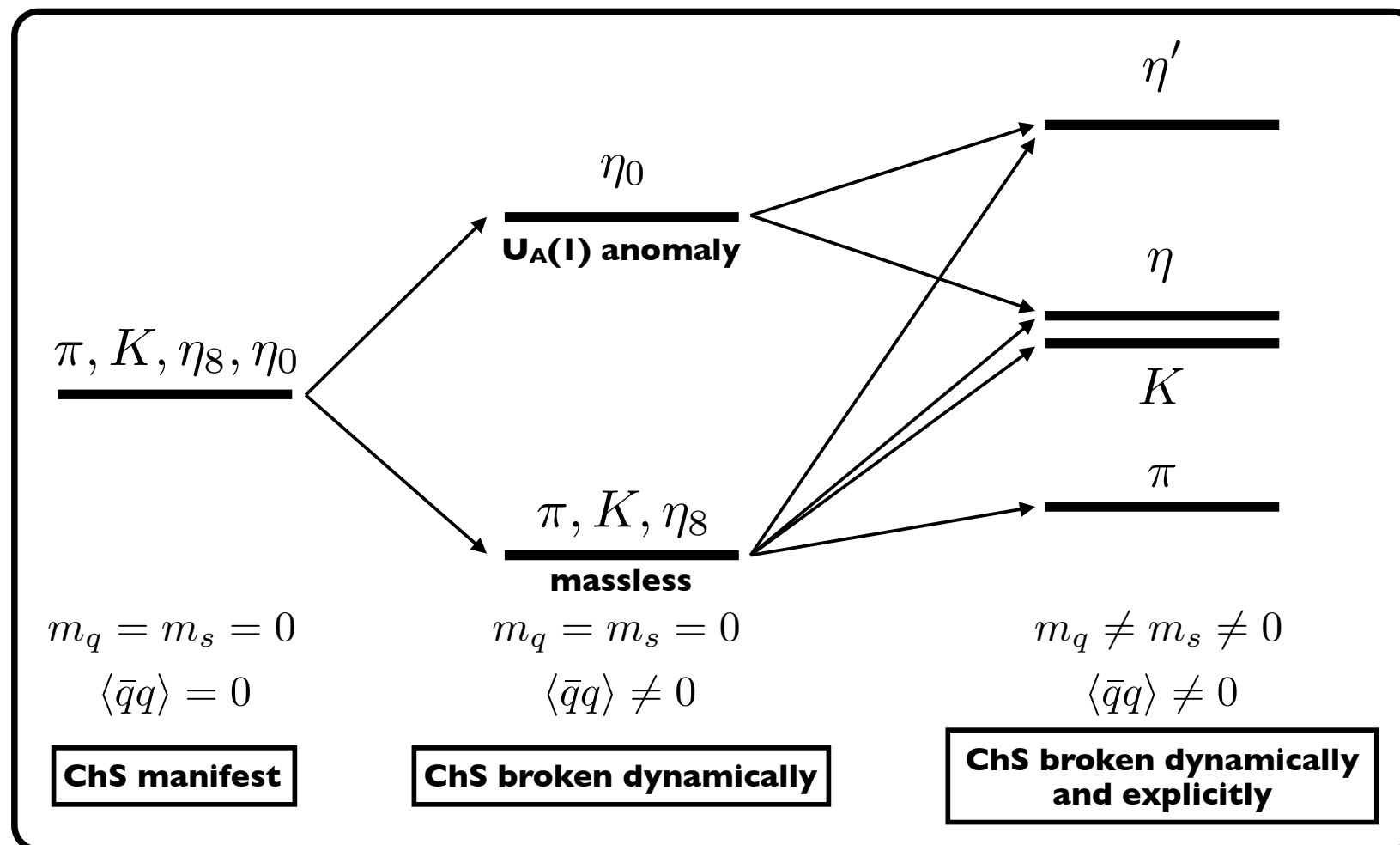
RCNP Osaka University, Universidade de Santiago de Compostela, Universität Giessen, Kyoto University, GSI, KVI-CART University of Groningen, Beihang University, The University of Tokyo, Nara Women's University, KEK, Tottori University, RIKEN Nishina Center, Tokyo Metropolitan University, Saint Mary's University, Comenius University Bratislava, Stefan Meyer Institut, Niigata University

η' meson



η' meson in vacuum

- Mass = **958 MeV/c²** (especially large), Width : 0.2 MeV, $J^P = 0^-$
- $U_A(1)$ anomaly and spontaneous breaking of chiral symmetry



H. Nagahiro, D. Jido *et al*,
 PRC 87, 045201 (2013).

D. Jido, H. Nagahiro, S. Hirenzaki,
 PRC 85, 032201 (2012).

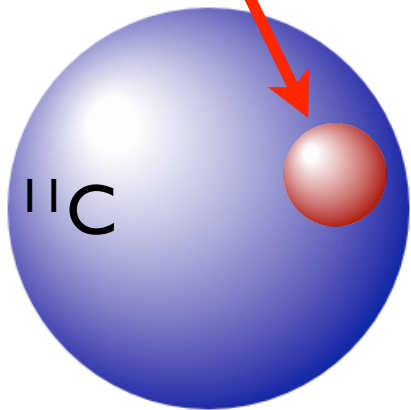
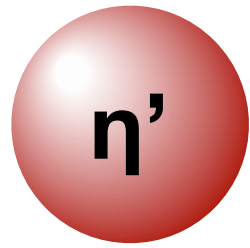
η' meson

η' meson in vacuum

- Mass = **958 MeV/c²** (especially large), Width : 0.2 MeV, $J^P = 0^-$
- $U_A(1)$ anomaly and spontaneous breaking of chiral symmetry

η' meson at nuclear density

- Partial restoration of chiral symmetry ($\langle \bar{q}q \rangle$ reduced $\sim 30\%$)
- Mass reduction is expected



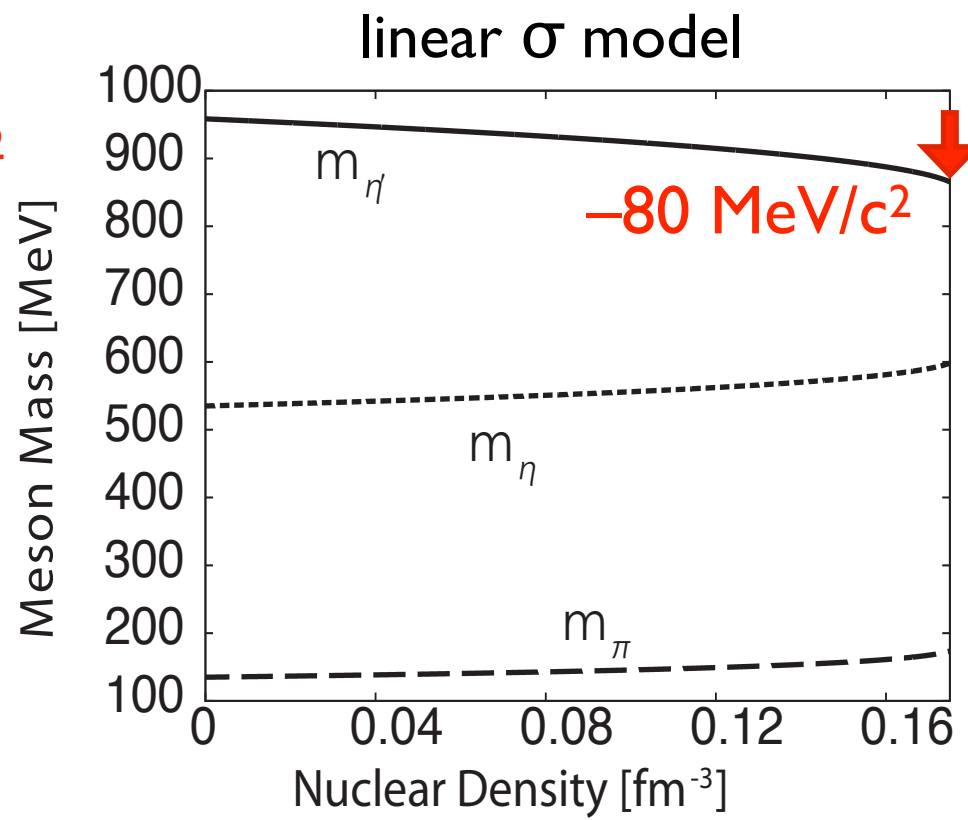
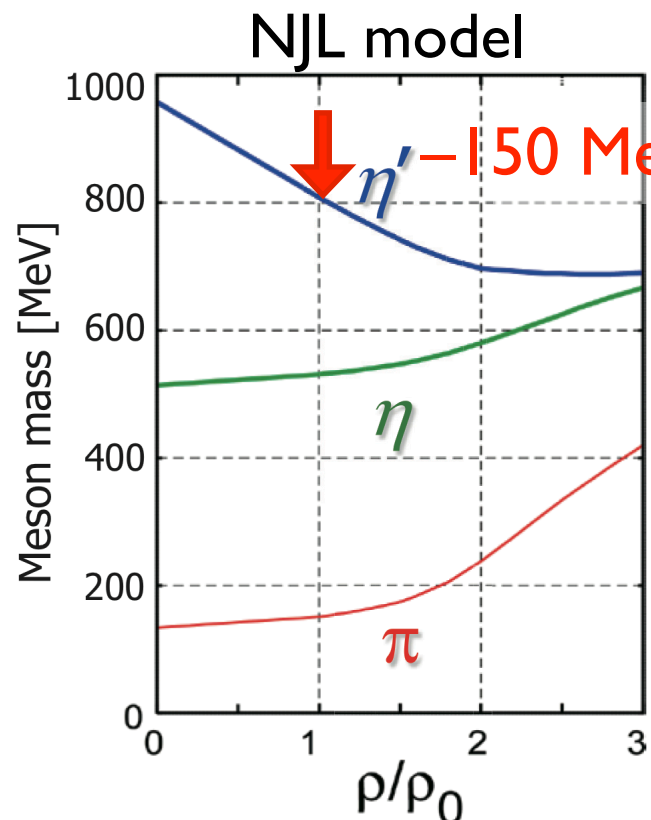
η' meson

η' meson in vacuum

- Mass = **958 MeV/c²** (especially large), Width : 0.2 MeV, $J^P = 0^-$
- $U_A(1)$ anomaly and spontaneous breaking of chiral symmetry

η' meson at nuclear density

- Partial restoration of chiral symmetry ($\langle \bar{q}q \rangle$ reduced $\sim 30\%$)
- Mass reduction is expected



QMC model :

$$\Delta m \sim -37 \text{ MeV}/c^2$$

(for $\theta_{\eta\eta'} = -20^\circ$)

H. Nagahiro *et al.*, PRC 74, 045203(2006).
 S. Sakai *et al.*, D. Jido, PRC 88, 064906 (2013).
 S.D. Bass, A.W. Thomas, PLB 634, 368 (2006).

η' -nucleus potential

η' -nucleus optical potential :

$$V_{\eta'} = (V_0 + iW_0) \frac{\rho(r)}{\rho_0}$$

$$V_0 = \Delta m(\rho_0), \quad W_0 = -\Gamma(\rho_0) / 2$$

Theoretical predictions

$$\Delta m(\rho_0) \sim -150 \text{ MeV}/c^2 \text{ (NJL)}, -80 \text{ MeV}/c^2 \text{ (linear } \sigma), -37 \text{ MeV}/c^2 \text{ (QMC)}$$

H. Nagahiro *et al.*, PRC 74, 045203(2006).

S. Sakai, D. Jido, PRC 88, 064906 (2013).

S.D. Bass, A.W. Thomas, PLB 634, 368 (2006).

η' -nucleus potential

η' -nucleus optical potential :

$$V_{\eta'} = (V_0 + iW_0) \frac{\rho(r)}{\rho_0}$$

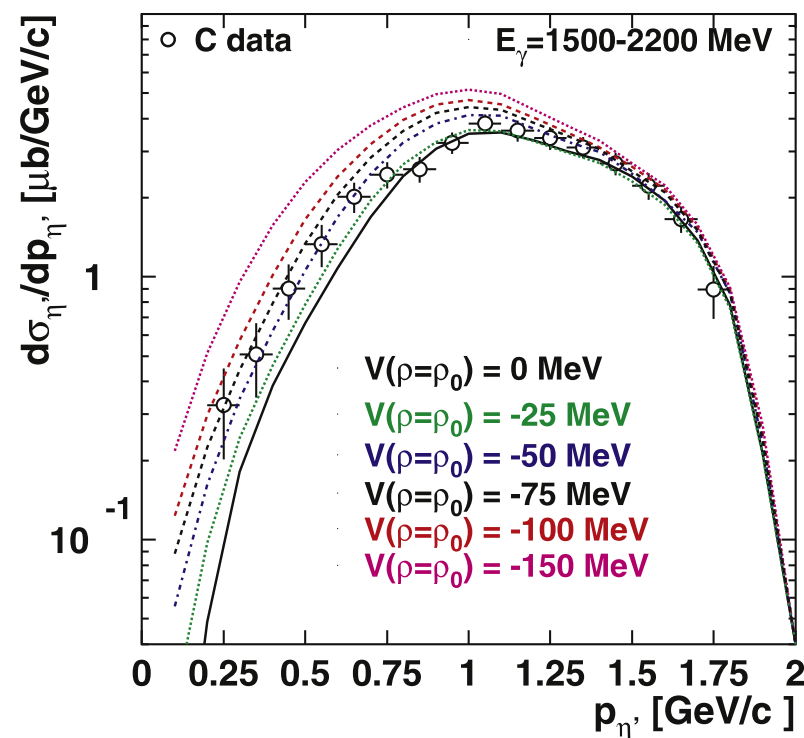
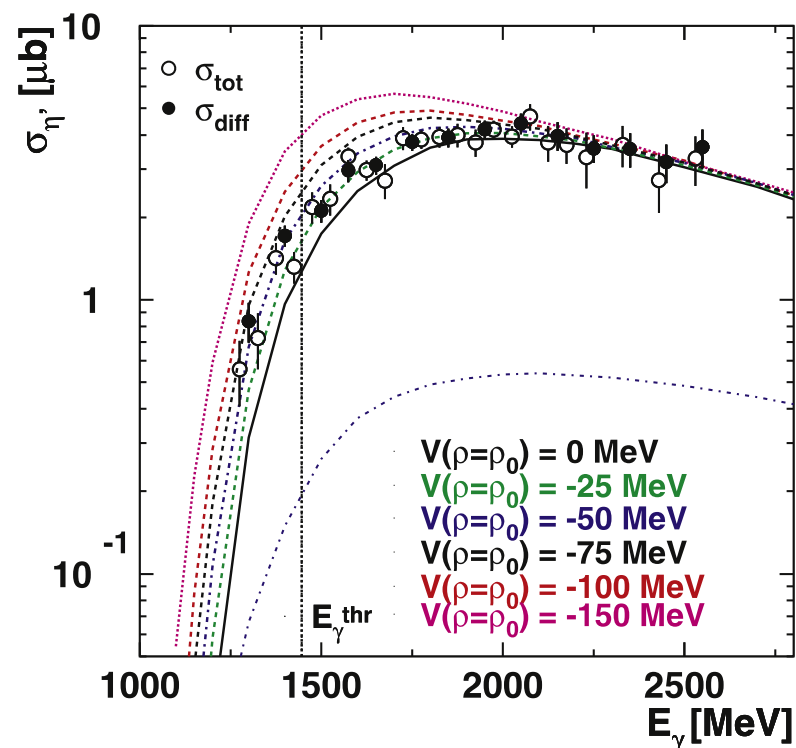
$$V_0 = \Delta m(\rho_0), \quad W_0 = -\Gamma(\rho_0) / 2$$

Theoretical predictions

$\Delta m(\rho_0) \sim -150 \text{ MeV}/c^2$ (NJL), $-80 \text{ MeV}/c^2$ (linear σ), $-37 \text{ MeV}/c^2$ (QMC)

Experimental indications (CBELSA/TAPS)

□ $V_0 \sim -40 \text{ MeV}$ (excitation function, mom. distribution)



M. Nanova *et al.*, PRC 94 025205 (2016).
M. Nanova *et al.*, PLB 727, 417 (2013).

η' photo-production
off C target

η' -nucleus potential

η' -nucleus optical potential :

$$V_{\eta'} = (V_0 + iW_0) \frac{\rho(r)}{\rho_0}$$

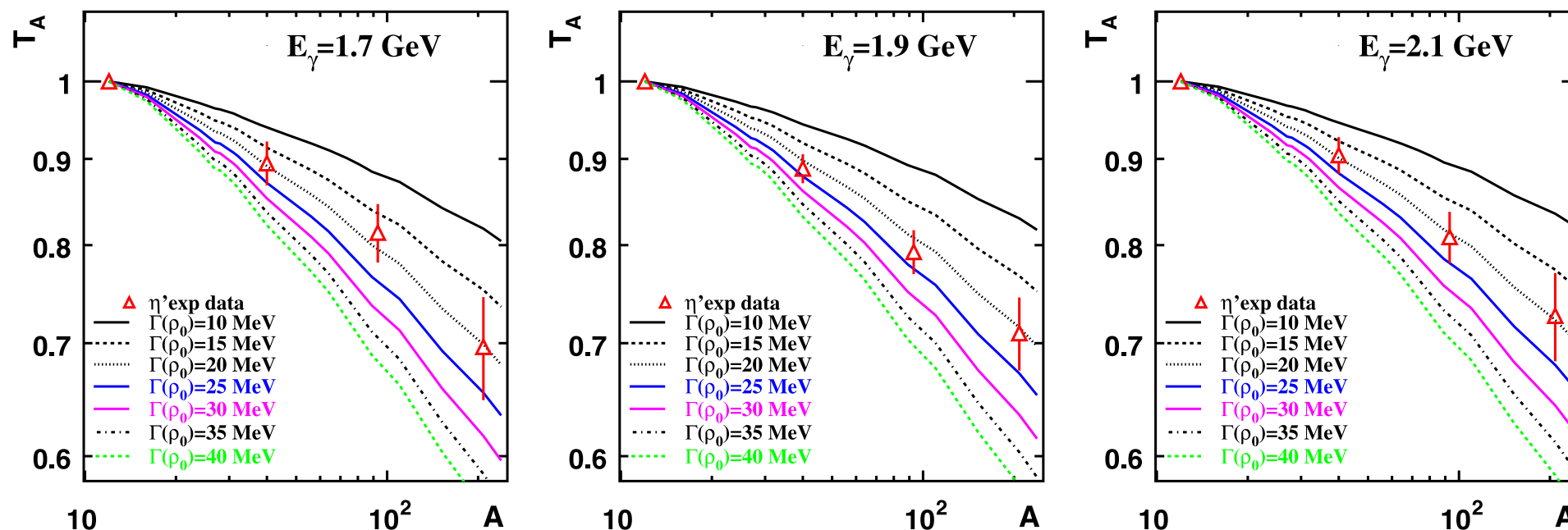
$$V_0 = \Delta m(\rho_0), \quad W_0 = -\Gamma(\rho_0) / 2$$

Theoretical predictions

$\Delta m(\rho_0) \sim -150 \text{ MeV}/c^2$ (NJL), $-80 \text{ MeV}/c^2$ (linear σ), $-37 \text{ MeV}/c^2$ (QMC)

Experimental indications (CBELSA/TAPS)

- $V_0 \sim -40 \text{ MeV}$ (excitation function, mom. distribution)
- $W_0 = -13 \pm 3(\text{stat}) \pm 3(\text{syst}) \text{ MeV}$ (transparency ratio)



M. Nanova *et al.*,
PLB 710, 600 (2012).

S. Friedrich *et al.*,
EPJA 52, 297 (2016).

η' -nucleus potential

η' -nucleus optical potential :

$$V_{\eta'} = (V_0 + iW_0) \frac{\rho(r)}{\rho_0}$$

$$V_0 = \Delta m(\rho_0), \quad W_0 = -\Gamma(\rho_0) / 2$$

Theoretical predictions

$\Delta m(\rho_0) \sim -150 \text{ MeV}/c^2$ (NJL), $-80 \text{ MeV}/c^2$ (linear σ), $-37 \text{ MeV}/c^2$ (QMC)

Experimental indications (CBELSA/TAPS)

- $V_0 \sim -40 \text{ MeV}$ (excitation function, mom. distribution)
- $W_0 = -13 \pm 3(\text{stat}) \pm 3(\text{syst}) \text{ MeV}$ (transparency ratio)

η' - p scattering length by COSY-11

E. Czerwiński et al., PRL 113, 062004 (2014)

○ $\text{Re}(a_{\eta'p}) = 0 \pm 0.43 \text{ fm}$, $\text{Im}(a_{\eta'p}) = 0.37_{-0.16}^{+0.40} \text{ fm}$

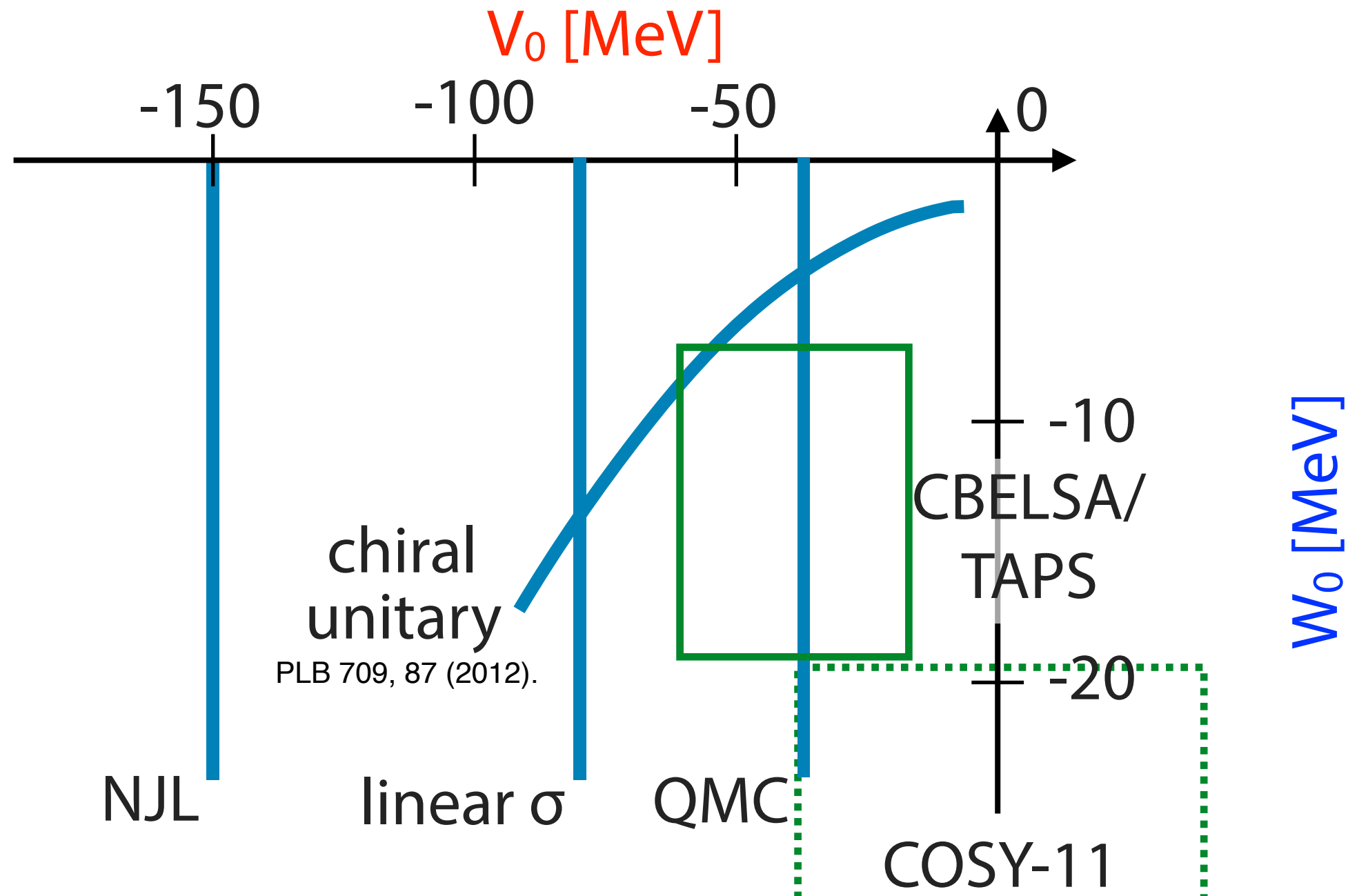
→ $|V_0| < 38 \text{ MeV}$, $W_0 = -(33_{-14}^{+40}) \text{ MeV}$ (low density approx.)

η' -nucleus potential

η' -nucleus optical potential :

$$V_{\eta'} = (V_0 + iW_0) \frac{\rho(r)}{\rho_0}$$

$$V_0 = \Delta m(\rho_0), \quad W_0 = -\Gamma(\rho_0) / 2$$

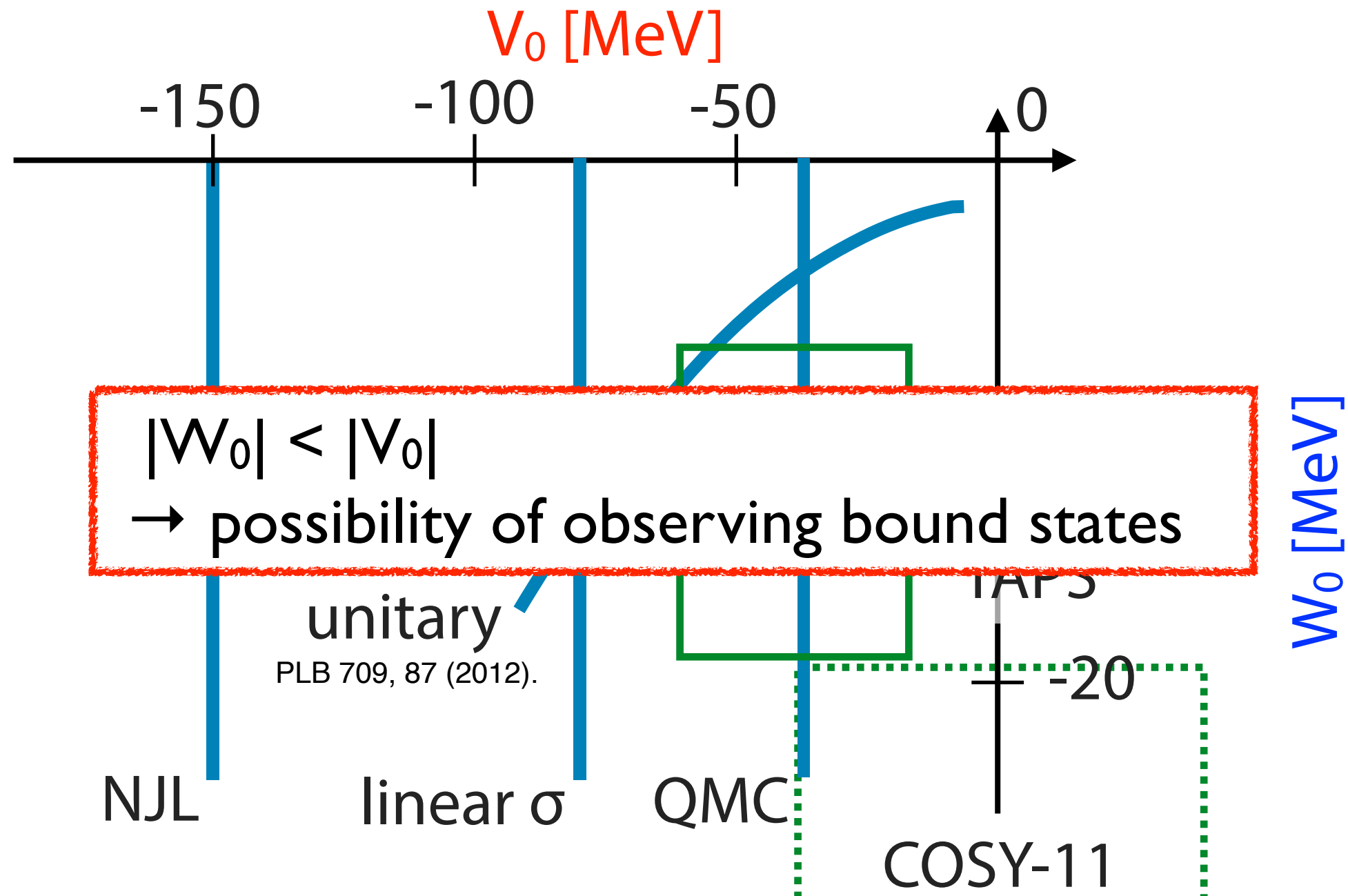


η' -nucleus potential

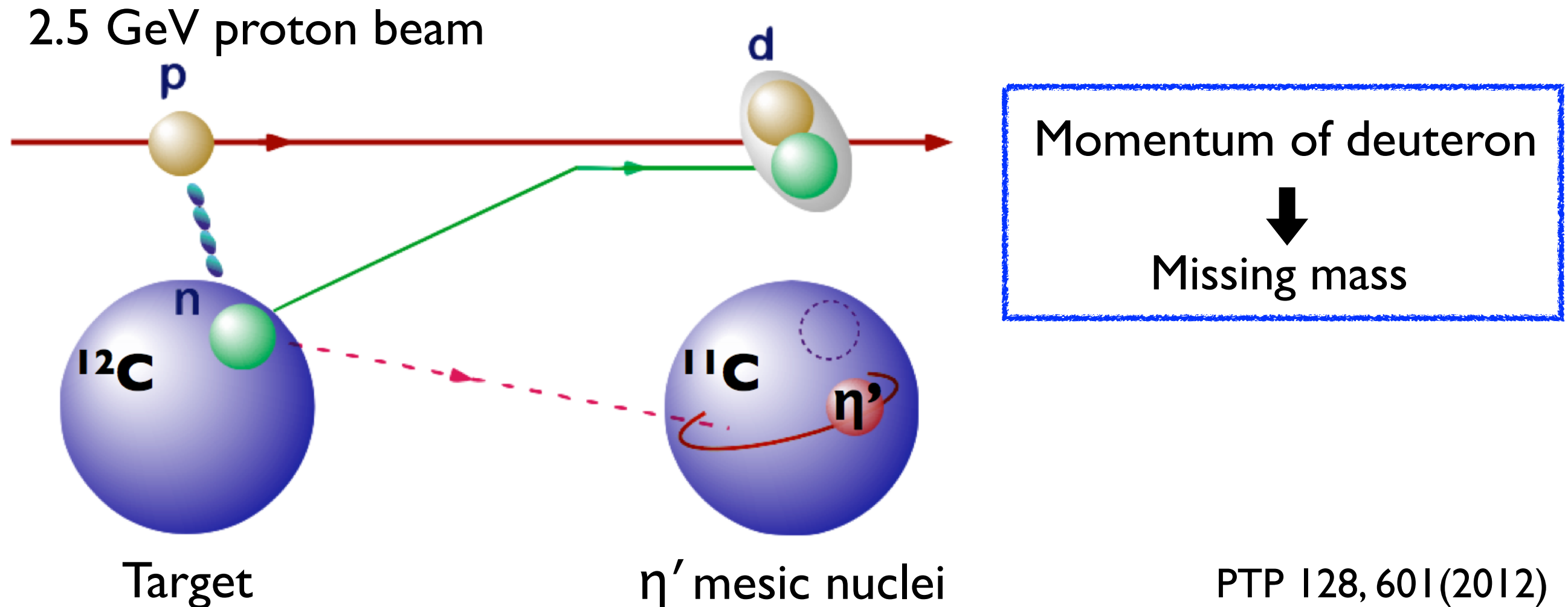
η' -nucleus optical potential :

$$V_{\eta'} = (V_0 + iW_0) \frac{\rho(r)}{\rho_0}$$

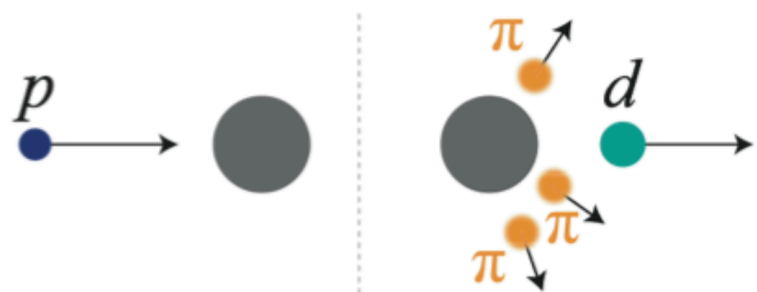
$$V_0 = \Delta m(\rho_0), \quad W_0 = -\Gamma(\rho_0) / 2$$



Missing-mass spectroscopy of $^{12}\text{C}(p,d)$ reaction ¹⁵



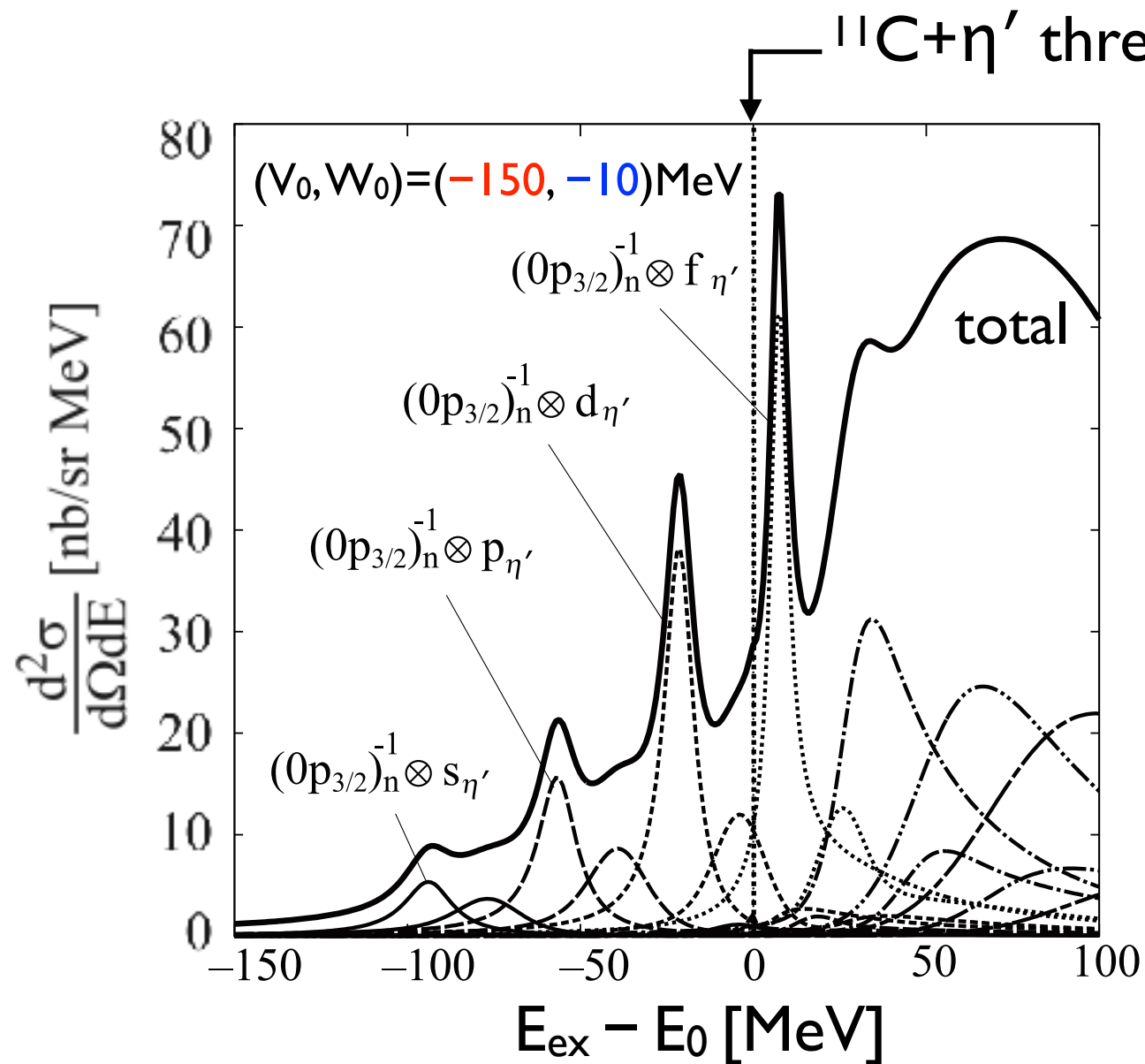
- overall structure w/o assuming decay process
- S/B ratio $\lesssim O(1/100)$ due to BG processes (e.g., $p+N \rightarrow d+\pi$'s)



high statistical sensitivity is essential

Theoretically calculated formation spectra

Calculated formation spectrum of $^{12}\text{C}(p,d)^{11}\text{C} \times \eta'$



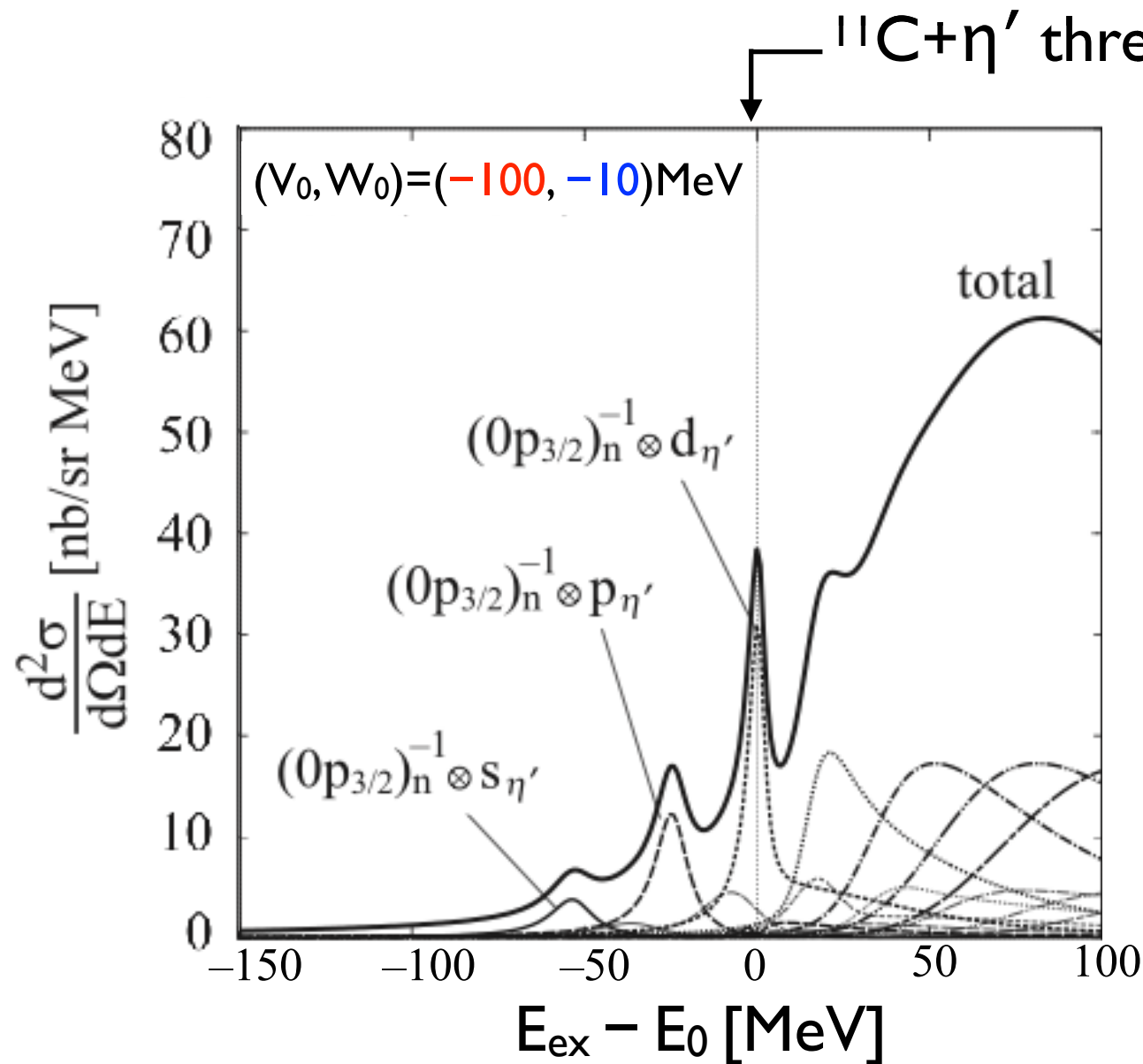
$$V_{\eta'} = (V_0 + iW_0) \frac{\rho(r)}{\rho_0}$$

H. Nagahiro *et al.*,
PRC 87, 045201 (2013)

- momentum transfer $\sim 400 \text{ MeV}/c$ at $T_p = 2.5 \text{ GeV}$
- enhanced excited states near η' emission threshold

Theoretically calculated formation spectra

Calculated formation spectrum of $^{12}\text{C}(p,d)^{11}\text{C} \times \eta'$



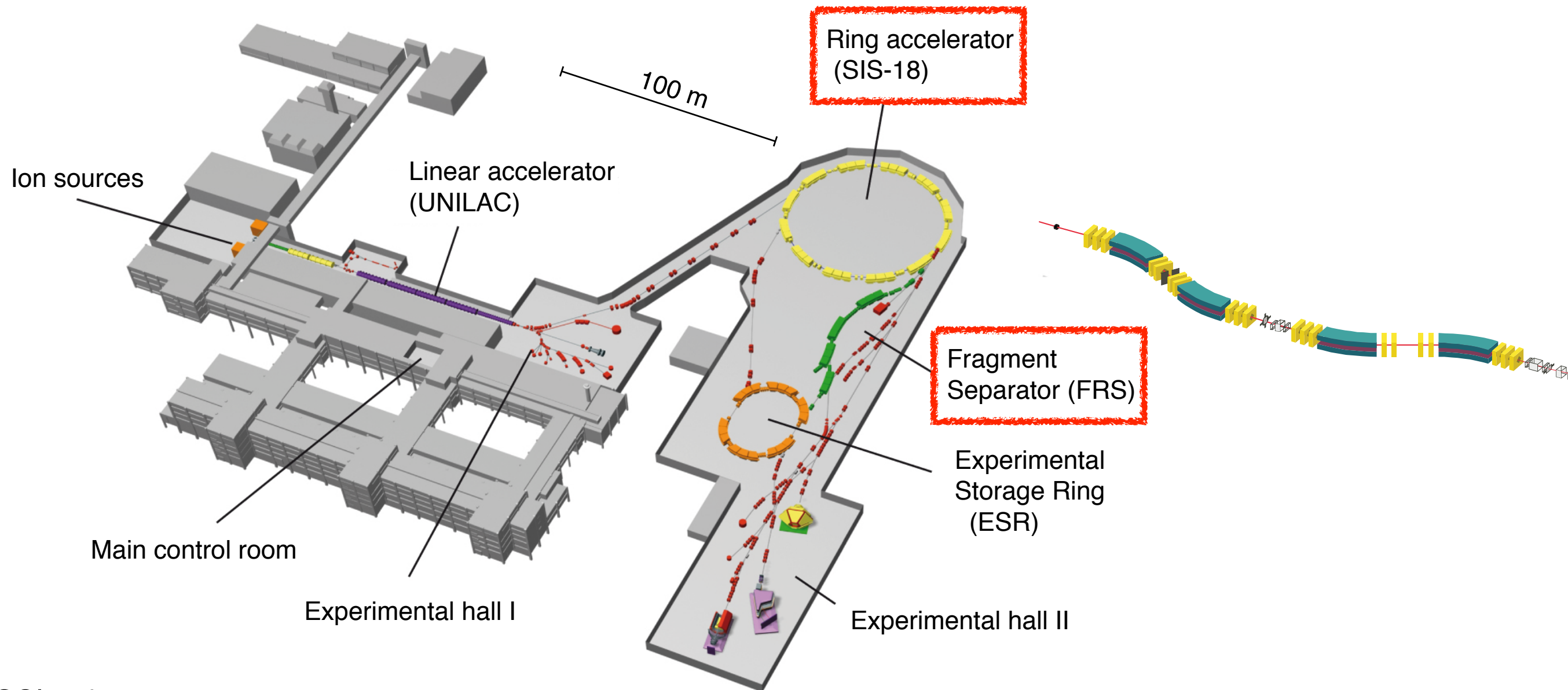
$$V_{\eta'} = (V_0 + iW_0) \frac{\rho(r)}{\rho_0}$$

H. Nagahiro *et al.*,
PRC 87, 045201 (2013)

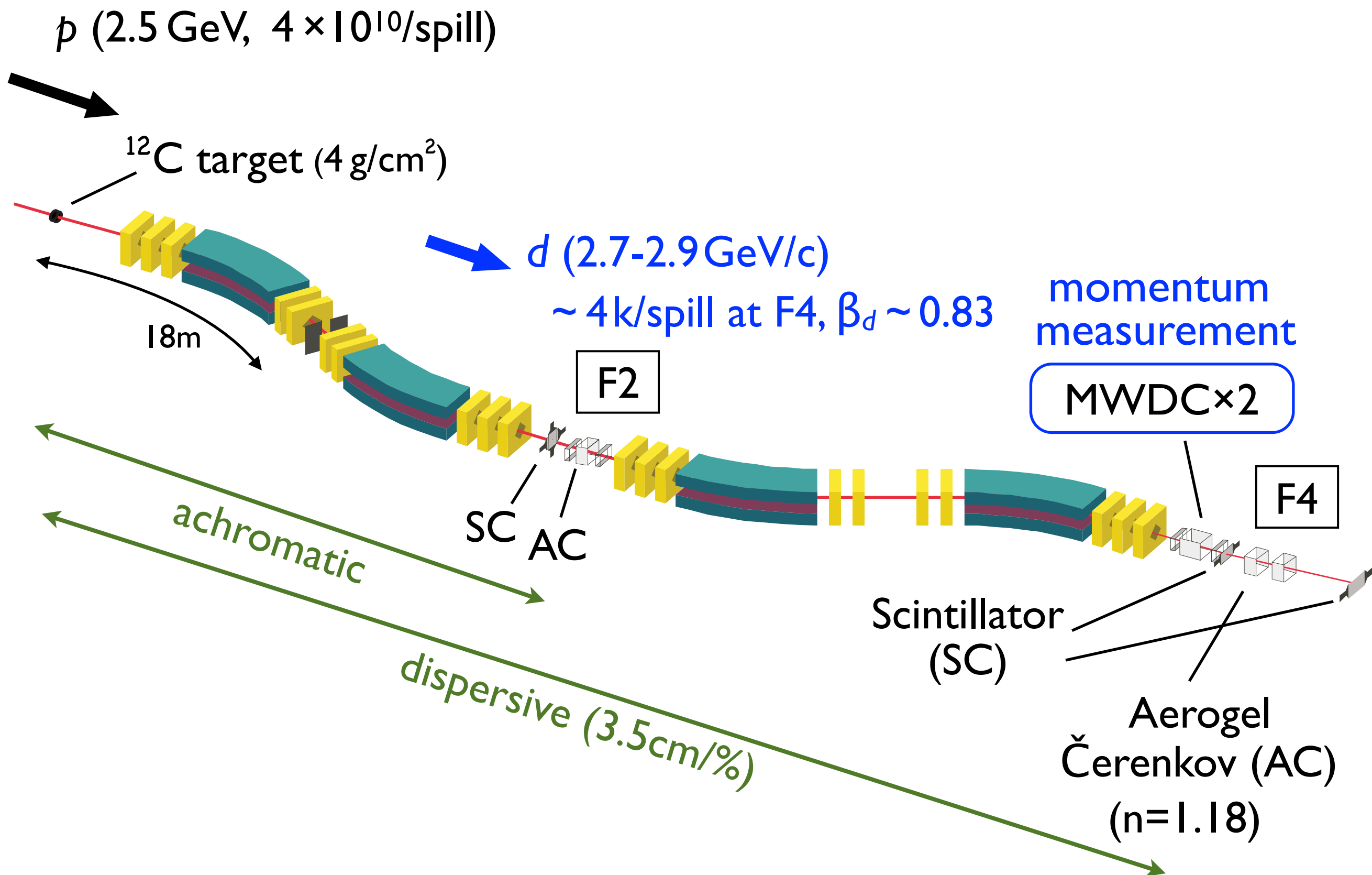
- momentum transfer $\sim 400 \text{ MeV}/c$ at $T_p = 2.5 \text{ GeV}$
- enhanced excited states near η' emission threshold

GSI facilities

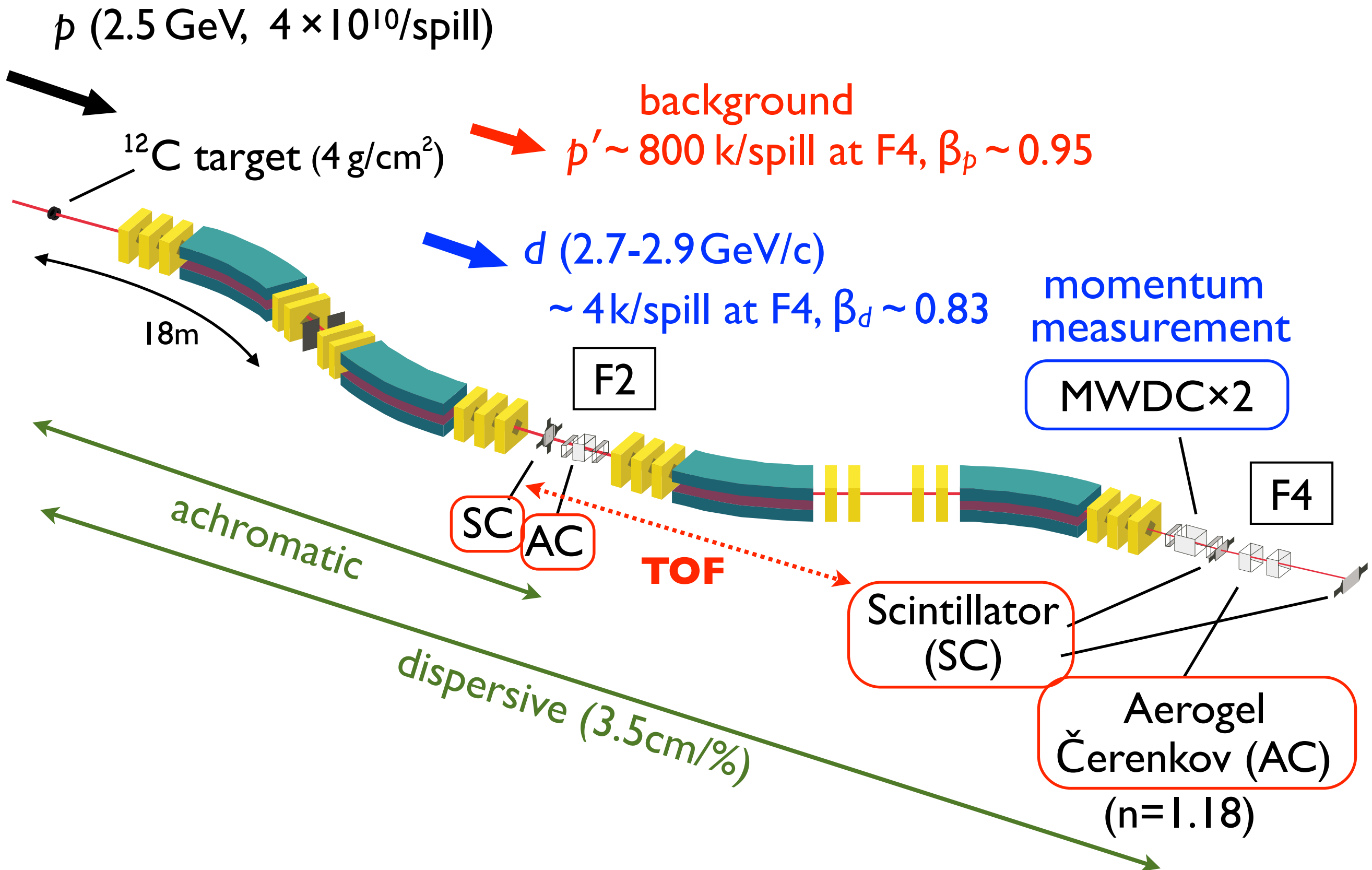
- SIS-18: 2.5 GeV proton beam
- Fragment Separator (FRS): high-resolution spectrometer + (instrumental) BG rejection



Experimental setup at FRS

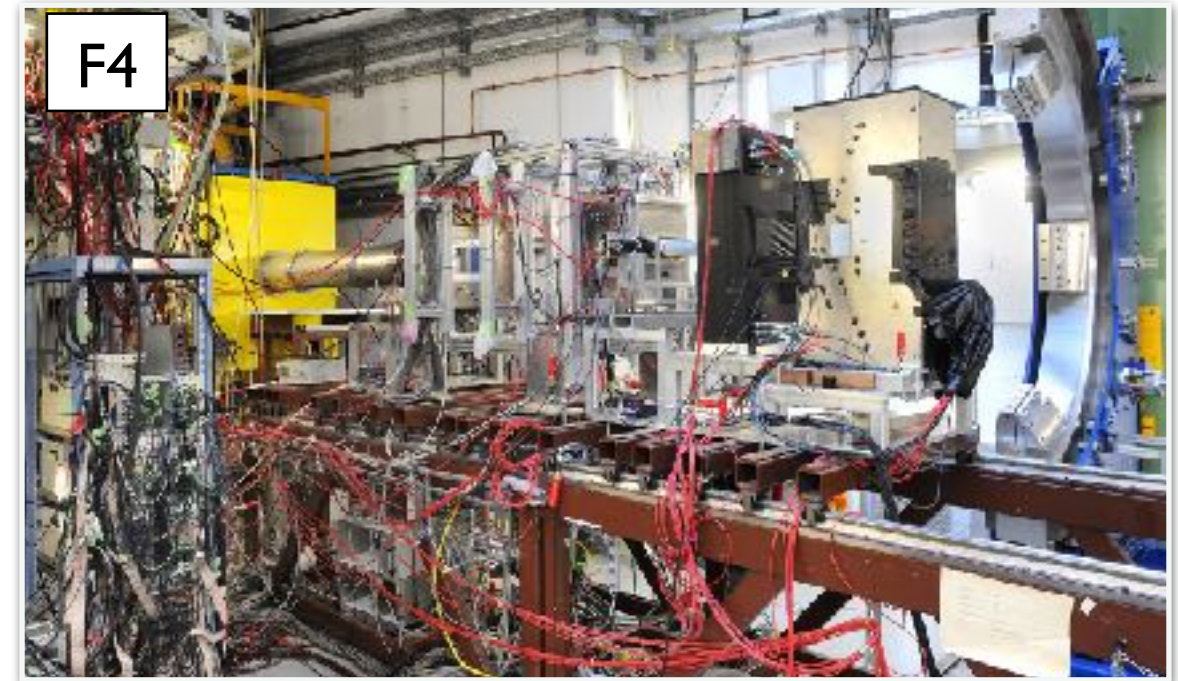
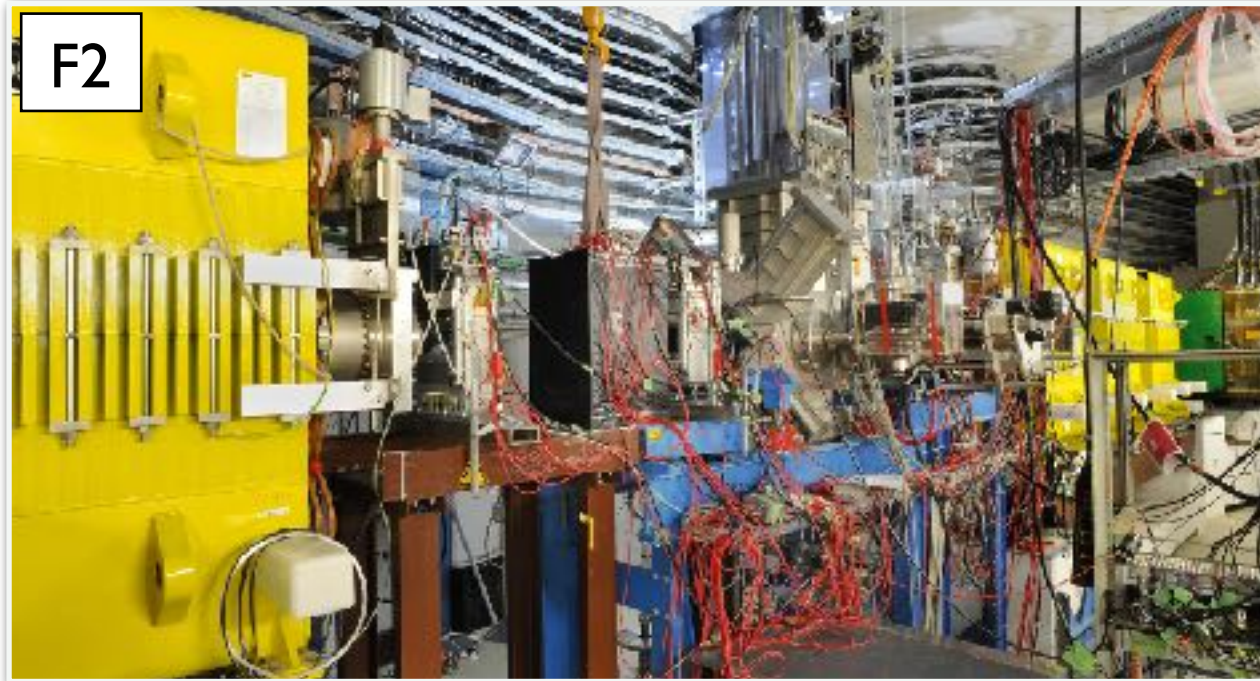


Experimental setup at FRS

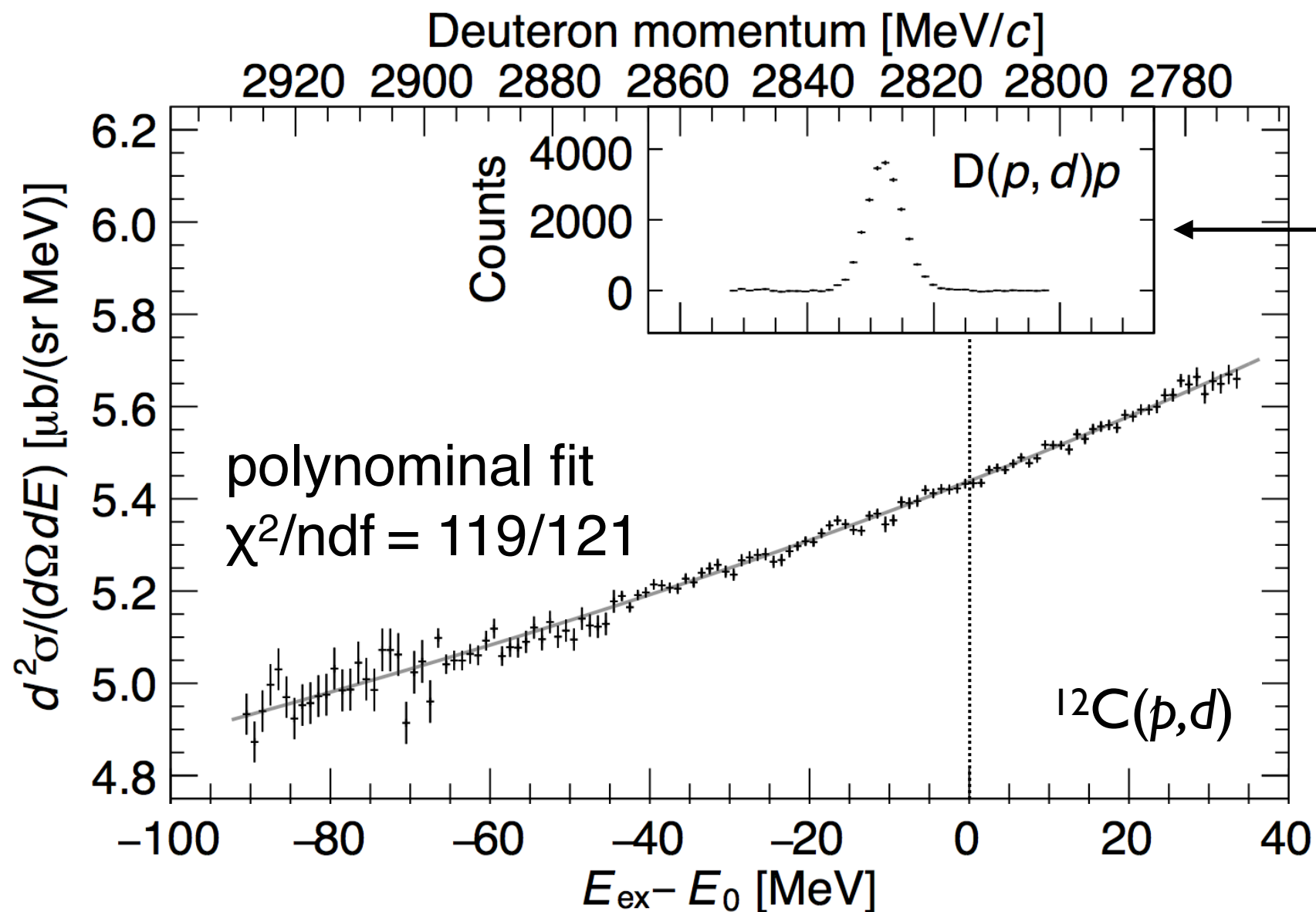


First experiment in 2014

- production run of $C(p,d)$ reaction at $T_p = 2.5$ GeV (~ 5 days)
- scaling momentum region of FRS
 - cover -90 to $+40$ MeV around η' threshold
- good statistics : $\sim O(10^7)$ deuteron events
- calibration with $D(p,d)p$ elastic scattering at $T_p = 1.6$ GeV



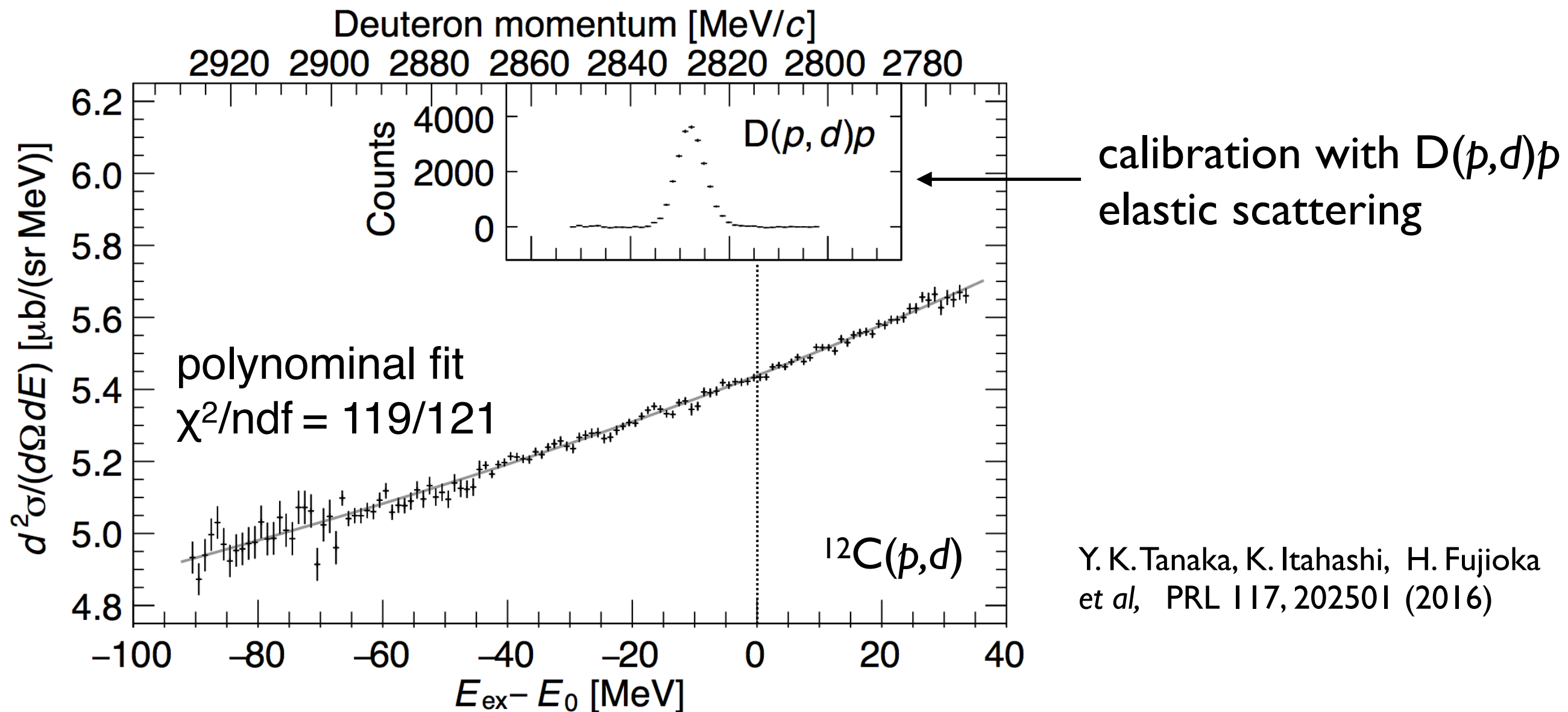
Results — excitation spectrum —



calibration with $D(p,d)p$
elastic scattering

Y. K. Tanaka, K. Itahashi, H. Fujioka
et al, PRL 117, 202501 (2016)

Results — excitation spectrum —

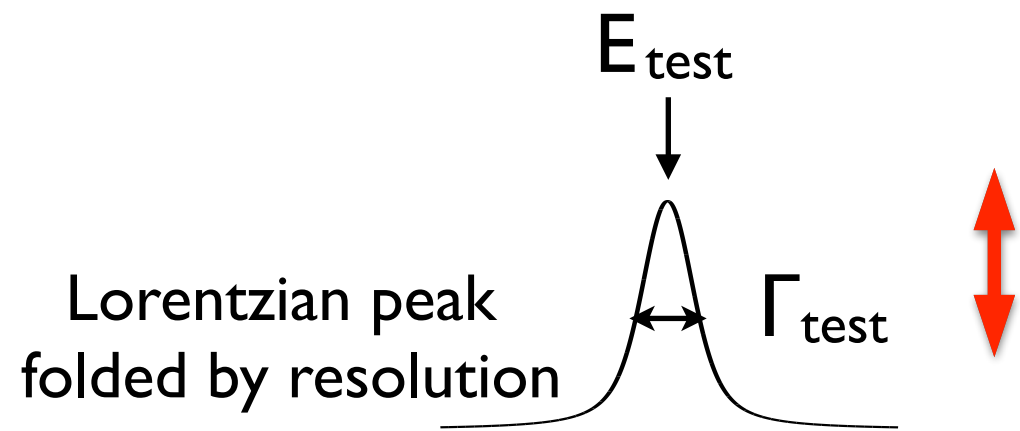


- good statistical sensitivity $\lesssim 1\%$ is achieved
- overall (p,d) cross section consistent with quasi-free multi- π production
- sufficient resolution 2.5 MeV(σ) achieved
- no significant peak structure is observed
 - upper limits for formation cross section of η' mesic states

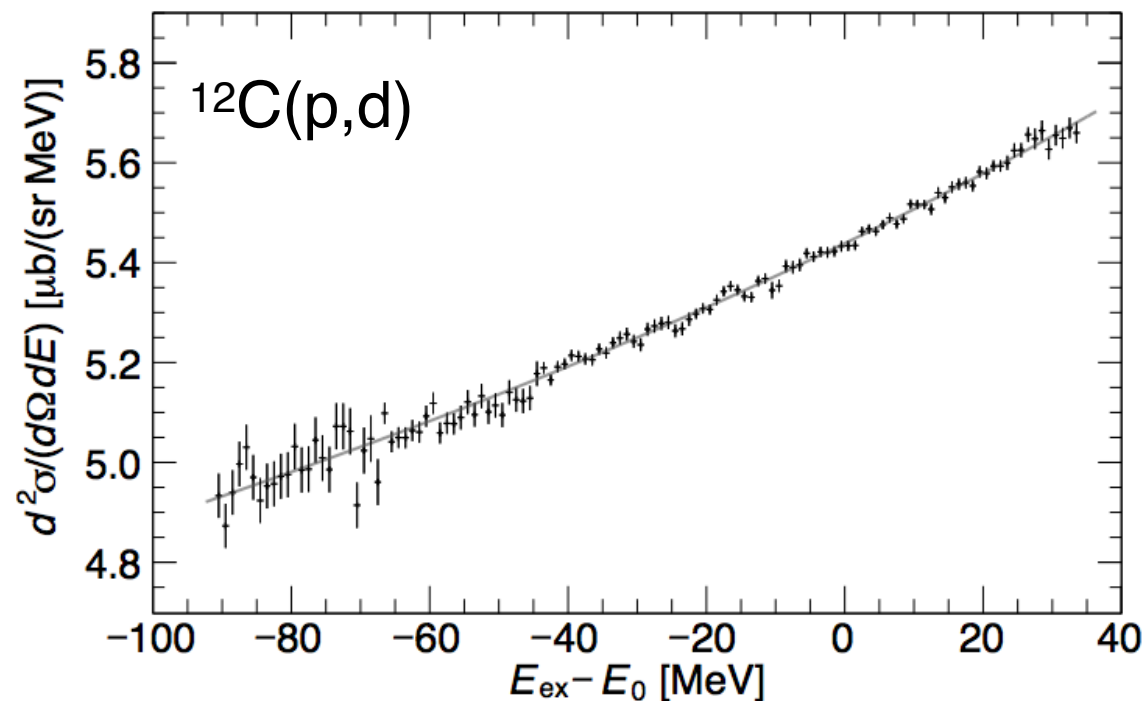
Upper limit of formation cross section

Upper limit of Lorentzian-shaped formation cross section

- fit function: $A \times \text{Voigt}(E; E_{\text{test}}, \Gamma_{\text{test}}, \sigma_{\text{exp}}) + \text{Pol3}(E; p_0, p_1, p_2, p_3)$

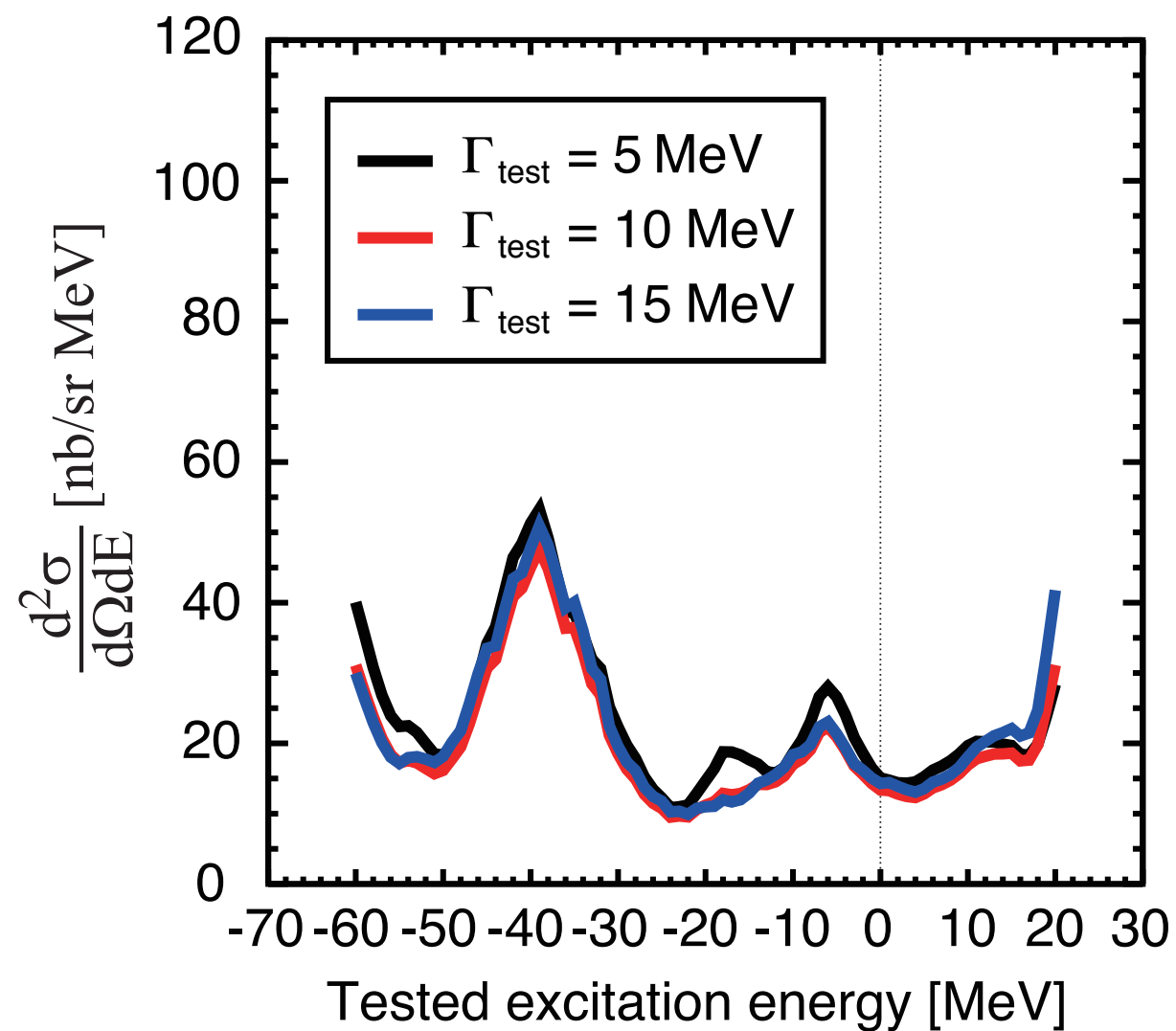


- evaluate upper limit of cross section for fixed $(E_{\text{test}}, \Gamma_{\text{test}})$
- repeat analysis for other $(E_{\text{test}}, \Gamma_{\text{test}})$



Upper limit of formation cross section

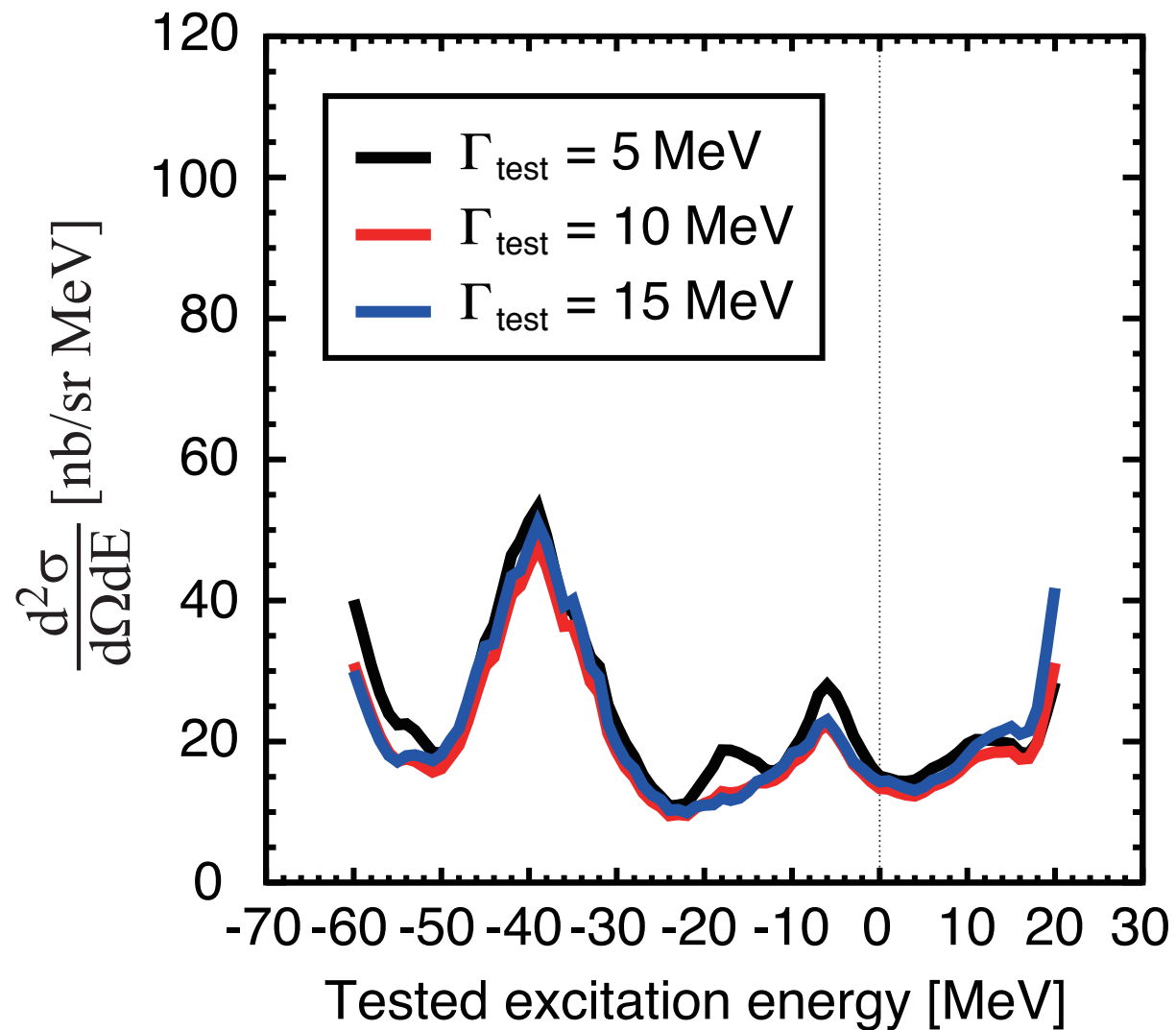
Obtained 95% C.L. upper limits
of Lorentzian peak height



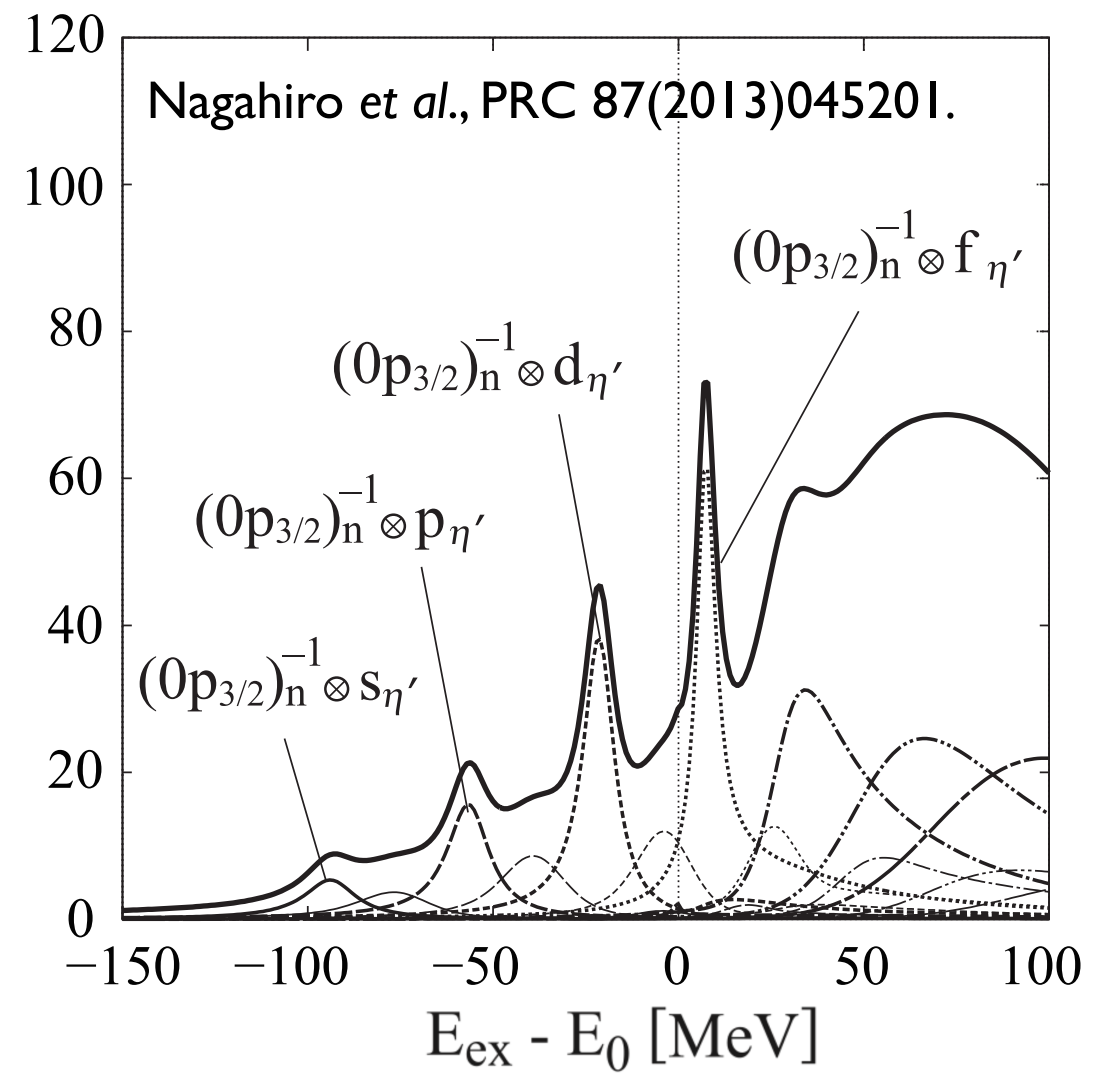
- high statistical sensitivity better than 1% is achieved (as intended)

Upper limit of formation cross section

Obtained 95% C.L. upper limits
of Lorentzian peak height



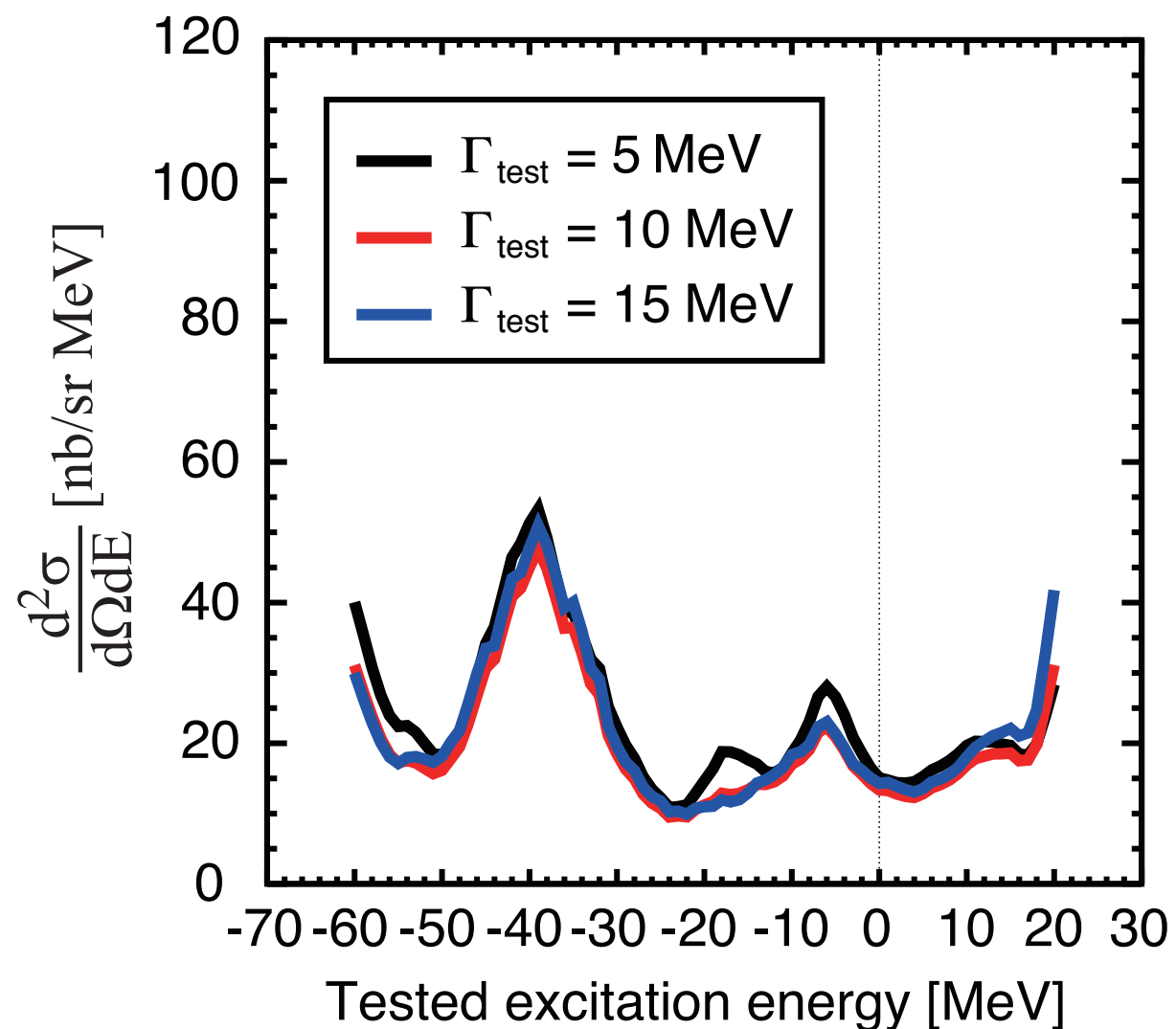
Theoretically expected spectrum
for $(V_0, W_0) = (-150, -10)$ MeV



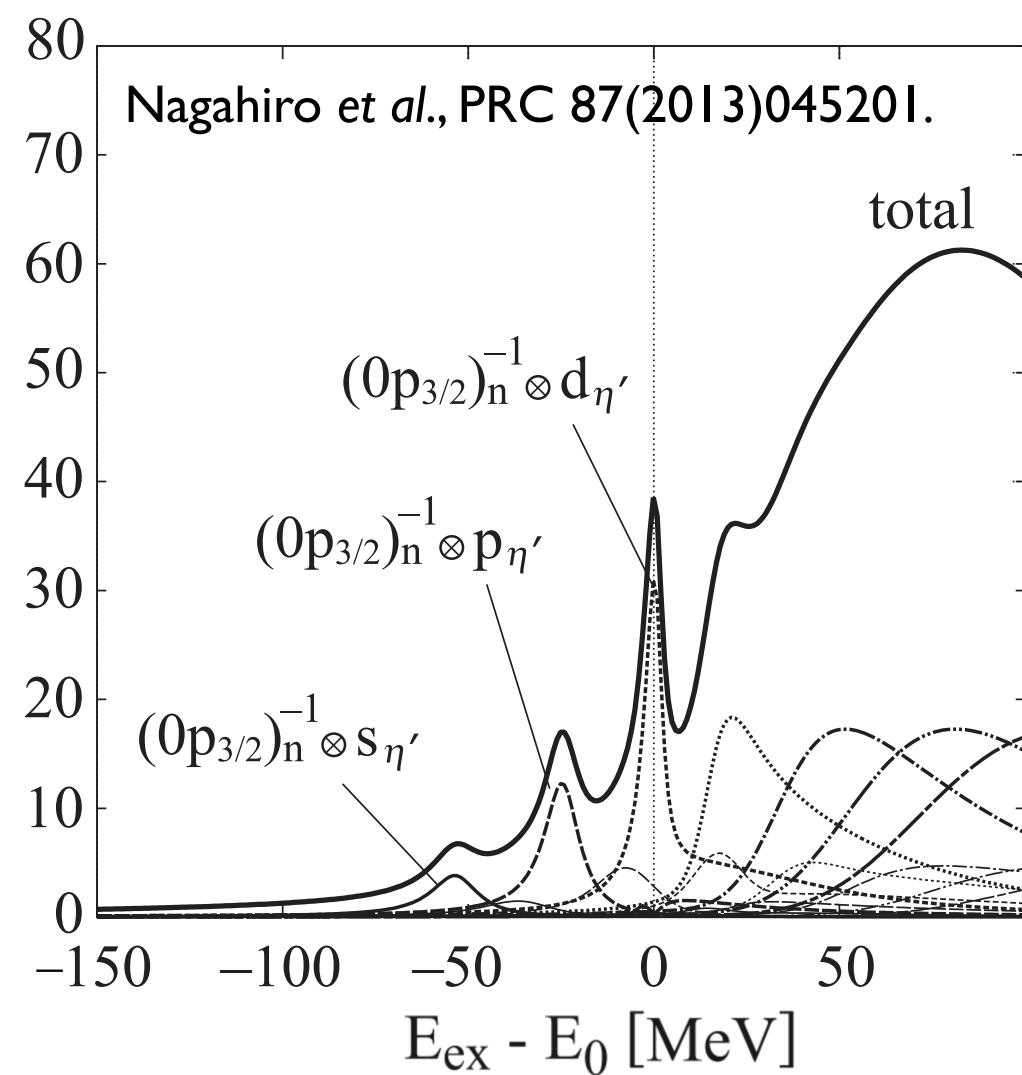
- high statistical sensitivity better than 1% is achieved (as intended)
- ~ 40 nb/(sr.MeV) peak expected for $(V_0, W_0) = (-150, -10)$ MeV is excluded at 95% C.L.

Upper limit of formation cross section

Obtained 95% C.L. upper limits
of Lorentzian peak height



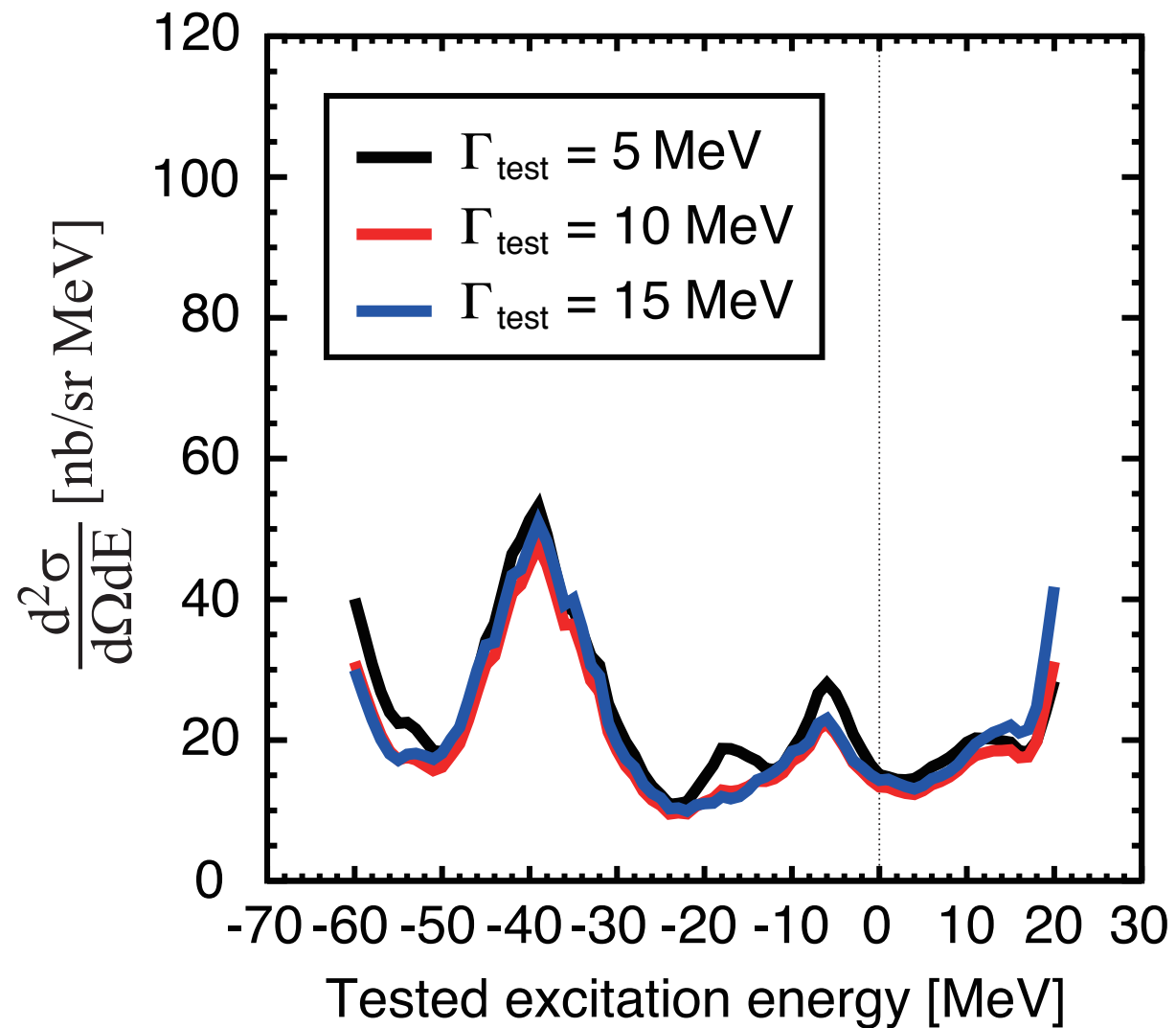
Theoretically expected spectrum
for $(V_0, W_0) = (-100, -10)$ MeV



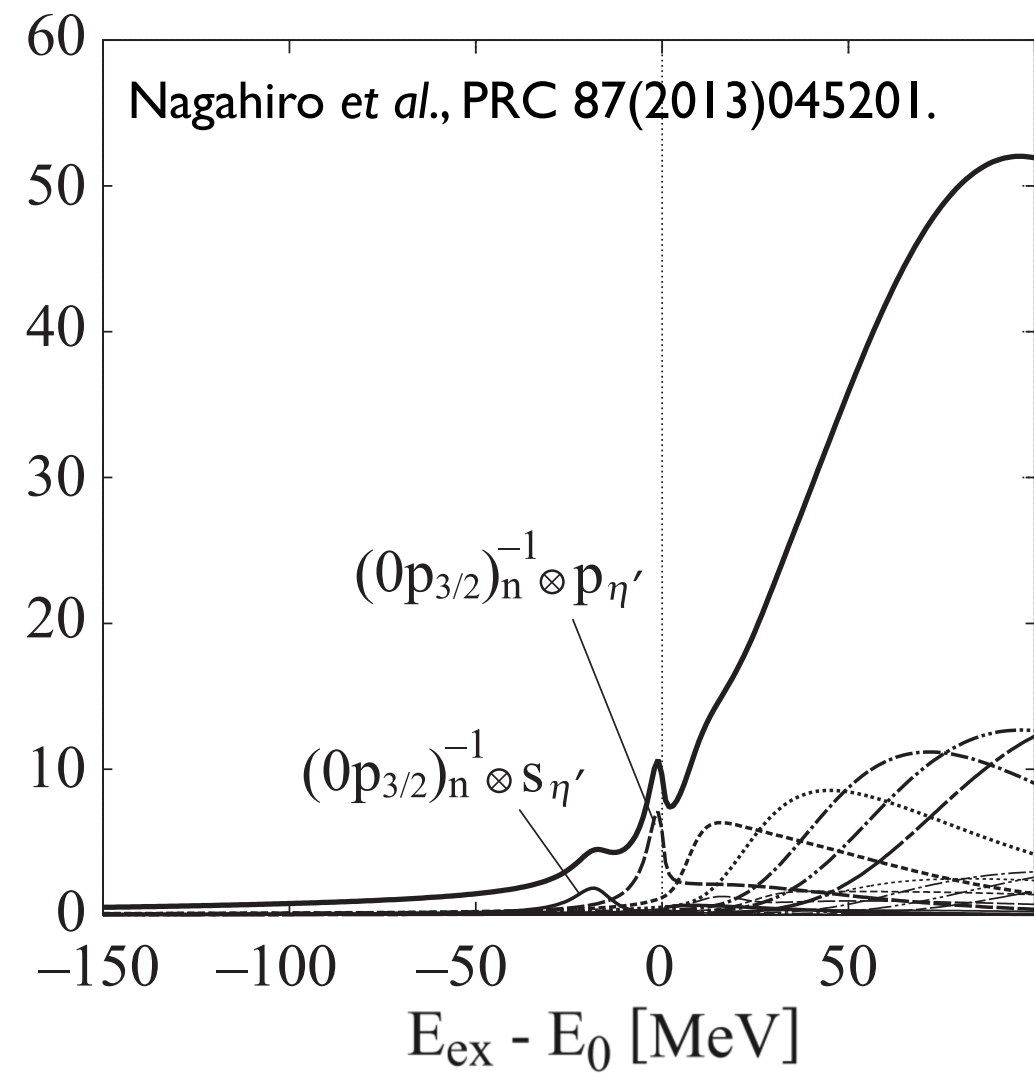
- high statistical sensitivity better than 1% is achieved (as intended)
- ~ 30 nb/(sr·MeV) peak expected for $(V_0, W_0) = (-100, -10)$ MeV is excluded at 95% C.L.

Upper limit of formation cross section

Obtained 95% C.L. upper limits
of Lorentzian peak height



Theoretically expected spectrum
for $(V_0, W_0) = (-50, -10)$ MeV

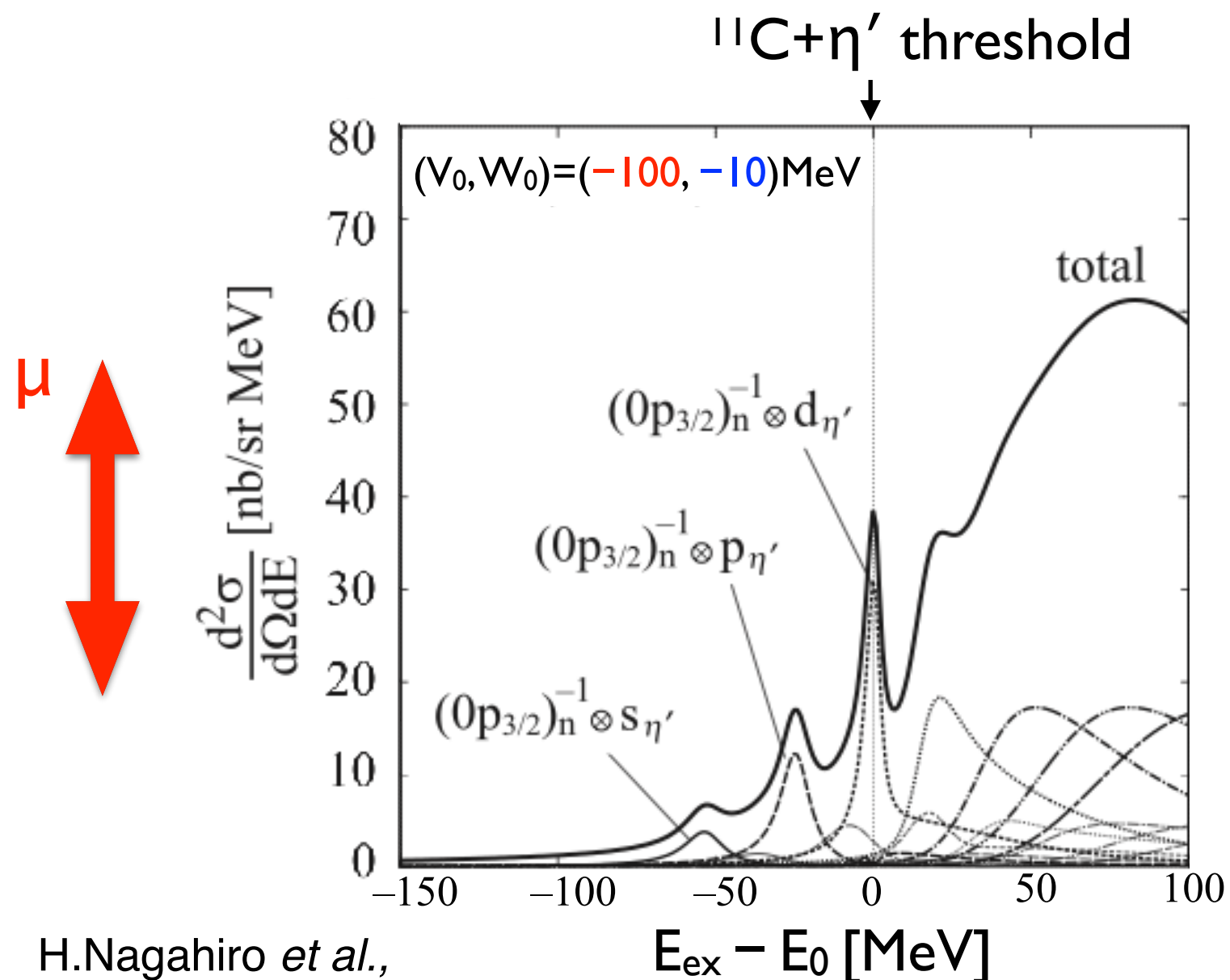


- high statistical sensitivity better than 1% is achieved (as intended)
- ~ 10 nb/(sr·MeV) peak expected for $(V_0, W_0) = (-50, -10)$ MeV is not in conflict with present data

Comparison with theoretical spectra

Analysis of possible scale μ for theoretically-calculated spectrum

- fit function: $\mu \times (d^2\sigma/d\Omega dE)^{\text{theory} \times \text{resolution}} + \text{Pol3}(E; p_0, p_1, p_2, p_3)$
- upper limit of μ at 95% C.L.



H. Nagahiro *et al.*,
PRC 87, 045201 (2013)

Comparison with theoretical spectra

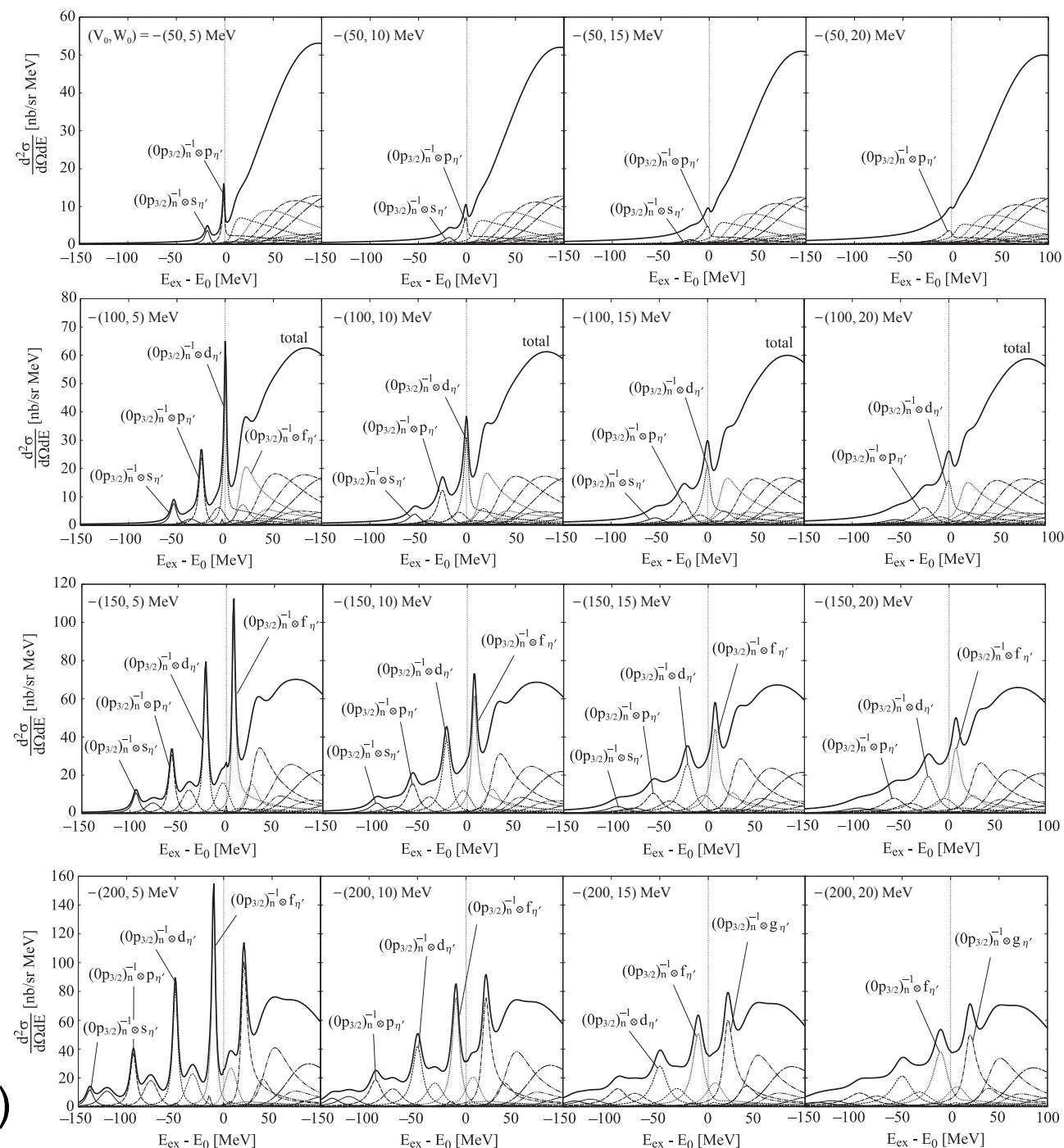
Analysis of possible scale μ for theoretically-calculated spectrum

- fit function: $\mu \times (d^2\sigma/d\Omega dE)^{\text{theory} \times \text{resolution}} + \text{Pol3}(E; p_0, p_1, p_2, p_3)$
- upper limit of μ at 95% C.L.

for various sets of potential (V_0, W_0)

$$-200 \text{ MeV} \leq V_0 \leq -50 \text{ MeV}$$

$$-25 \text{ MeV} \leq W_0 \leq -5 \text{ MeV}$$



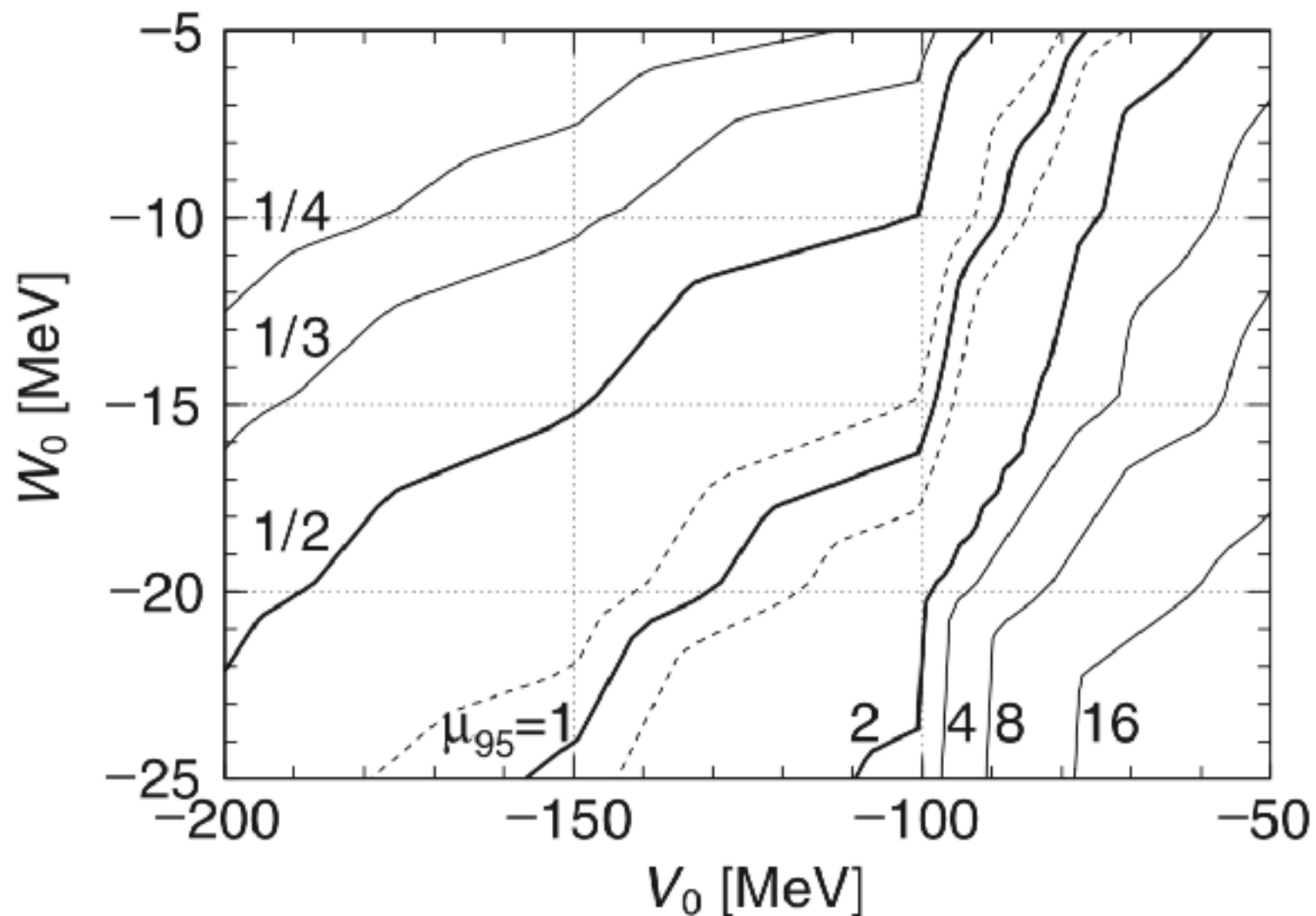
H.Nagahiro *et al.*,
PRC 87, 045201 (2013)

Comparison with theoretical spectra

Analysis of possible scale μ for theoretically-calculated spectrum

- fit function: $\mu \times (d^2\sigma/d\Omega dE)^{\text{theory} \times \text{resolution}} + \text{Pol3}(E; p_0, p_1, p_2, p_3)$
- upper limit of μ at 95% C.L.

upper limit of μ (contour plot)



$$V_{\eta'} = (V_0 + iW_0) \frac{\rho(r)}{\rho_0}$$

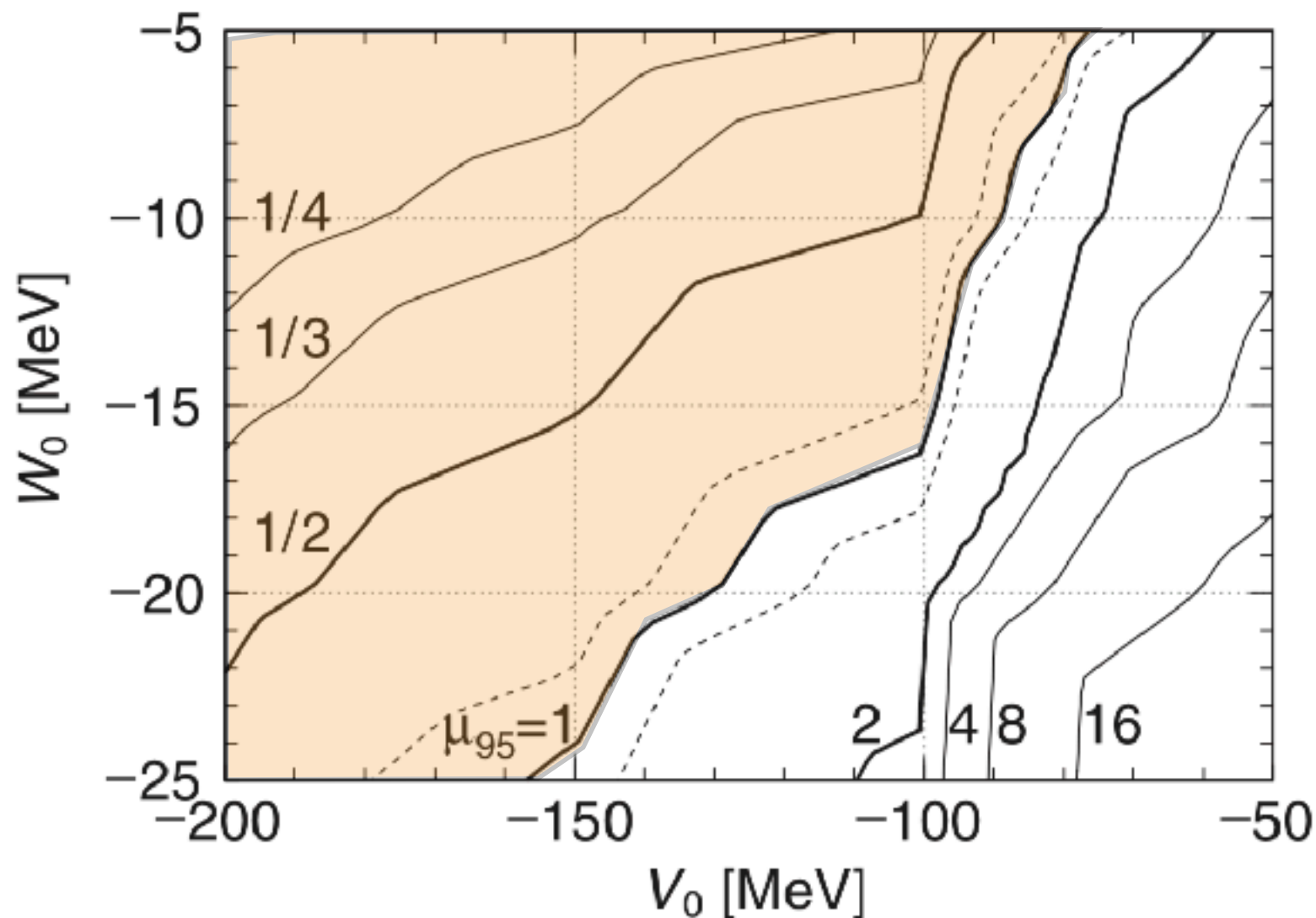
Y. K. Tanaka, K. Itahashi, H. Fujioka *et al*,
PRC 97, 015202 (2018)

Comparison with theoretical spectra

Analysis of possible scale μ for theoretically-calculated spectrum

- fit function: $\mu \times (d^2\sigma/d\Omega dE)^{\text{theory} \times \text{resolution}} + \text{Pol3}(E; p_0, p_1, p_2, p_3)$
- upper limit of μ at 95% C.L.

upper limit of μ (contour plot)



$$V_{\eta'} = (V_0 + iW_0) \frac{\rho(r)}{\rho_0}$$

(V_0, W_0) with $\mu_{\text{limit}} < 1$ is excluded under this comparison

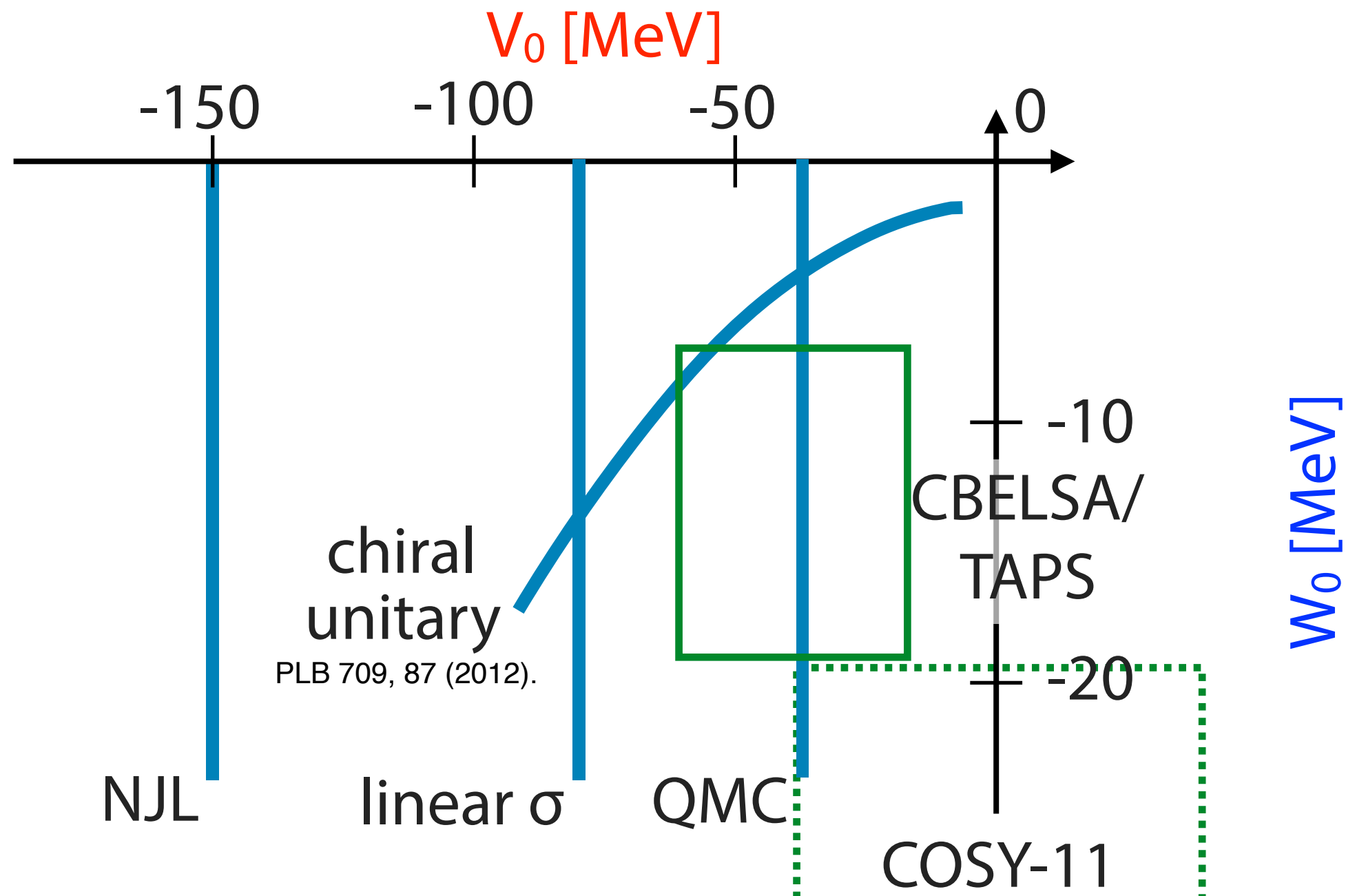
$|V_0| \sim 150$ MeV (NJL)
for $|W_0| \sim 10$ MeV

Y. K. Tanaka, K. Itahashi, H. Fujioka *et al*,
PRC 97, 015202 (2018)

Comparison with theoretical spectra

Analysis of possible scale μ for theoretically-calculated spectrum

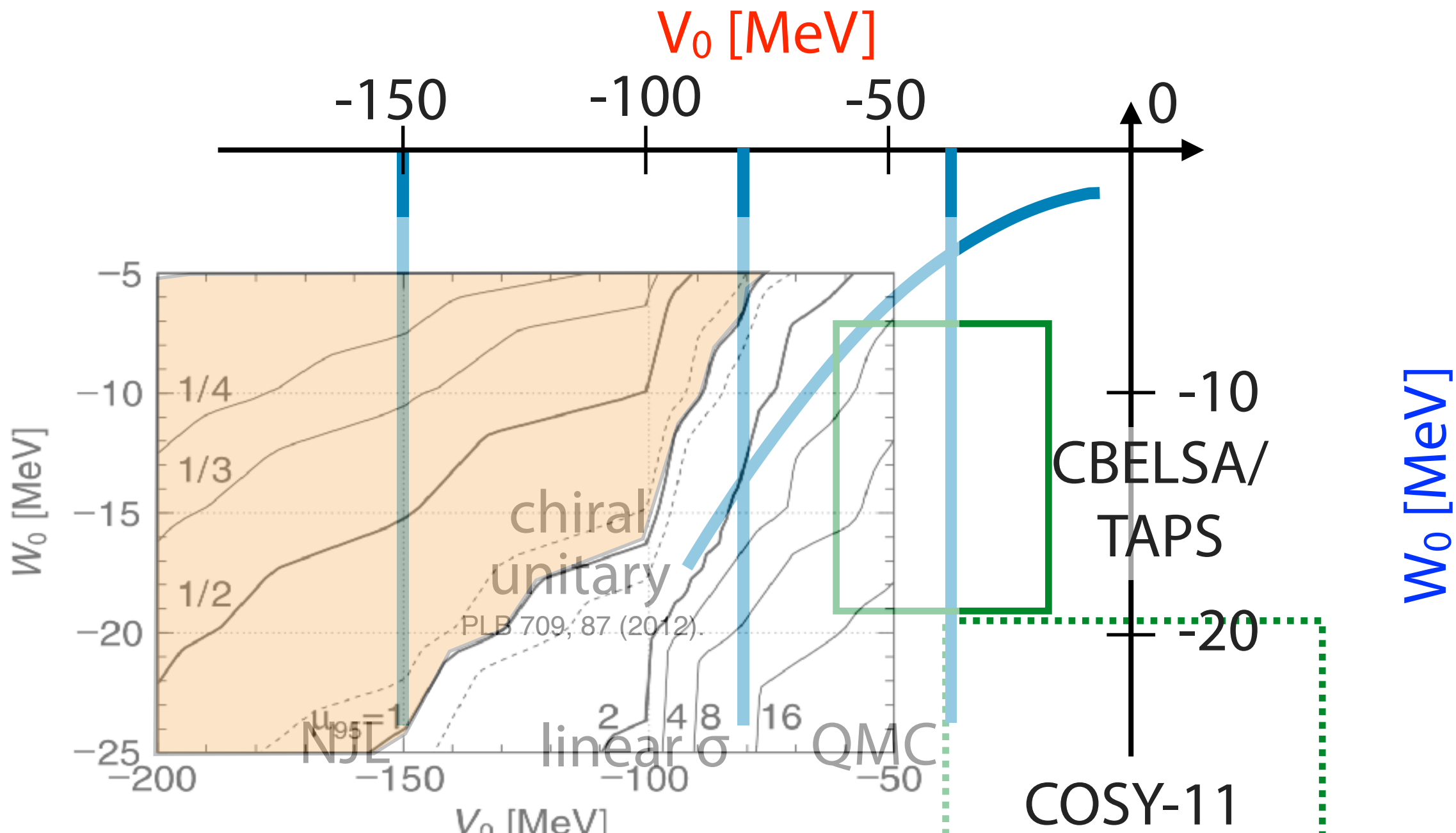
- fit function: $\mu \times (d^2\sigma/d\Omega dE)^{\text{theory} \times \text{resolution}} + \text{Pol3}(E; p_0, p_1, p_2, p_3)$
- upper limit of μ at 95% C.L.



Comparison with theoretical spectra

Analysis of possible scale μ for theoretically-calculated spectrum

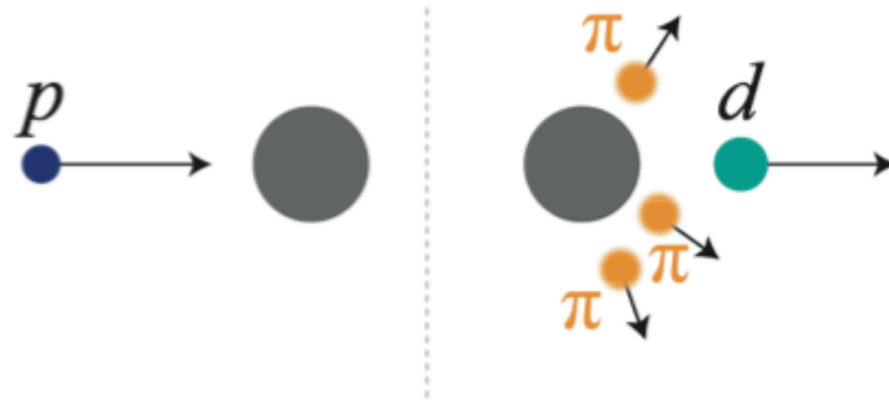
- fit function: $\mu \times (d^2\sigma/d\Omega dE)^{\text{theory} \times \text{resolution}} + \text{Pol3}(E; p_0, p_1, p_2, p_3)$
- upper limit of μ at 95% C.L.



Semi-exclusive measurement by tagging decay

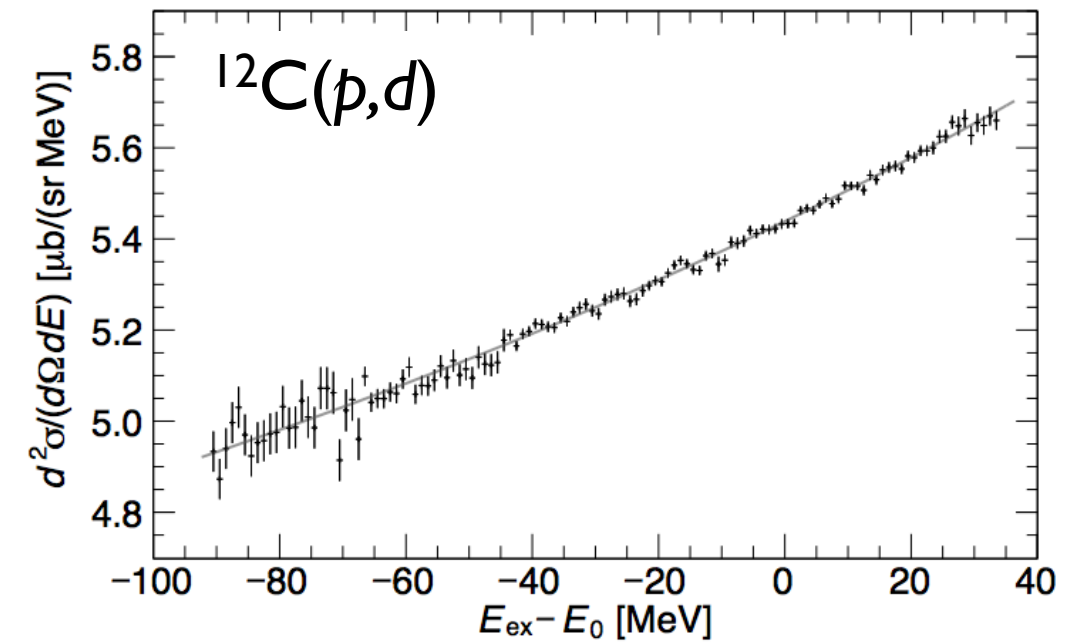
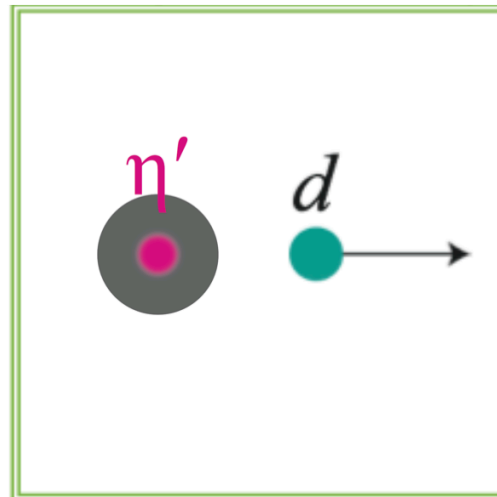
Background

multi- π
production



Signal

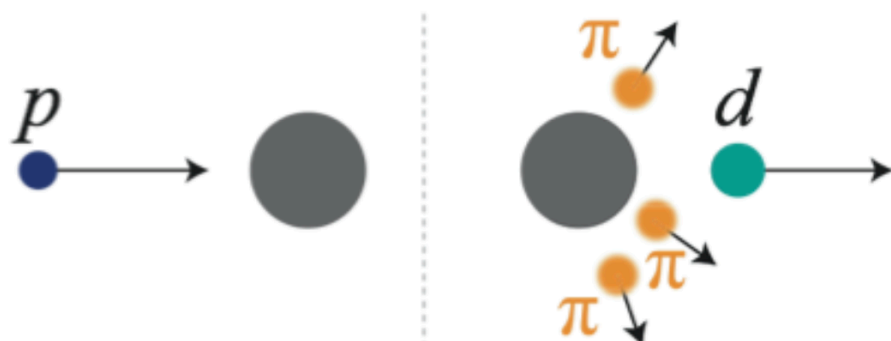
η' -mesic nuclei
formation



Semi-exclusive measurement by tagging decay

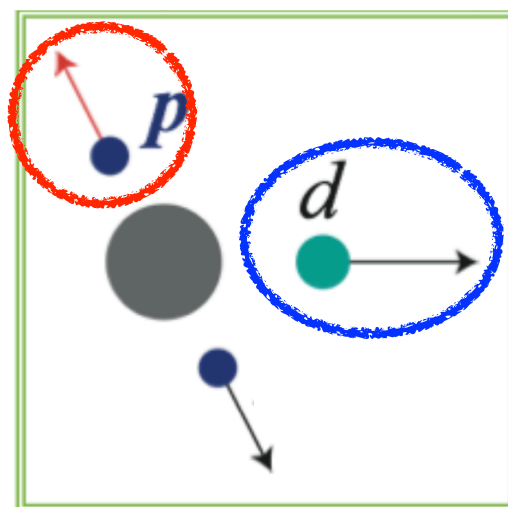
Background

multi- π
production



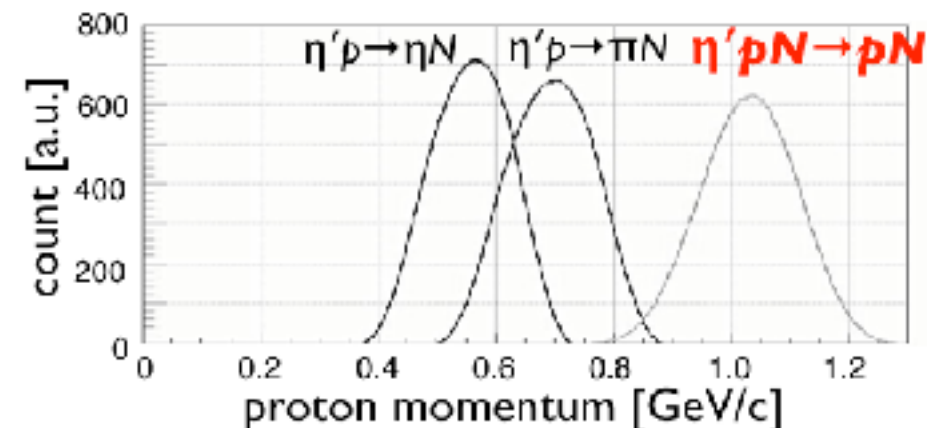
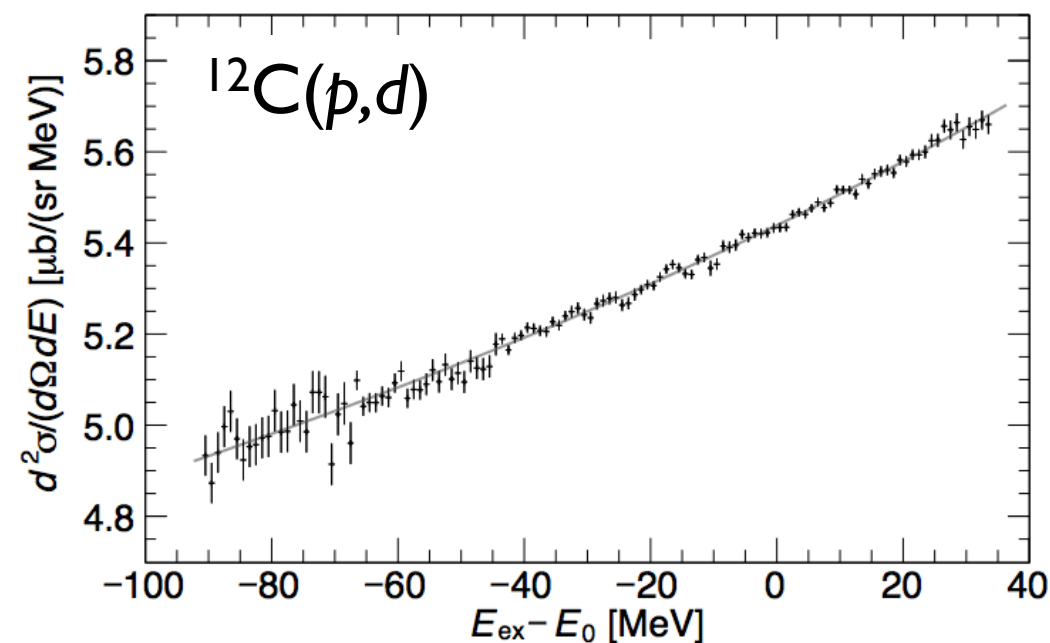
Signal

η' -mesic nuclei
formation



$\eta' NN \rightarrow NN, \eta' N \rightarrow \eta N, \pi N$

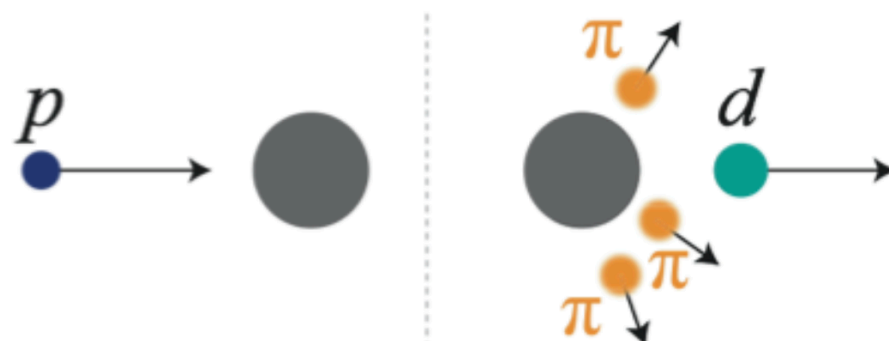
Coincidence measurement of
decay proton and **forward deuteron**



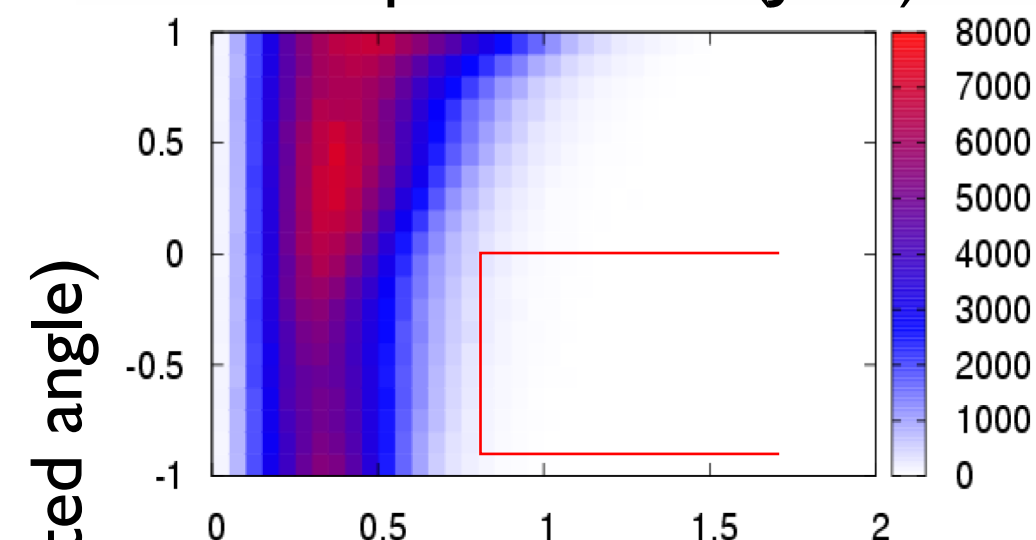
Semi-exclusive measurement by tagging decay

Background

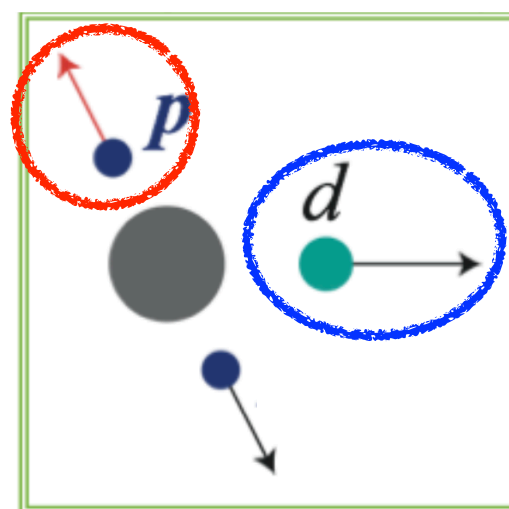
multi- π
production



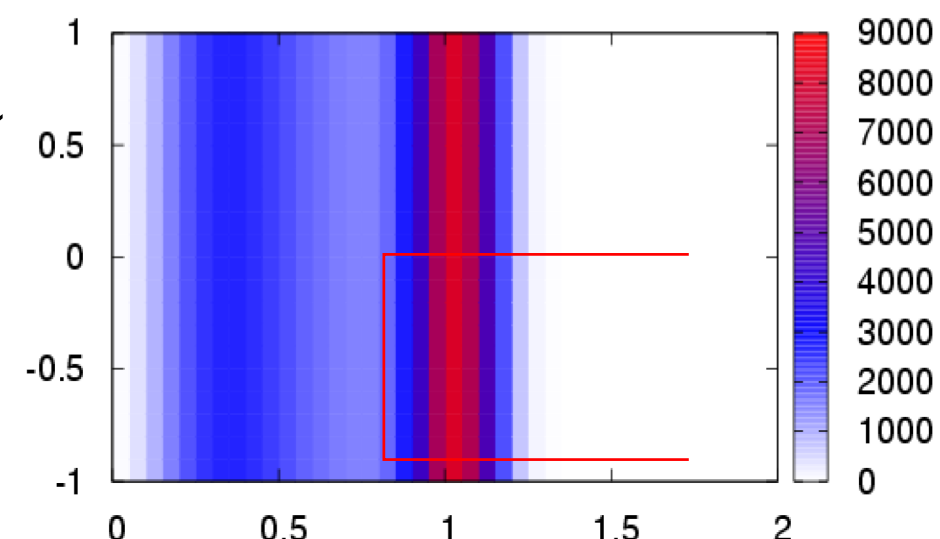
Calculation by microscopic
transport model (JAM)



Signal
 η' -mesic nuclei
formation



$\eta' NN \rightarrow NN$



Proton Momentum [GeV/c]

Coincidence measurement of
decay proton and **forward deuteron**

Y. Higashi

→ factor ~ 100 improvement
in Signal / BG ratio

Proposal of $^{12}\text{C}(p, dp)$ reaction measurement

SEARCH FOR η' -MESIC NUCLEI IN $^{12}\text{C}(p, dp)$ REACTION

Spokesperson: K. Itahashi

Co-spokesperson: Y.K. Tanaka

η -PRiME Collaboration includes

K. Itahashi¹, Y. K. Tanaka², Y. Ayyad³, S. Bagchi², J. Benlliure⁴, T. Dickel², H. Fujioka⁵, H. Geissel^{2,6}, F. Goldenbaum⁷, C. Guo⁸, E. Gutz⁶, E. Haettner², M. N. Harakeh⁹, R. S. Hayano¹⁰, S. Hirenzaki¹¹, C. Hornung⁶, Y. Igarashi¹², N. Ikeno¹³, M. Iwasaki¹, D. Jido¹⁴, N. Kalantar-Nayestanaki⁹, R. Kanungo¹⁵, B. Kindler², R. Knöbel^{2,6}, D. Kostyleva², N. Kurz², N. Kuzminchuk², B. Lommel², V. Metag⁶, P. Moskal¹⁶, I. Mukha², T. Nagae⁵, H. Nagahiro¹¹, M. Nanova⁶, T. Nishi¹, H. J. Ong¹⁷, H. Outa¹, S. Pietri², W. Plass², A. Prochazka², S. Purushothaman², C. Rappold², M. P. Reiter², J. Ritman⁷, J. L. Rodríguez-Sánchez⁴, O. Rundel¹⁶, T. Saito², C. Scheidenberger^{2,6}, H. Simon², B. Sitar¹⁸, M. Skurzok¹⁶, P. Strmen¹⁸, B. Sun⁸, K. Suzuki¹⁹, I. Szarka¹⁸, M. Takechi²⁰, I. Tanihata^{8,17}, S. Terashima⁸, Y. N. Watanabe¹⁰, H. Weick², E. Widmann¹⁹, J. S. Winfield², X. Xu⁸, and J. Zhao⁸.

¹RIKEN Nishina Center, ²GSI Helmholtzzentrum für Schwerionenforschung, ³LBNL, ⁴Universidade de Santiago de Compostela, ⁵Kyoto University, ⁶Universität Giessen, ⁷IKP, FZ Jülich, ⁸Beihang University, ⁹KVI-CART, University of Groningen, ¹⁰The University of Tokyo, ¹¹Nara Women's University, ¹²KEK, ¹³Tottori University, ¹⁴Tokyo Metropolitan University, ¹⁵Saint Mary's University, ¹⁶Jagiellonian University, ¹⁷RCNP, Osaka University, ¹⁸Comenius University Bratislava, ¹⁹Stefan-Meyer-Institut für subatomare Physik, and ²⁰Niigata University.

Abstract

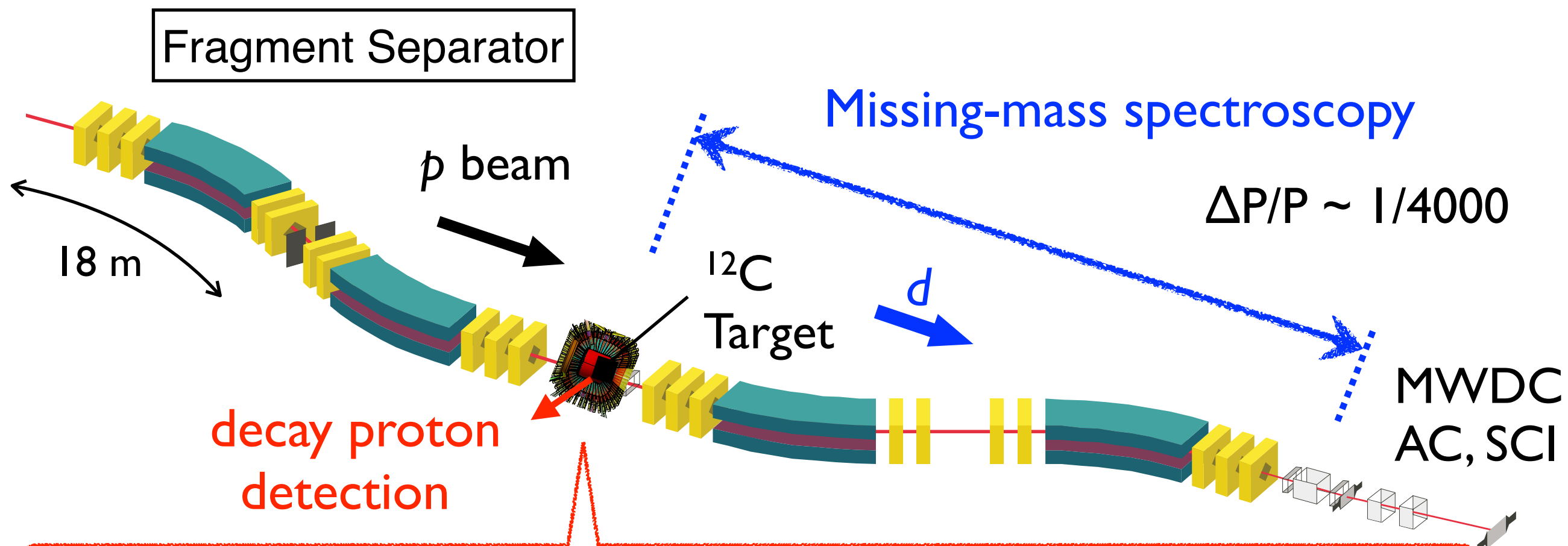
We propose to measure excitation spectrum of ^{11}C near the η' -production threshold in order to search for narrow structures due to formation of η' -mesic nuclei, bound systems of an η' meson and a nucleus. The expected spectra vary according to the assumed η' -nucleus interaction for which we have very limited knowledge. We have a concrete and strategic experimental

approved
proposal
in GPAC (2017)

using WASA central
detector at FRS-GSI

S490 experiment at GSI (scheduled in 2022 Feb.--Mar.)

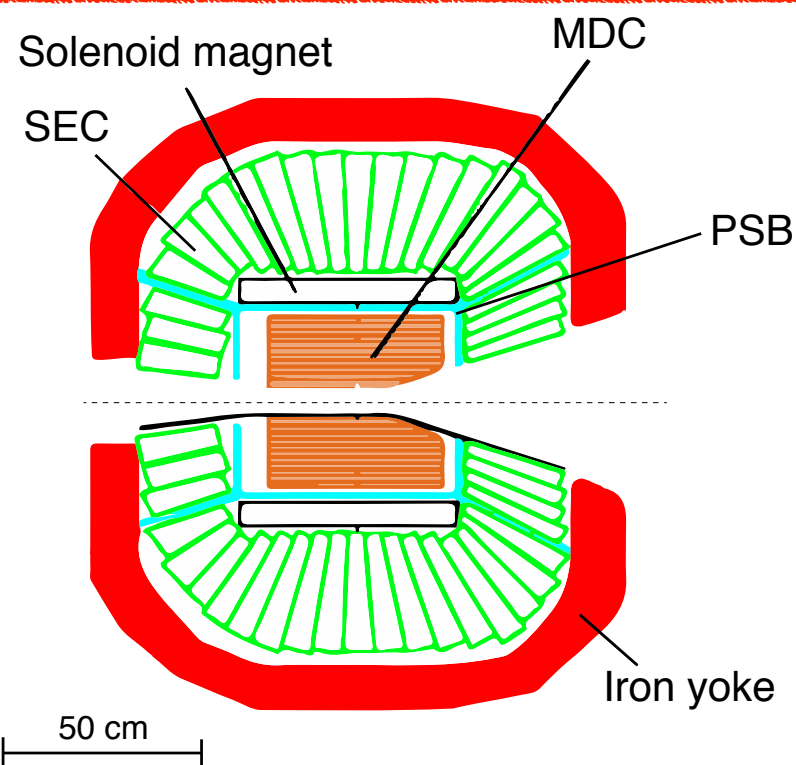
Experimental setup with WASA at FRS



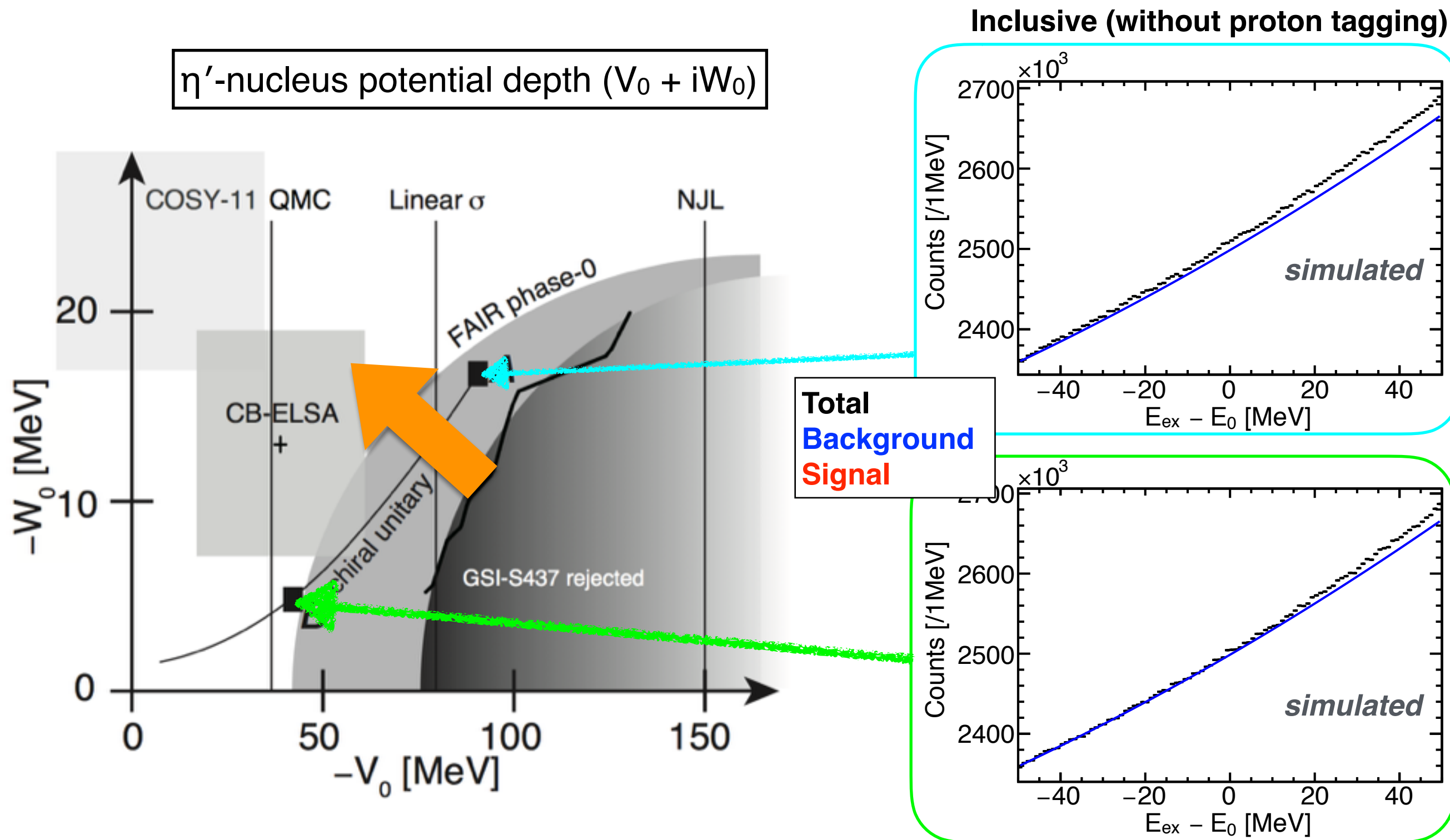
WASA Central Detector

operated @COSY
(2006–2014)

- ◇ Superconducting solenoid magnet (~ 1.3 T)
- ◇ Mini drift chamber (MDC) for tracking
- ◇ Plastic scintillator barrel (PSB) for $\Delta E, \text{TOF}$
- ◇ CsI Electromagnetic calorimeter (SEC)



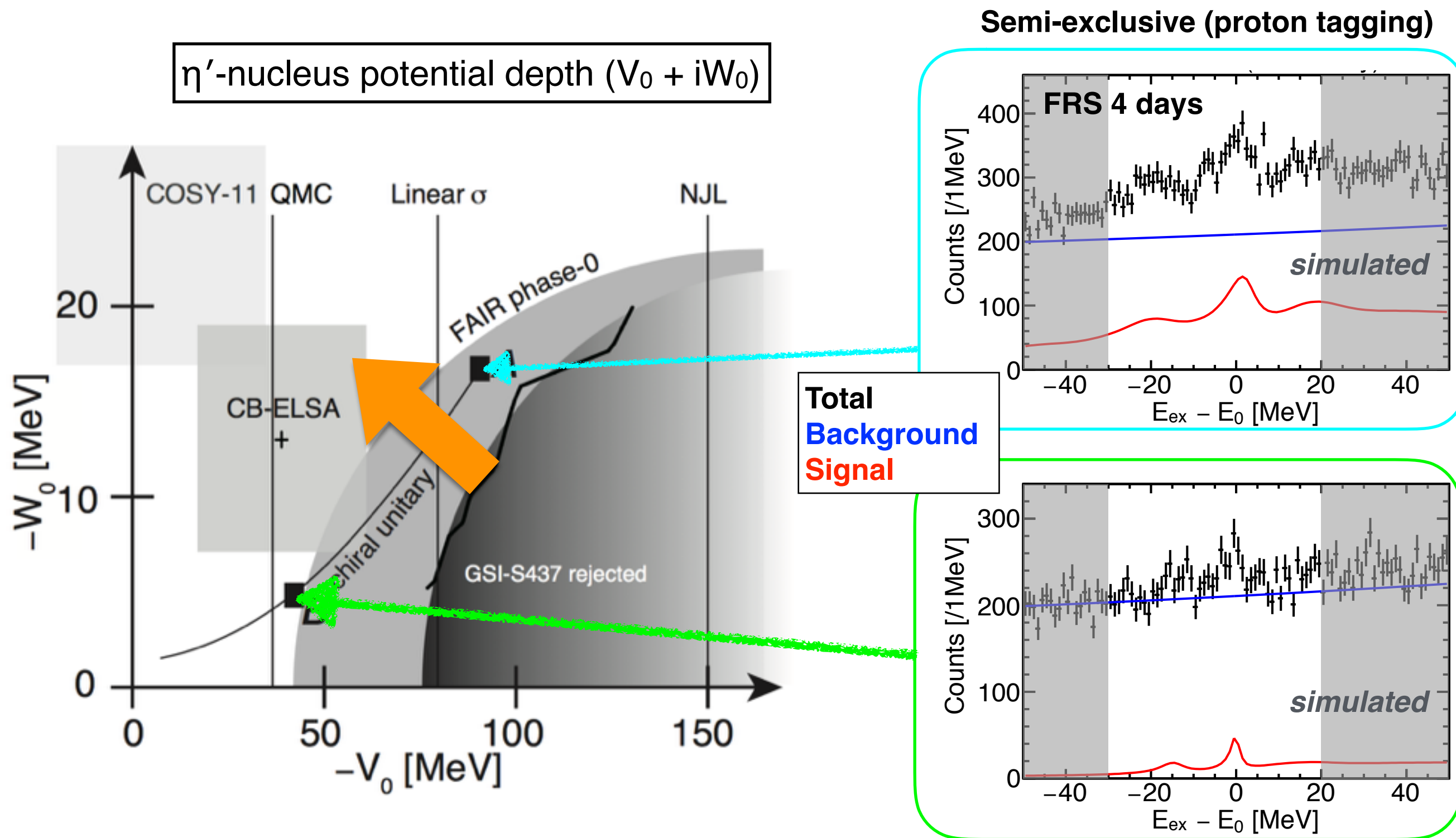
Expected spectra in semi-exclusive measurement



◇ Assumed branching ratio (to $\eta' NN \rightarrow NN$) $\sim 50\%$

H.Nagahiro *et al.*, PRC 87, 045201 (2013), Phys. Lett. B 709, 87 (2012).

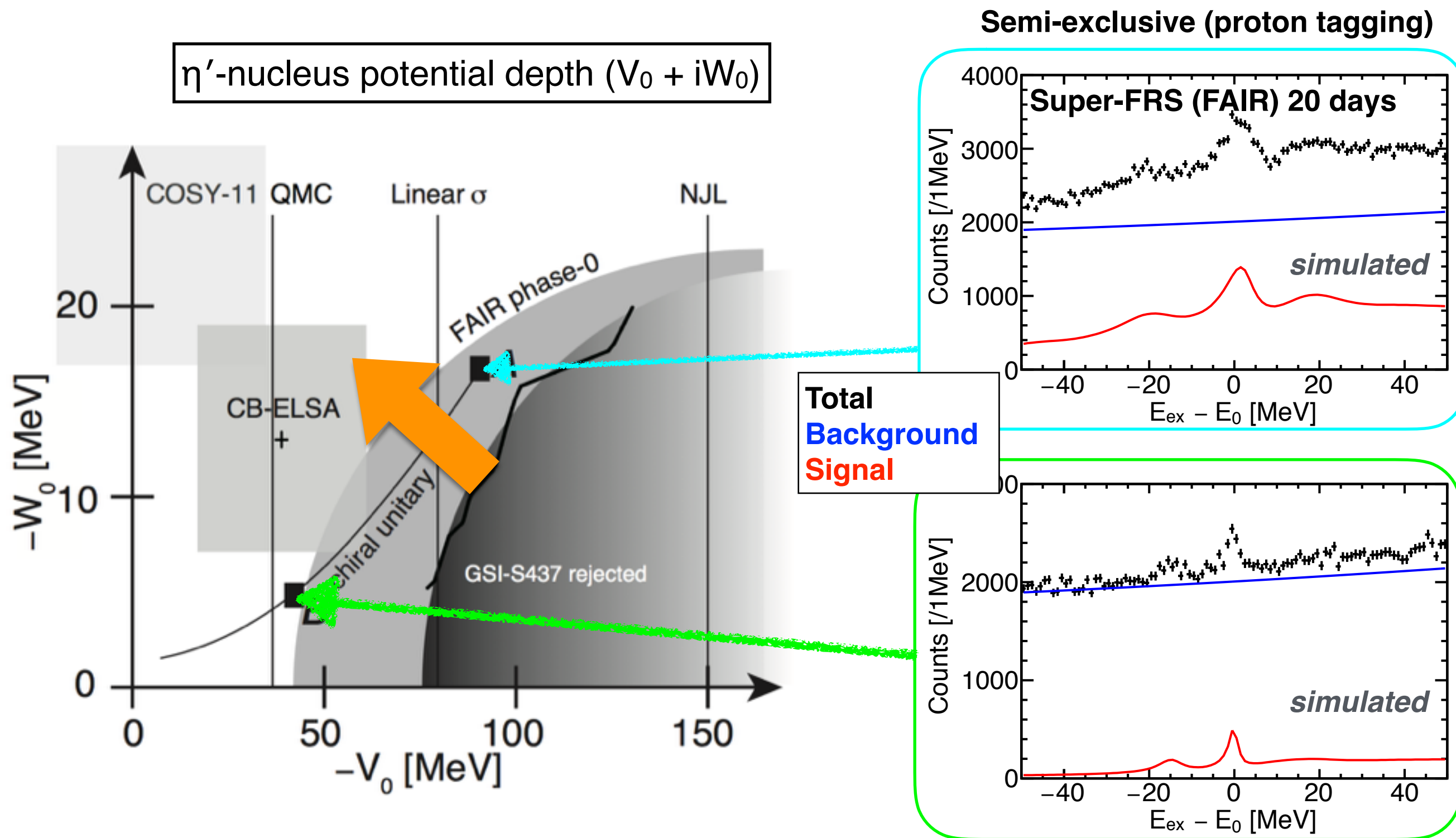
Expected spectra in semi-exclusive measurement



◇ Assumed branching ratio (to $\eta' NN \rightarrow NN$) $\sim 50\%$

H.Nagahiro *et al.*, PRC 87, 045201 (2013), Phys. Lett. B 709, 87 (2012).

Expected spectra in semi-exclusive measurement



◇ Assumed branching ratio (to $\eta' NN \rightarrow NN$) $\sim 50\%$

H.Nagahiro *et al.*, PRC 87, 045201 (2013), Phys. Lett. B 709, 87 (2012).

Transportation of WASA from COSY to GSI

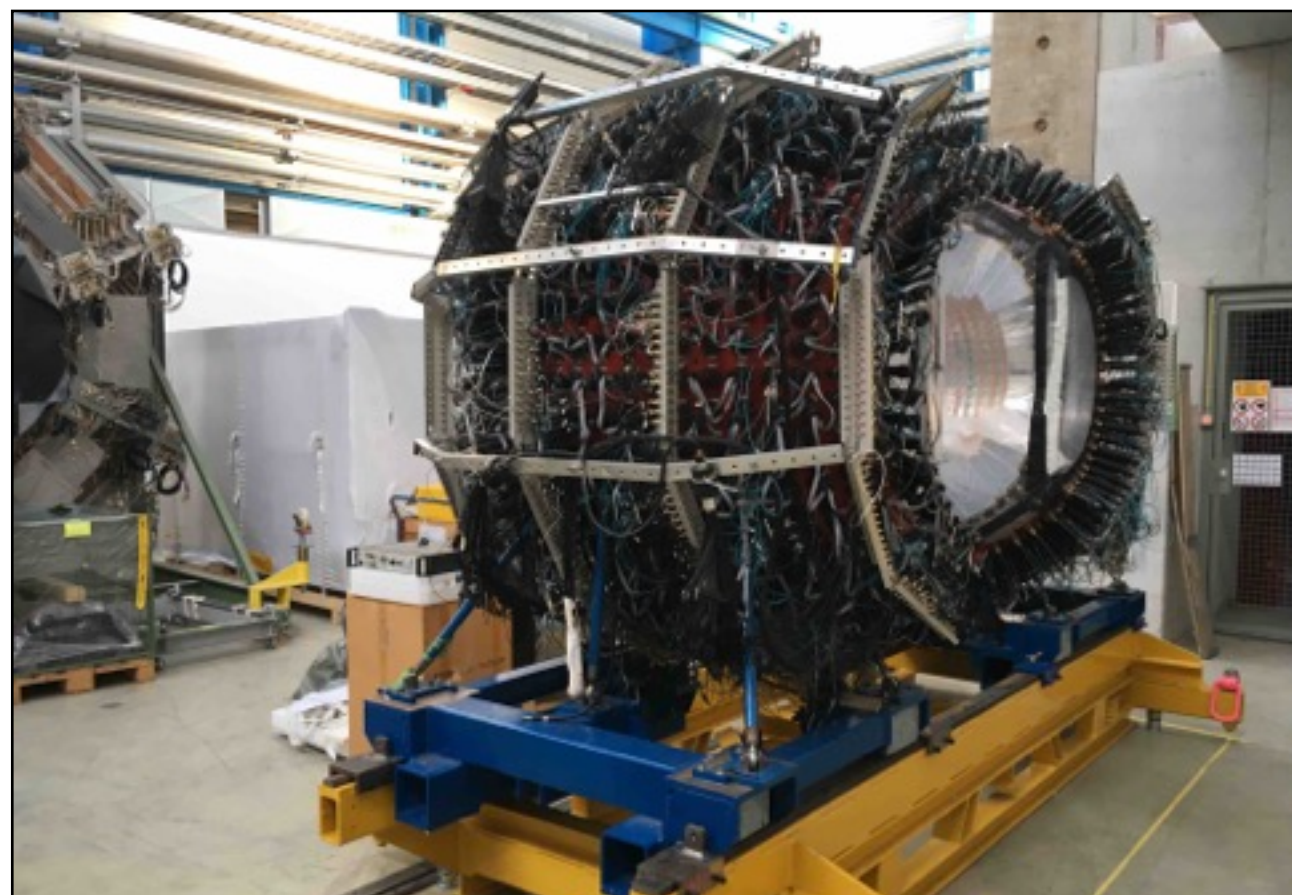


Transportation of all items
needed for FAIR phase-0

completed in 2019/March

@ COSY, FZ-Jülich

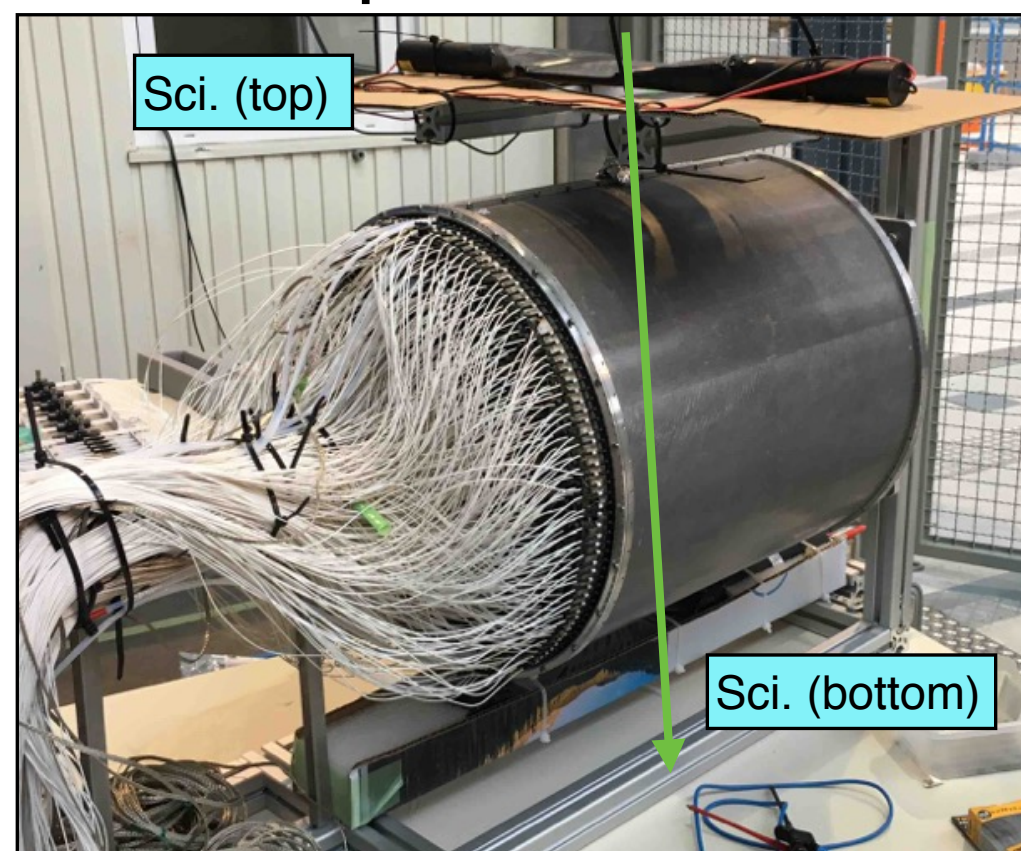
Testing area @ GSI



Testing WASA-MDC at FRS/GSI

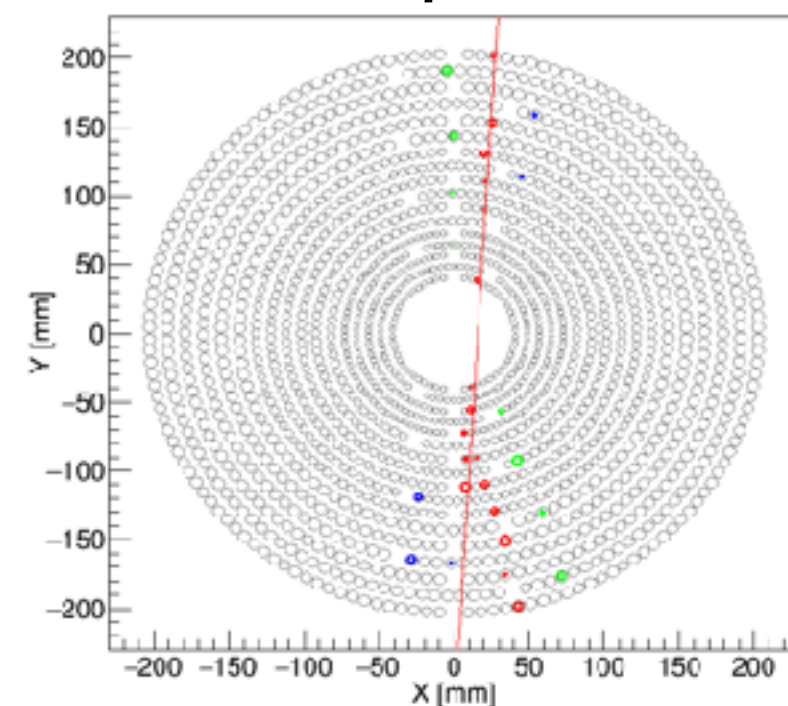
- ◇ Drift chambers base on straw tubes for charged particle tracking in the solenoid magnet
- ◇ 17 cylindrical layers (9 layers parallel to z axis, 8 layers “stereo”), in total 1738 channels
- ◇ Cosmic-ray test has been already performed in 2018-2019

test setup at WASA container

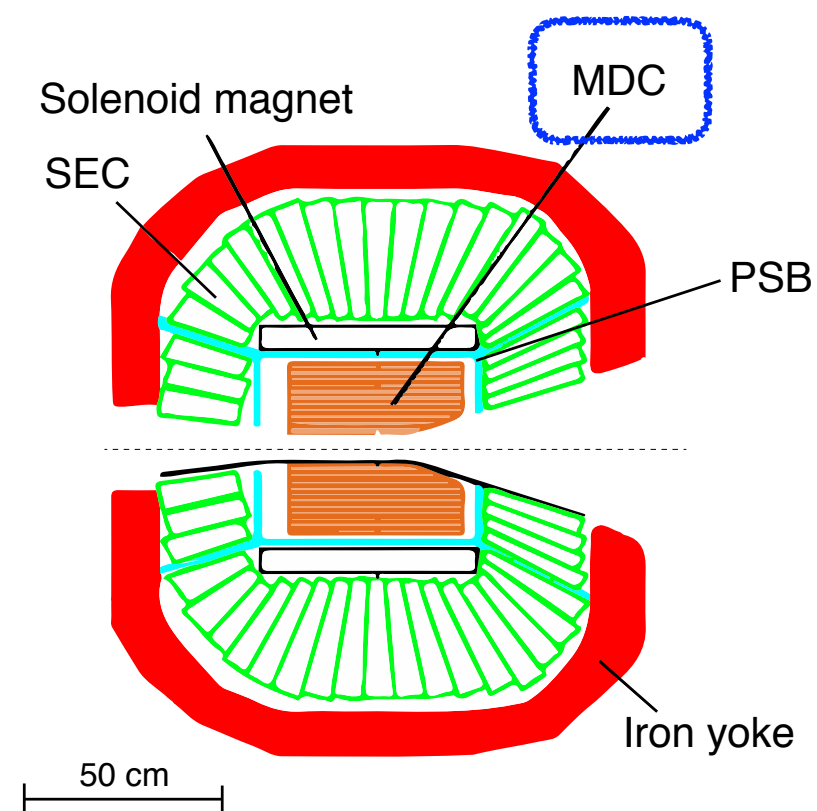


Trigger = Scintillator (Top and Bottom) coincidence

x-y projection of cosmic particles



axial / stereo(+) / stereo(-)

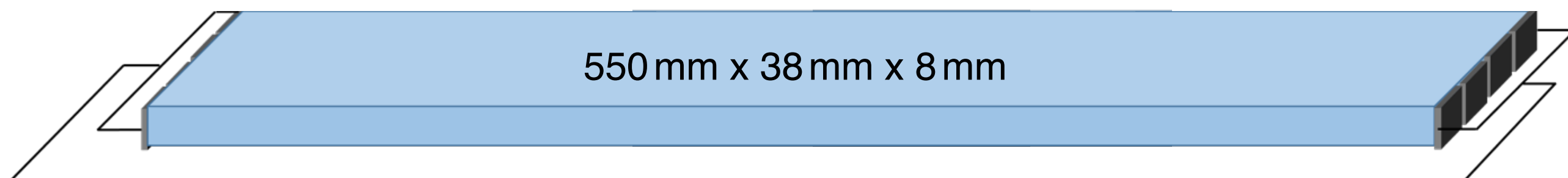


Upgrading PSB (plastic scintillator barrel)

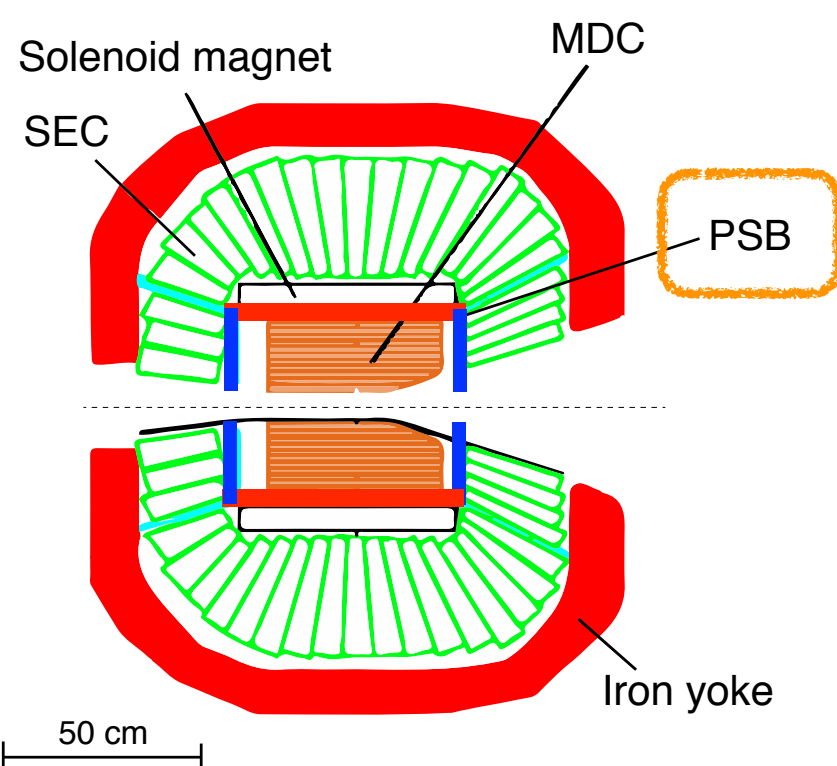
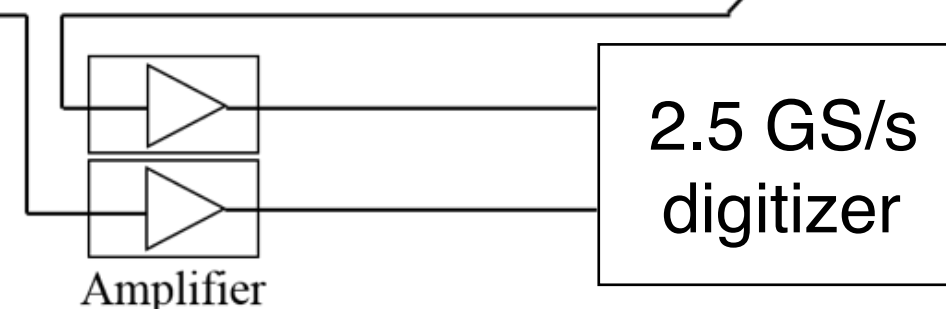
Prototype: MPPC readout at both sides to improve time resolution

ELJEN-EJ230 plastic (attenuation $L = 1.2$ m)

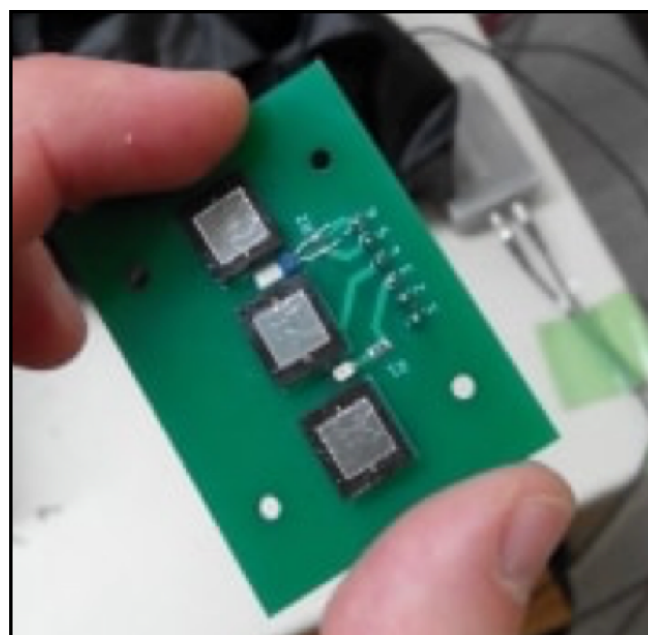
MPPC (Hamamatsu S13360), 6×6 mm²



R. Sekiya, Y.K.Tanaka, K.Itahashi, V. Drozd,
H. Fujioka, S. Y. Matsumoto, T. R. Saito, K. Suzuki,



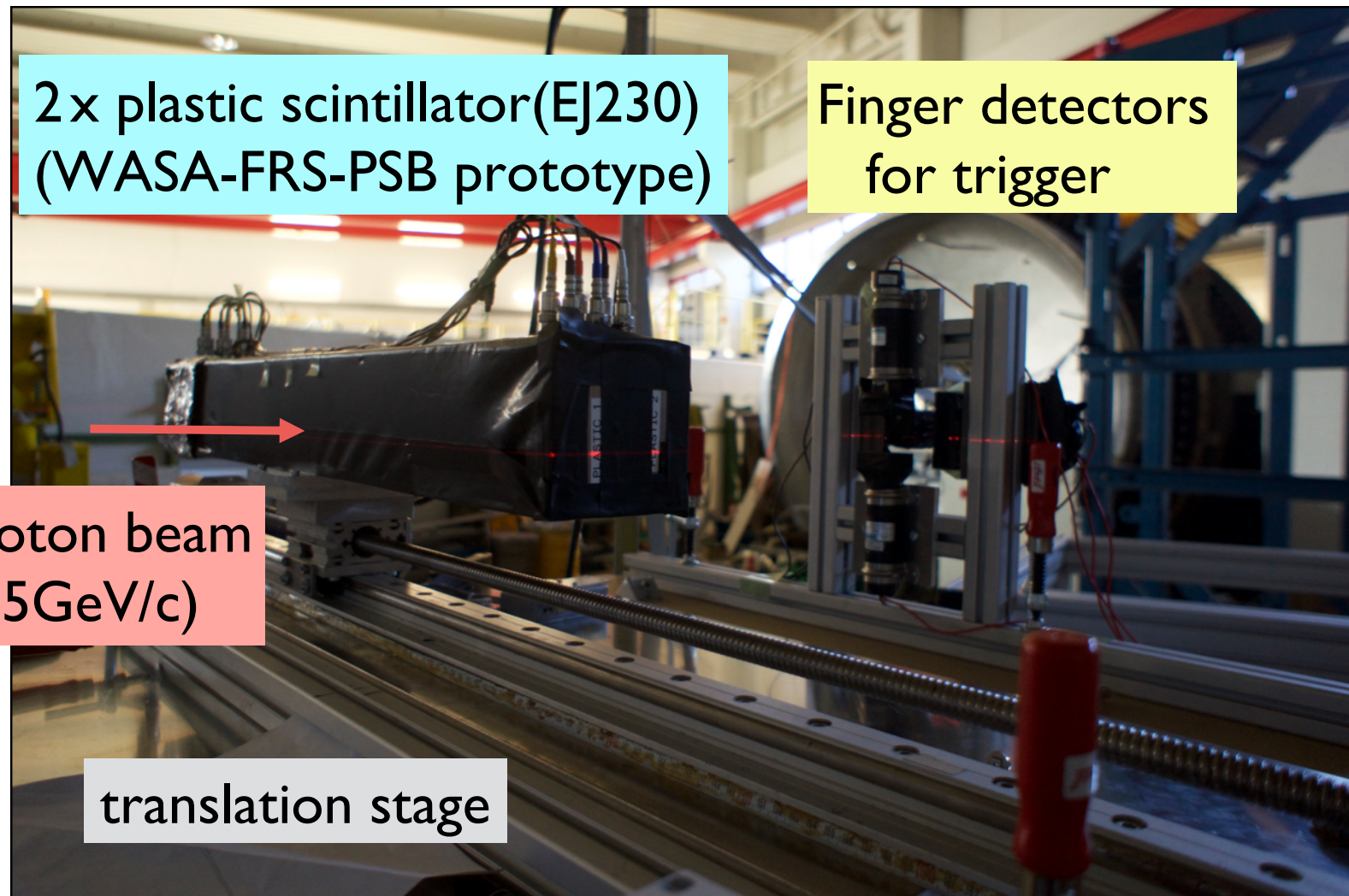
MPPC board



Amplifier

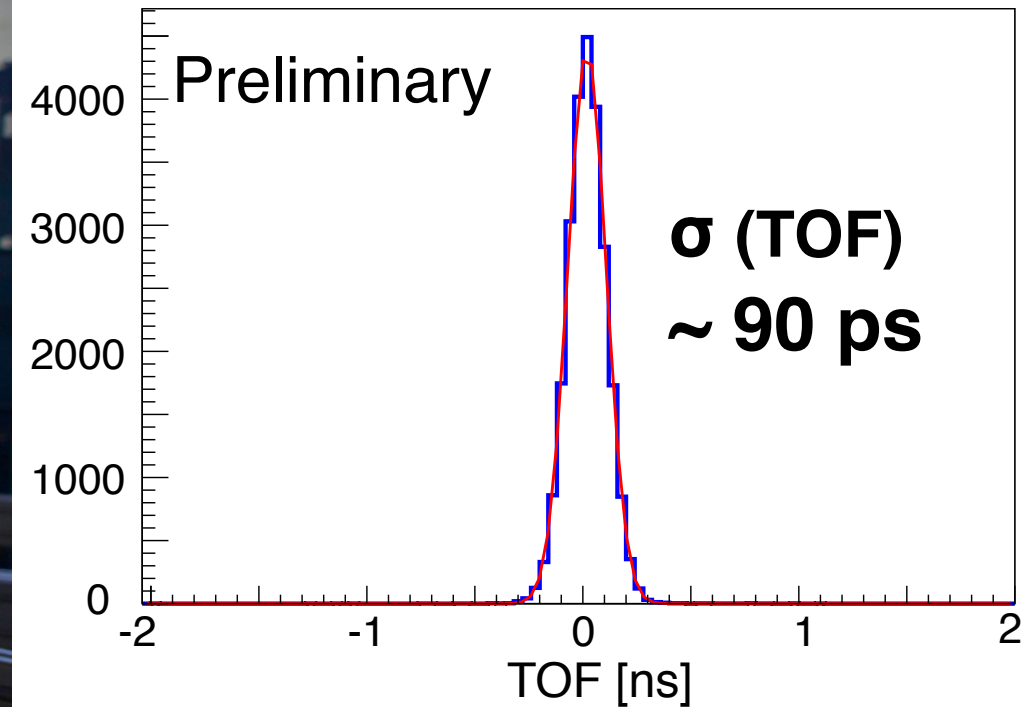


Test of new PSB prototype using proton beam



2019 Feb., at COSY, Jülich

Example:
3MPPC in series, 0° , $V_{\text{over}} = 5\text{V}$



$\rightarrow \sigma_{\text{PSB}} \sim 60$ ps
for 2.5 GeV/c proton

We performed systematic studies of the time resolution by changing ...

- ◇ Bias voltage
- ◇ Number of connected SiPMs
- ◇ Hit position
- ◇ Incident beam angles
- ◇ Readout electronics

WASA Superconducting Solenoid Magnet

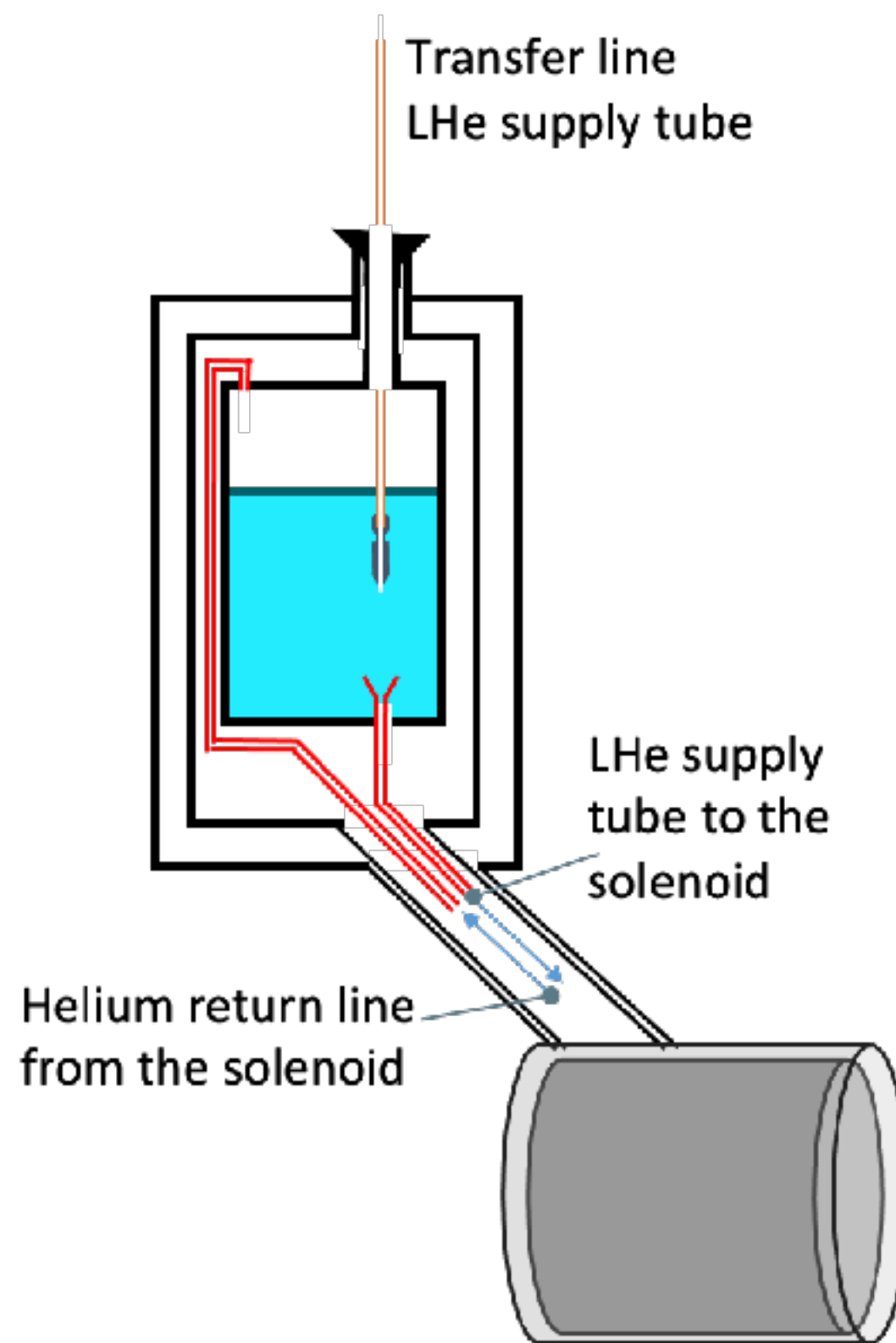
WASA solenoid magnet

- superconducting magnet, $B_{\max} \sim 1.3 \text{ T}$
- cooling with Liquid He, 4.5 K

Superconducting coil	
Inner/outer radius [mm]	267.8 / 288.8
Superconductor (stabilizer)	NbTi/Cu (pure Al)
Total winding length	465 mm
Maximum central magnetic flux density, B_c	1.3 T
Field uniformity in the MDC	1.22 T $\pm 20\%$
Cooling	Liquid He, 4.5°K
Cryostat	
Material	Aluminium
Inner / outer radius [mm]	245 / 325
Overall length [mm]	555
SCS wall thickness (coil+cryostat) [radl]	0.18

Table 5: Main parameters of the superconducting coil and its cryostat.

PhD Thesis , R.Ruber



WASA Superconducting Solenoid Magnet

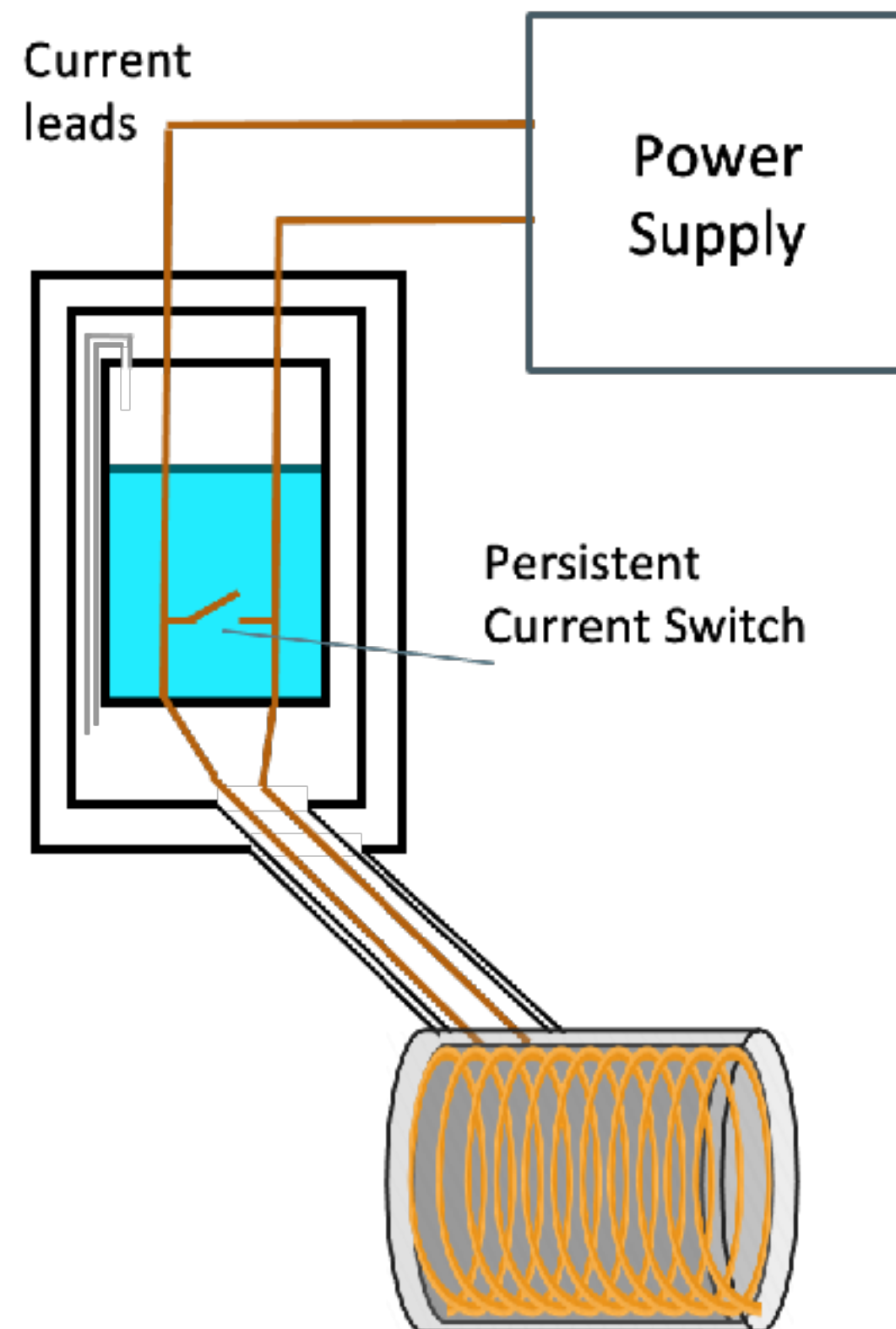
WASA solenoid magnet

- superconducting magnet, $B_{\max} \sim 1.3 \text{ T}$
- cooling with Liquid He, 4.5 K

Superconducting coil	
Inner/outer radius [mm]	267.8 / 288.8
Superconductor (stabilizer)	NbTi/Cu (pure Al)
Total winding length	465 mm
Maximum central magnetic flux density, B_c	1.3 T
Field uniformity in the MDC	1.22 T $\pm 20\%$
Cooling	Liquid He, 4.5°K
Cryostat	
Material	Aluminium
Inner / outer radius [mm]	245 / 325
Overall length [mm]	555
SCS wall thickness (coil+cryostat) [radl]	0.18

Table 5: Main parameters of the superconducting coil and its cryostat.

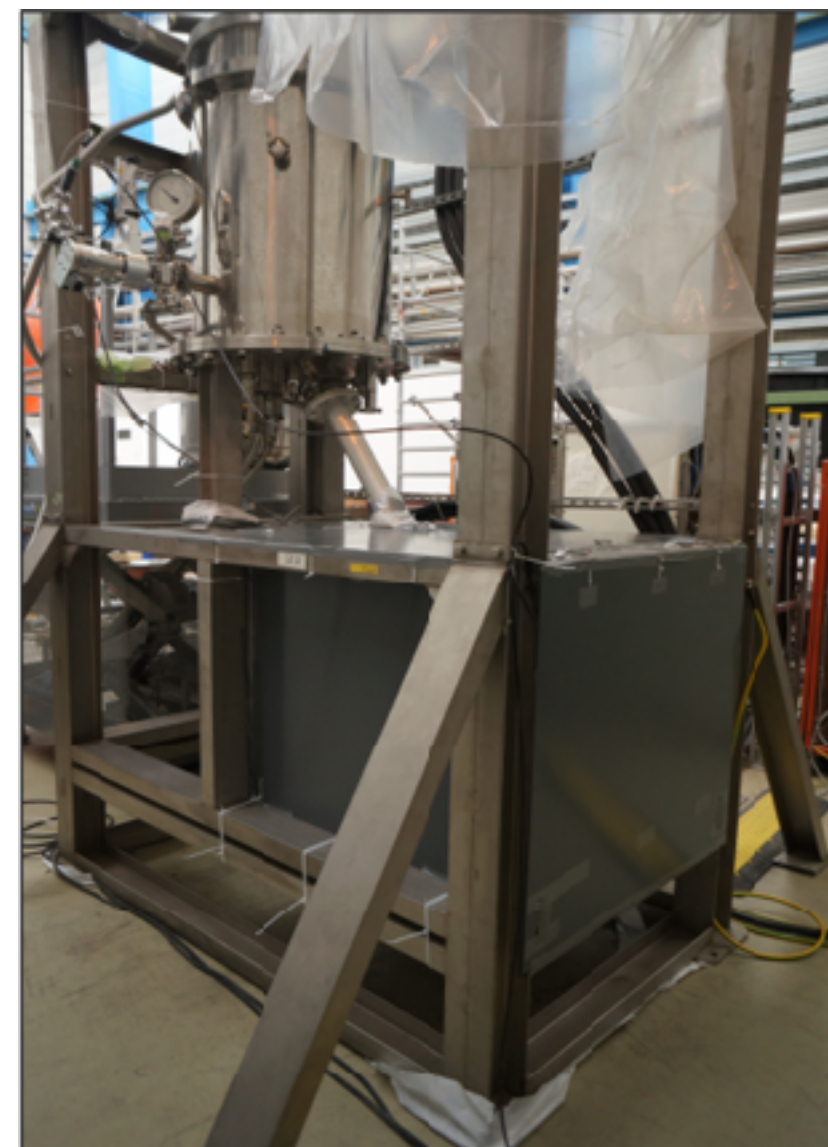
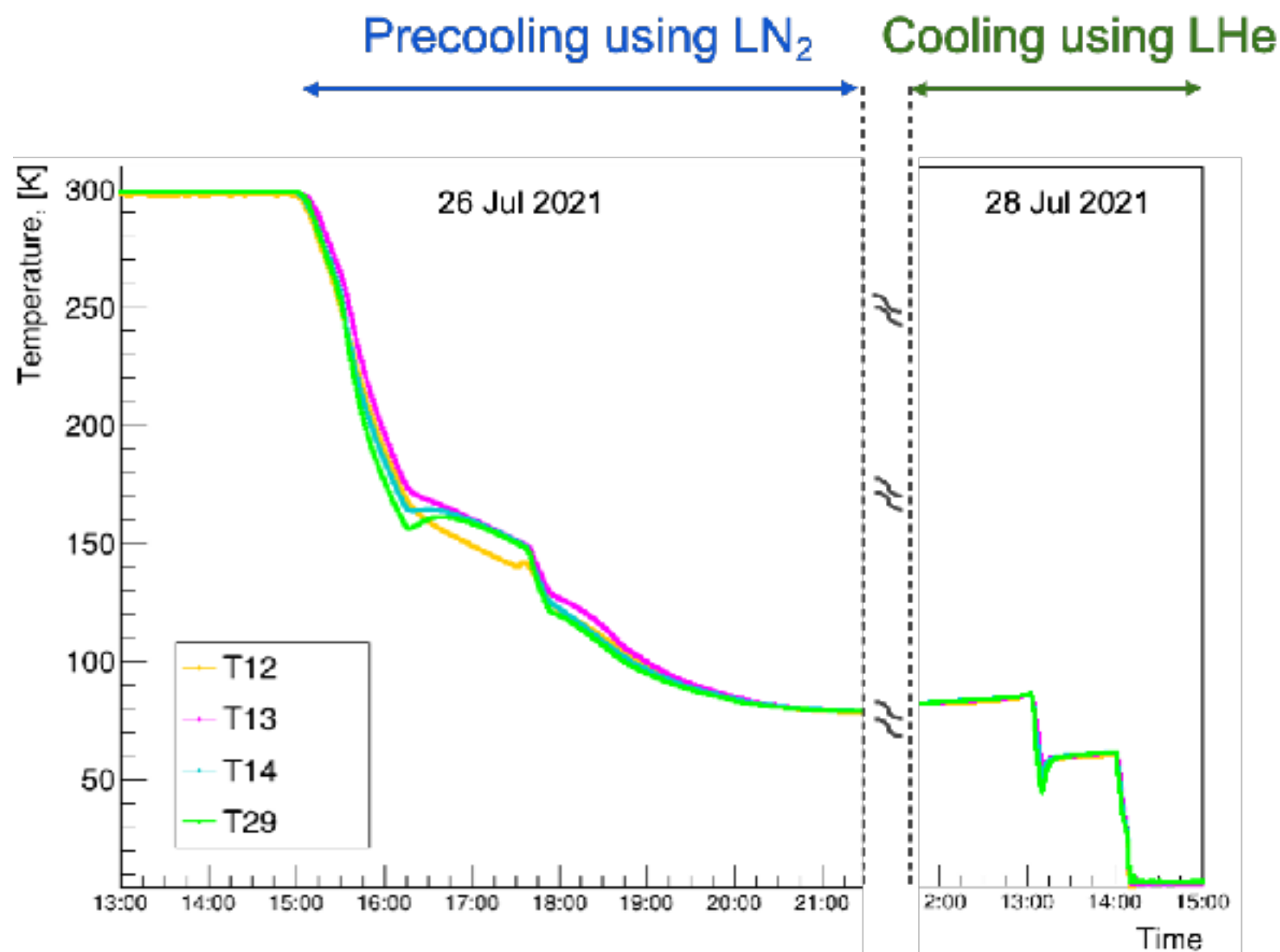
PhD Thesis , R.Ruber



Superconducting Solenoid Magnet

Test Phase at FOPI area (2019-2021)

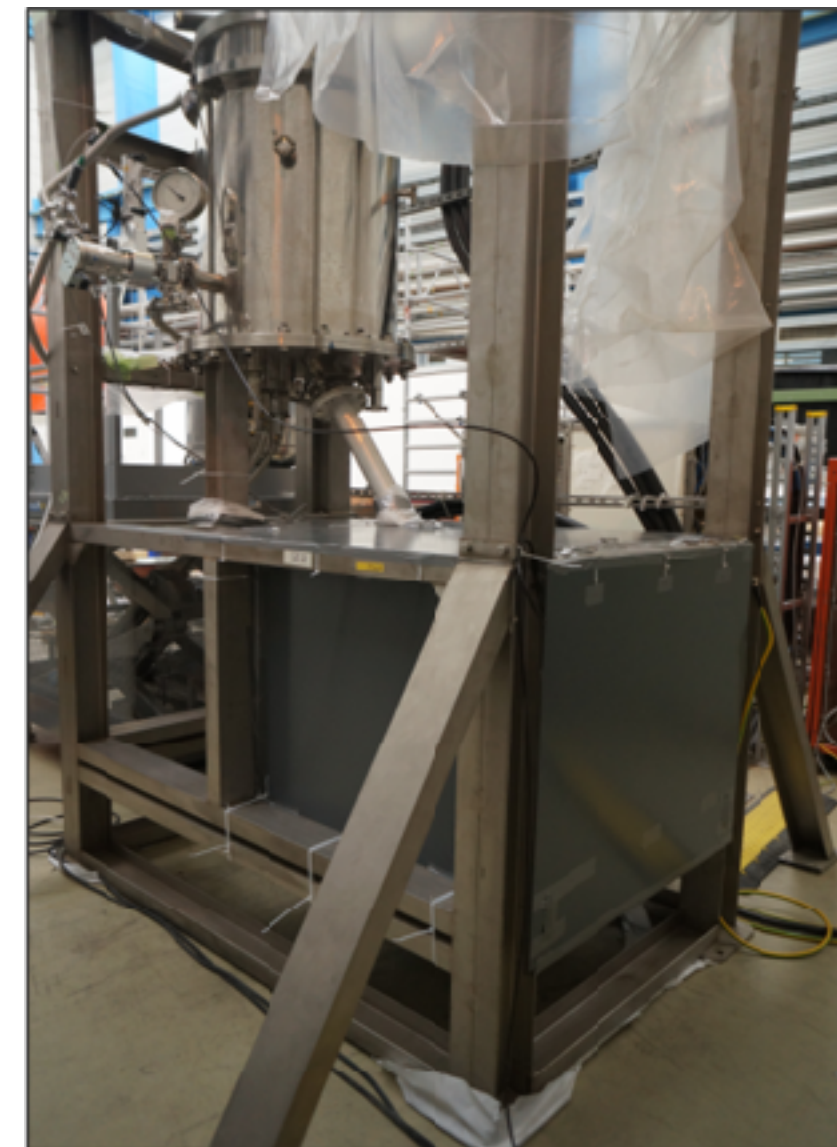
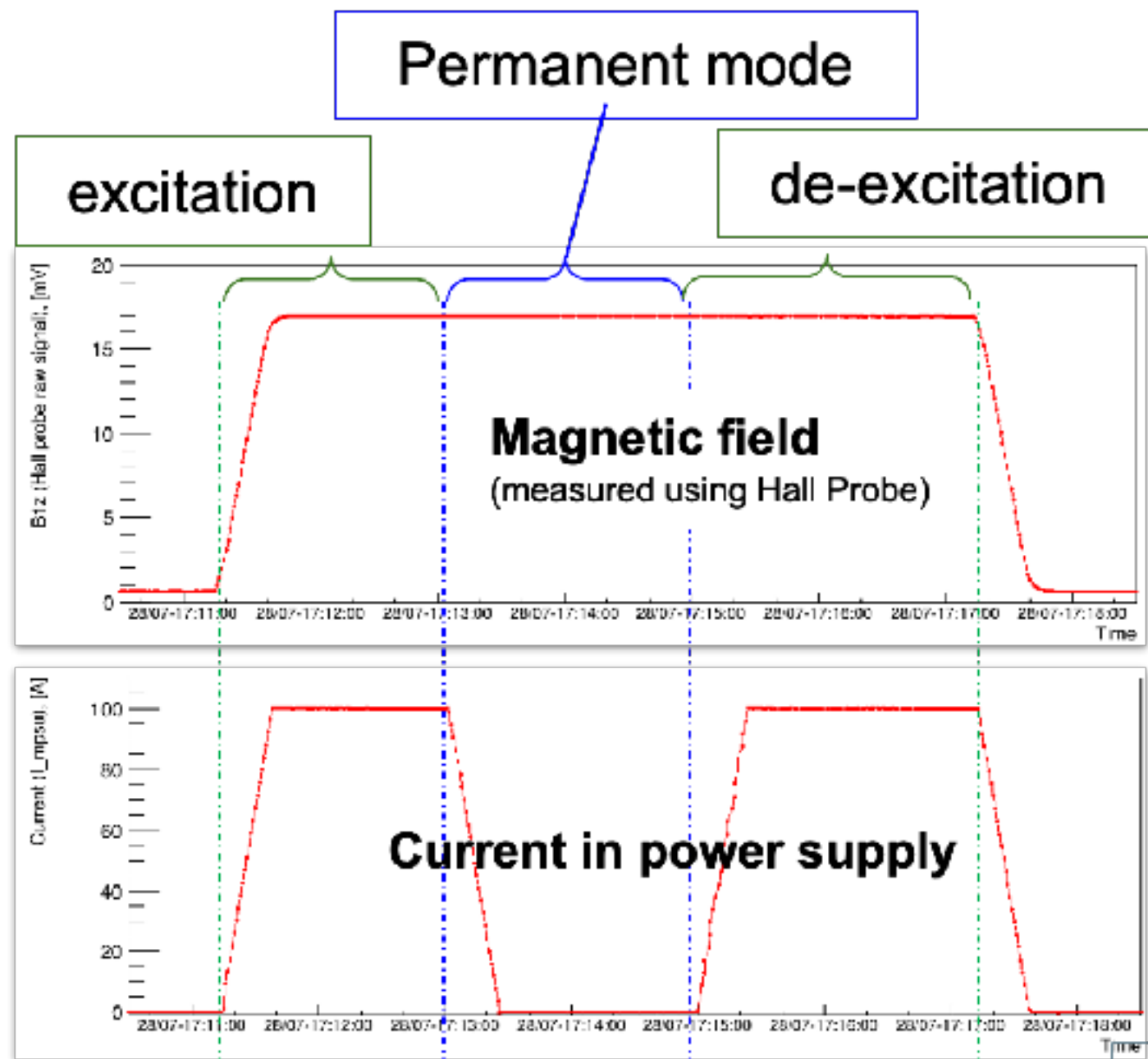
- ✓ Cooling tests down to **4.5 K**
- ✓ Excitation tests
- ✓ Development of the control and monitoring system



Superconducting Solenoid Magnet

Test Phase at FOPI area (2019-2021)

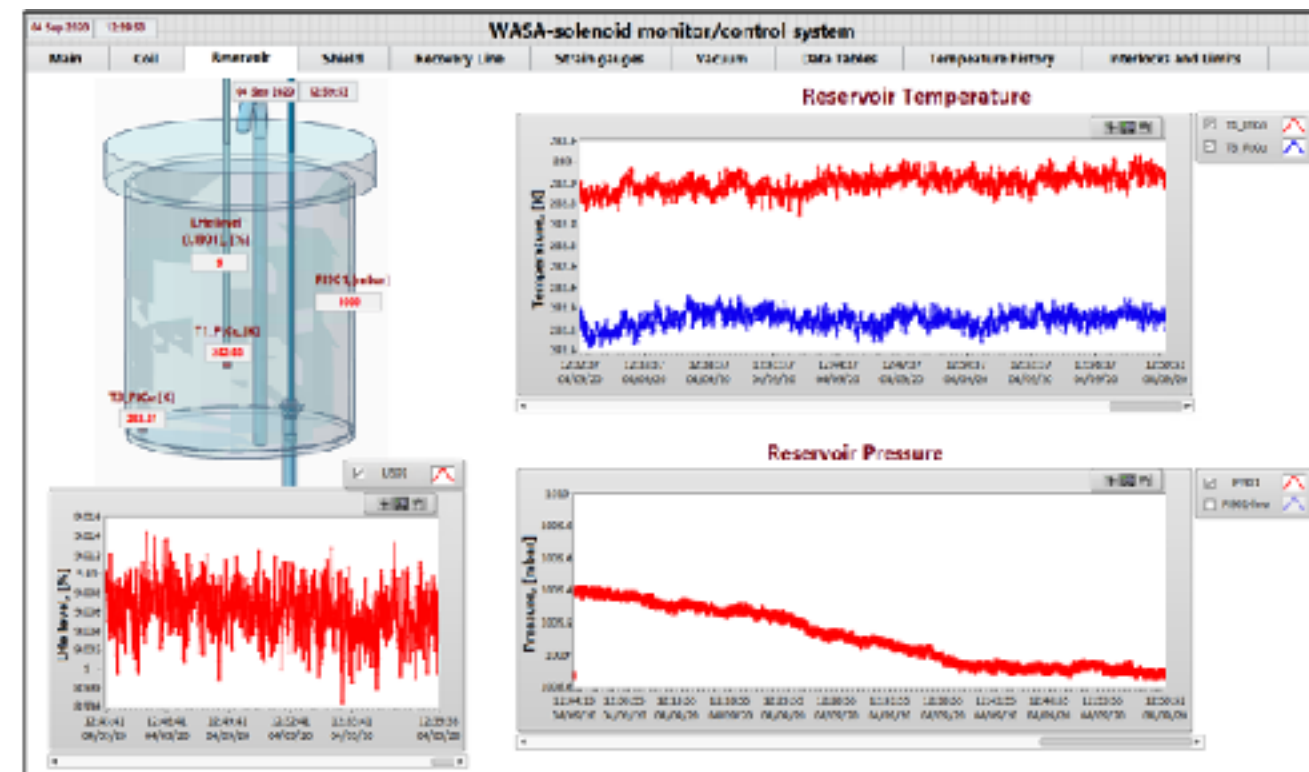
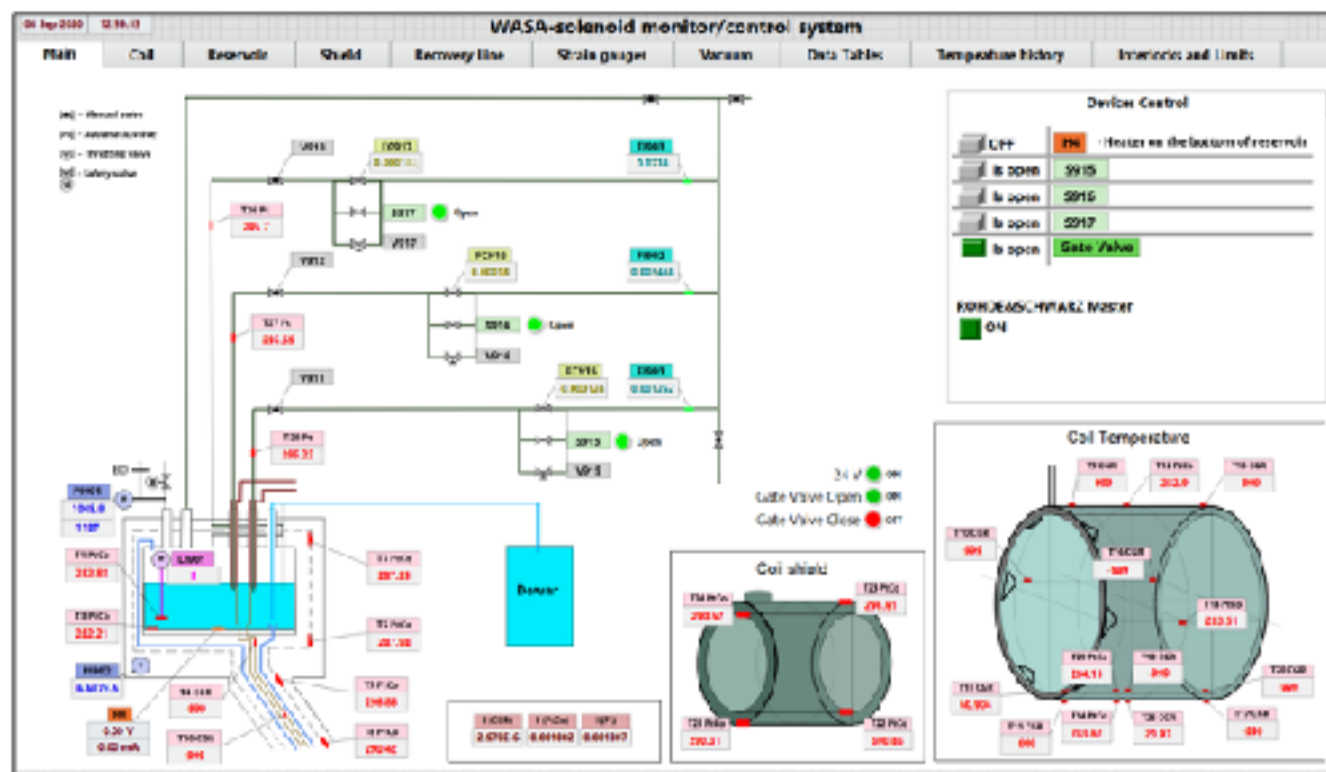
- ✓ Cooling tests down to **4.5 K**
- ✓ Excitation tests
- ✓ Development of the control and monitoring system



Superconducting Solenoid Magnet

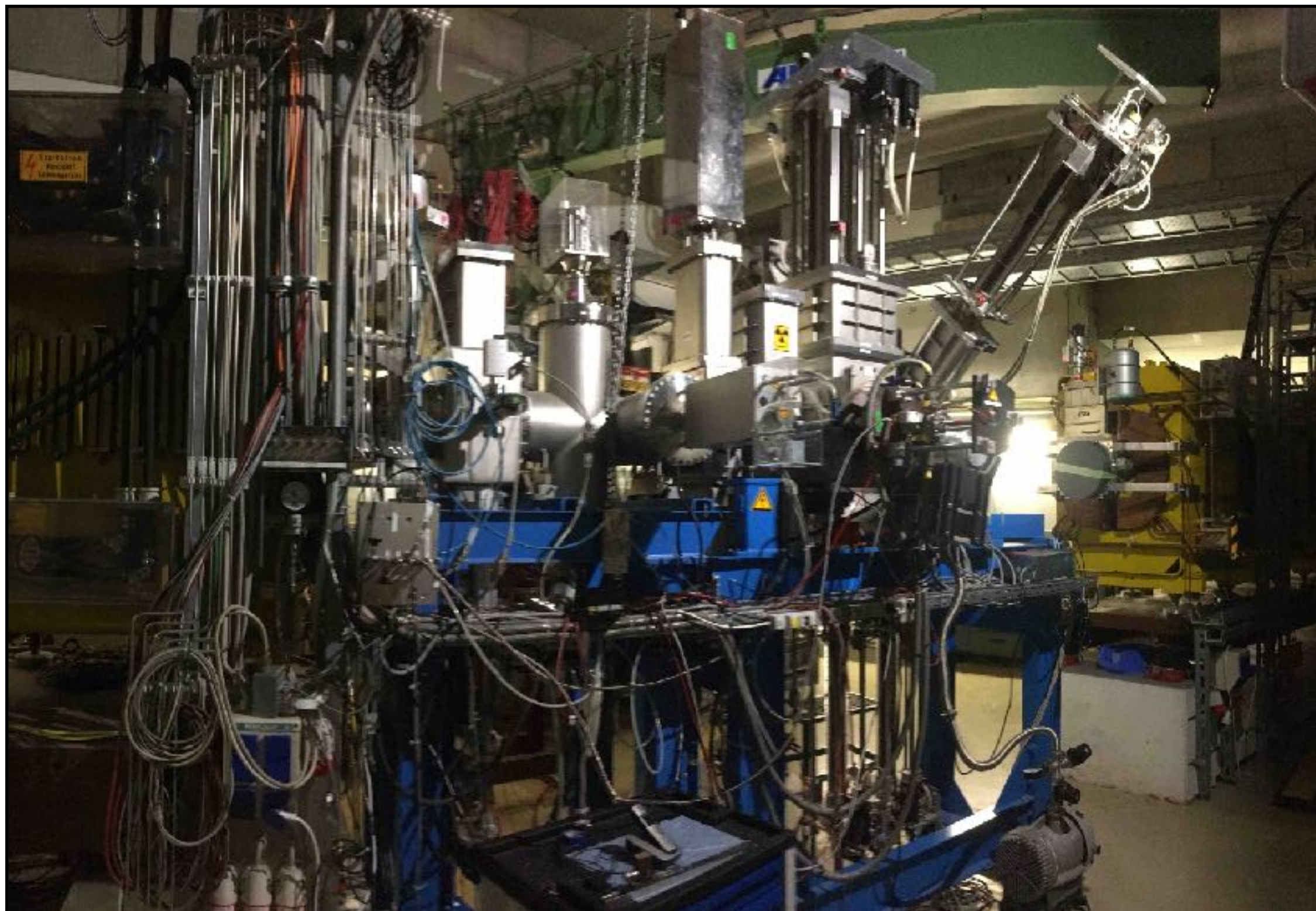
Test Phase at FOPI area (2019-2021)

- ✓ Cooling tests down to **4.5 K**
- ✓ Excitation tests
- ✓ Development of the control and monitoring system



WASA Installation at GSI-FRS F2

2021 June standard FRS-F2



essential devices for separation and identification of fragments for NUSTAR experiments

WASA Installation at GSI-FRS F2

2021 July: Roof was opened; FRS standard chamber was removed



WASA Installation at GSI-FRS F2

2021 August: Installation of Csl Rail structure



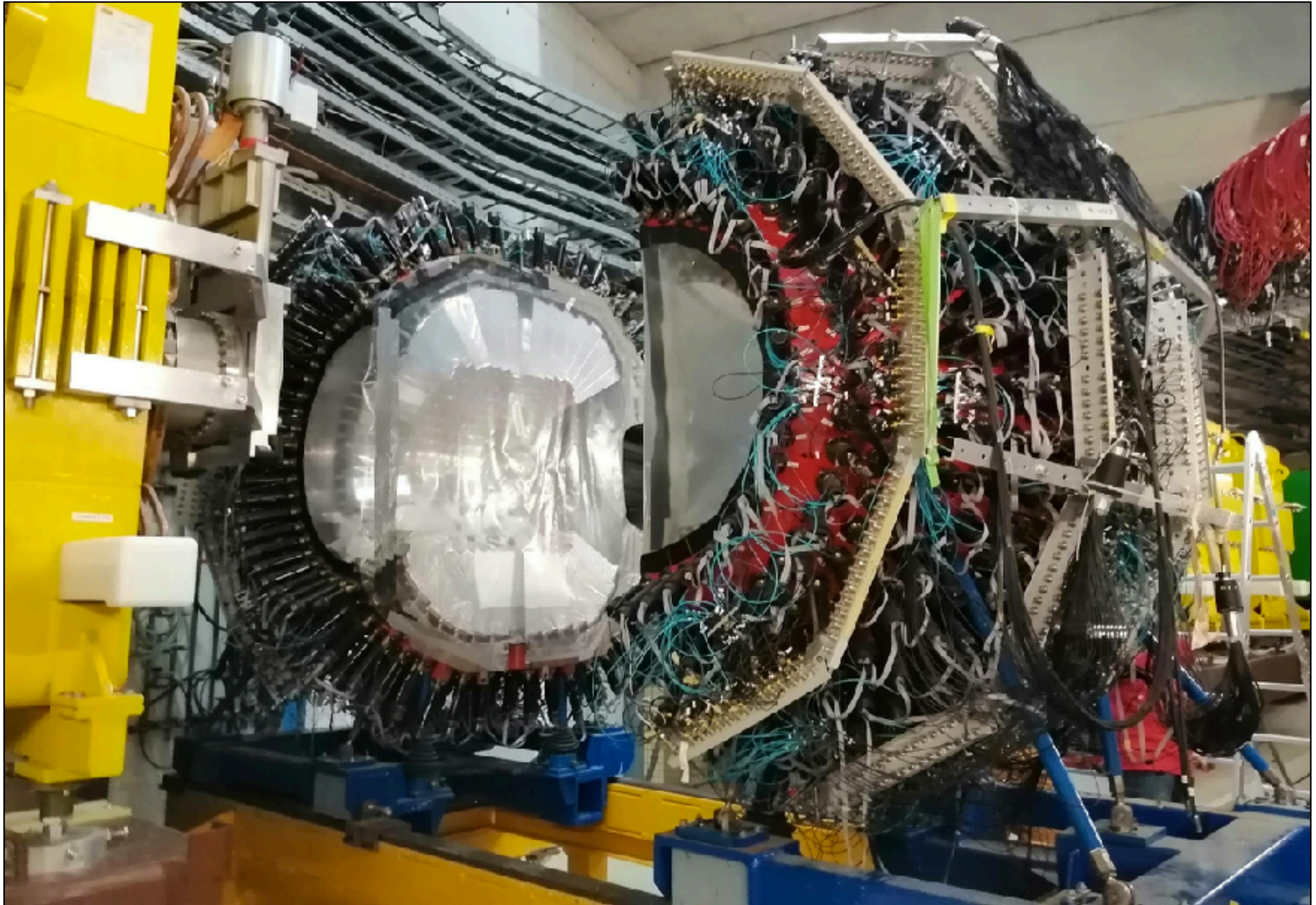
WASA Installation at GSI-FRS F2

2021 August: Installation of CsI Rail structure



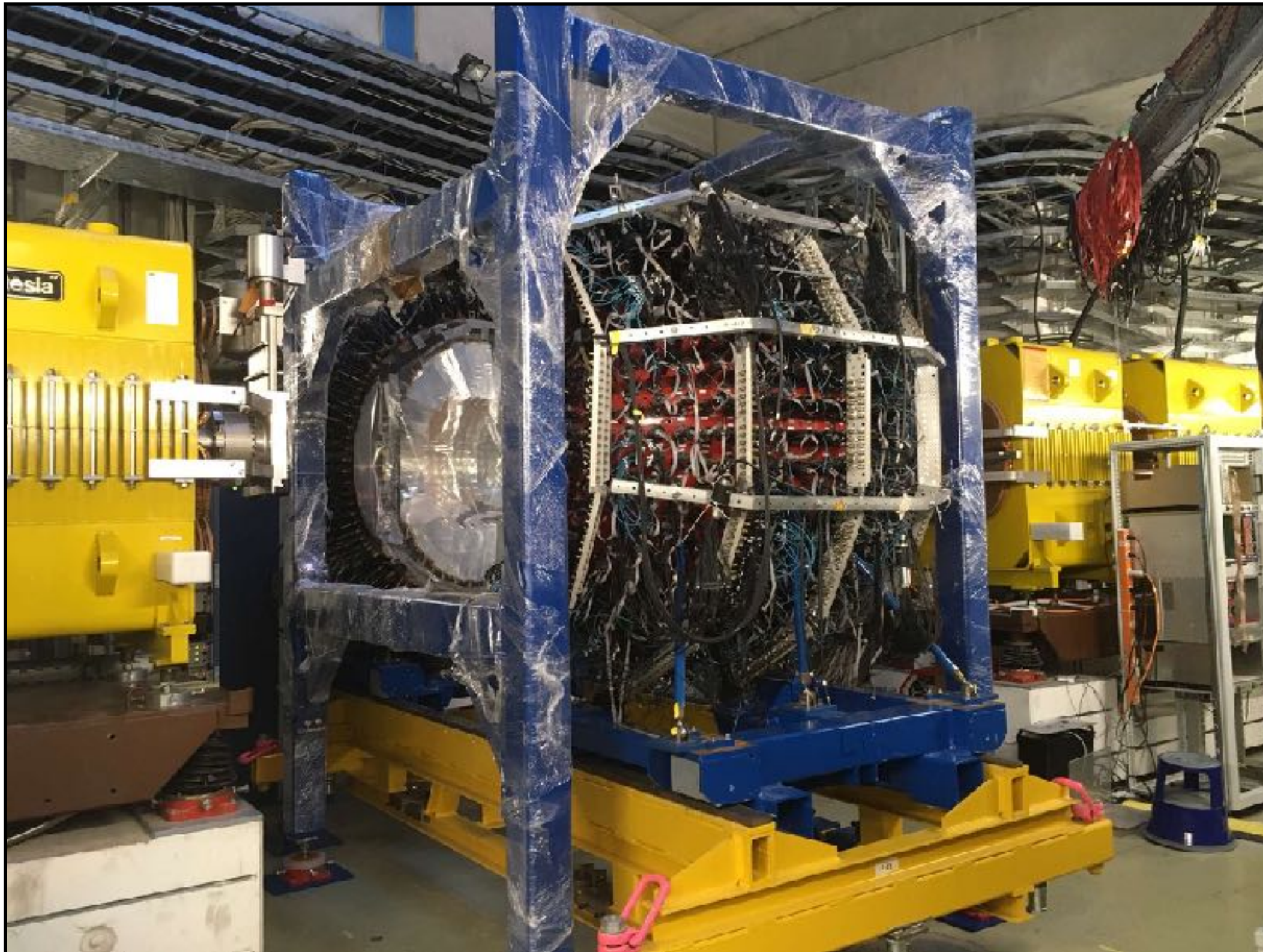
WASA Installation at GSI-FRS F2

2021 August: Installation of CsI Rail structure



WASA Installation at GSI-FRS F2

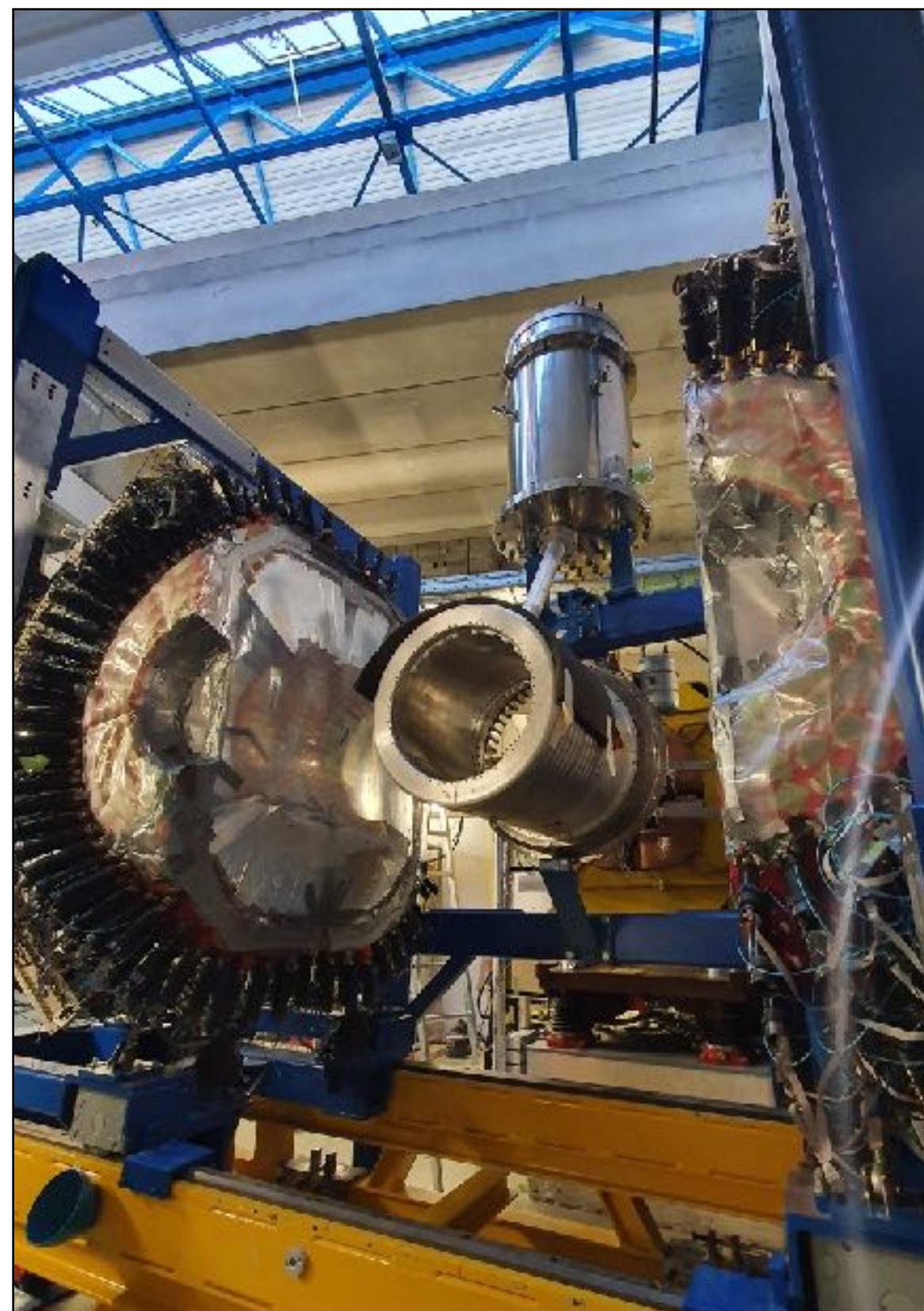
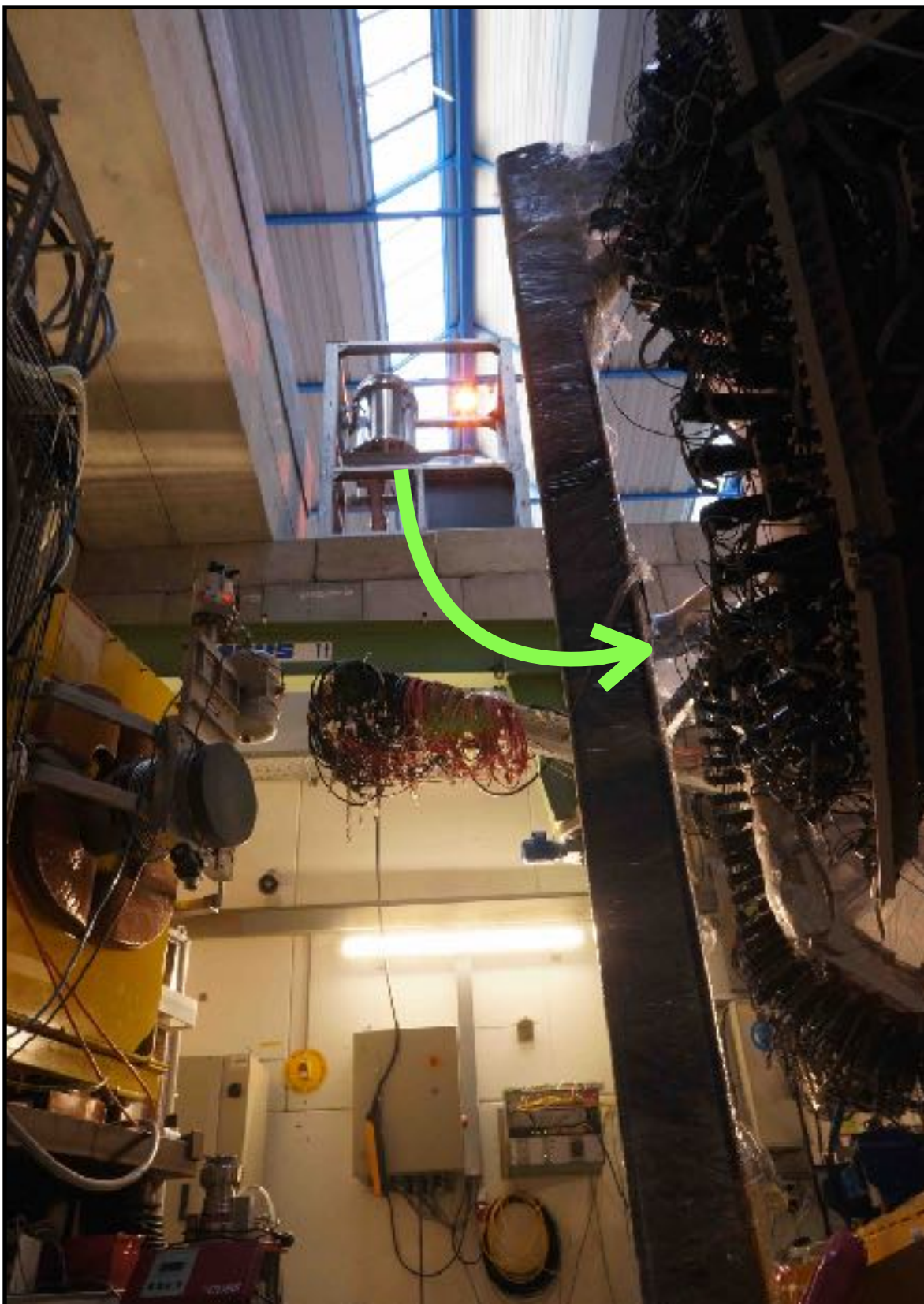
2021 September: Installation of Support frame for Magnet



WASA Installation at GSI-FRS F2

October 5, 2021

Installation of Support frame for Magnet



WASA Installation at GSI-FRS F2

October-November, 2021

Installation LHe transfer line from 3000L LHe storage dewar



WASA Installation at GSI-FRS F2

November, 2021

Installation of inner detectors

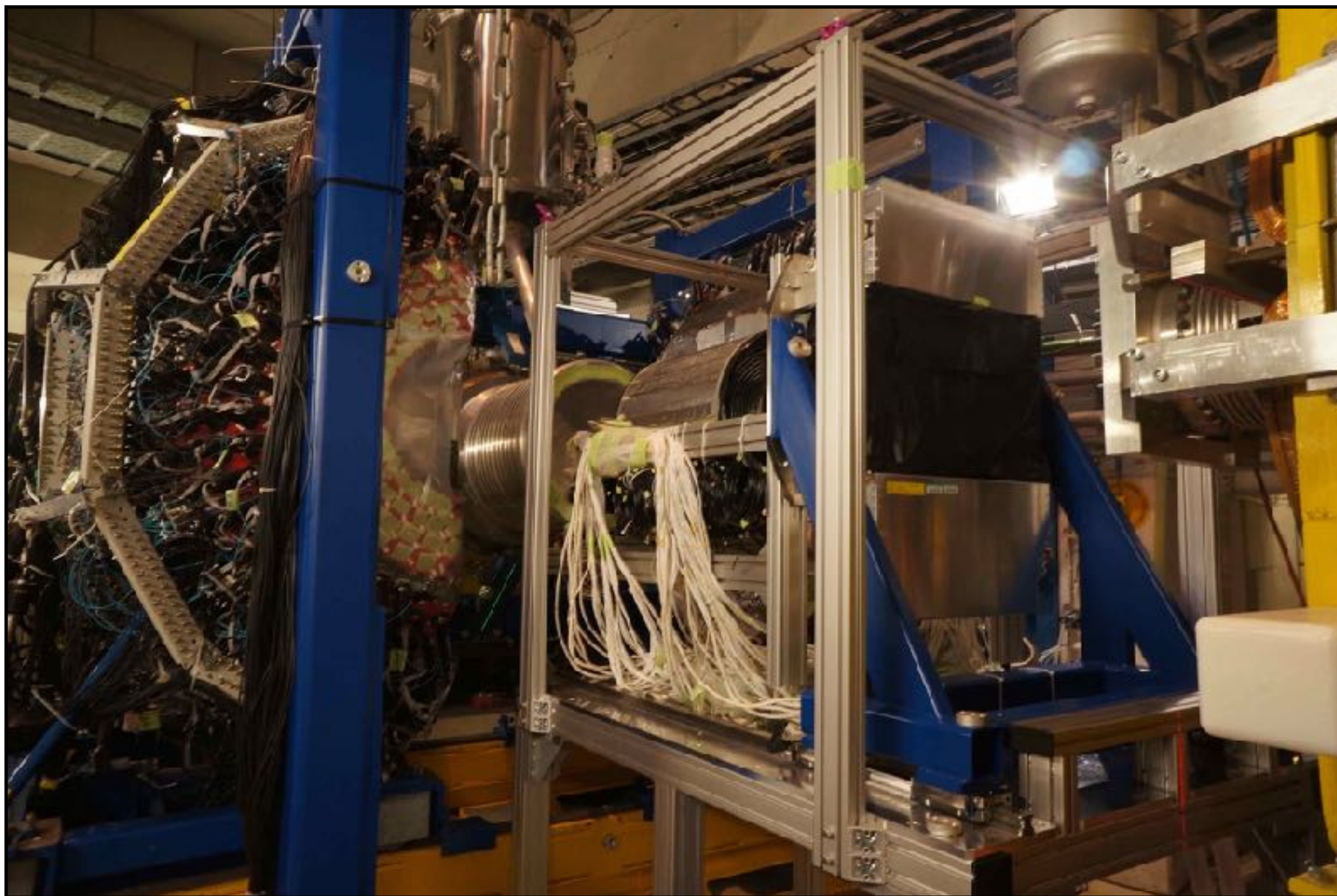


MDC+PSB+miniFiber were integrated to the MDC structure and these were installed as one unit

WASA Installation at GSI-FRS F2

November, 2021

Installation of inner detectors

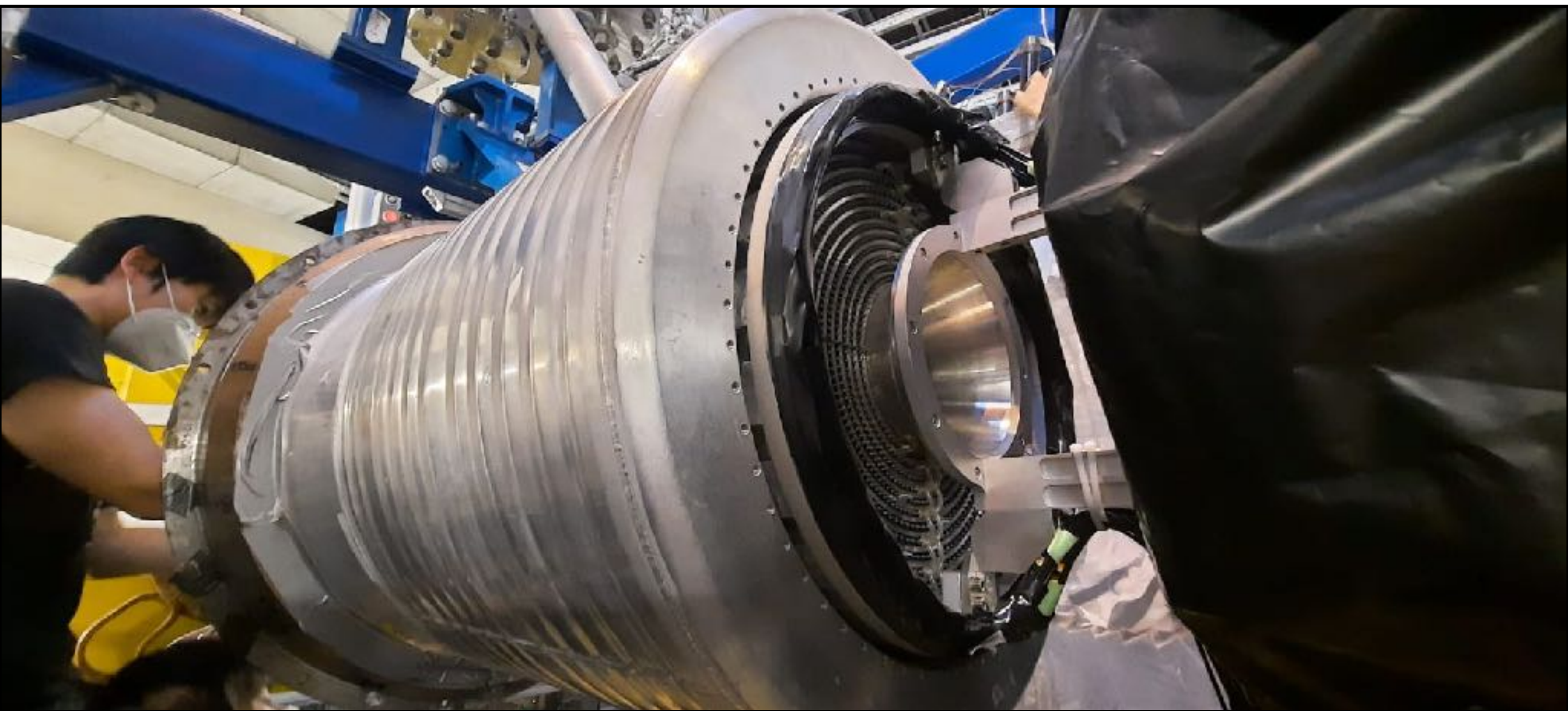


MDC+PSB+miniFiber were integrated to the MDC structure and these were installed as one unit

WASA Installation at GSI-FRS F2

November, 2021

Installation of inner detectors

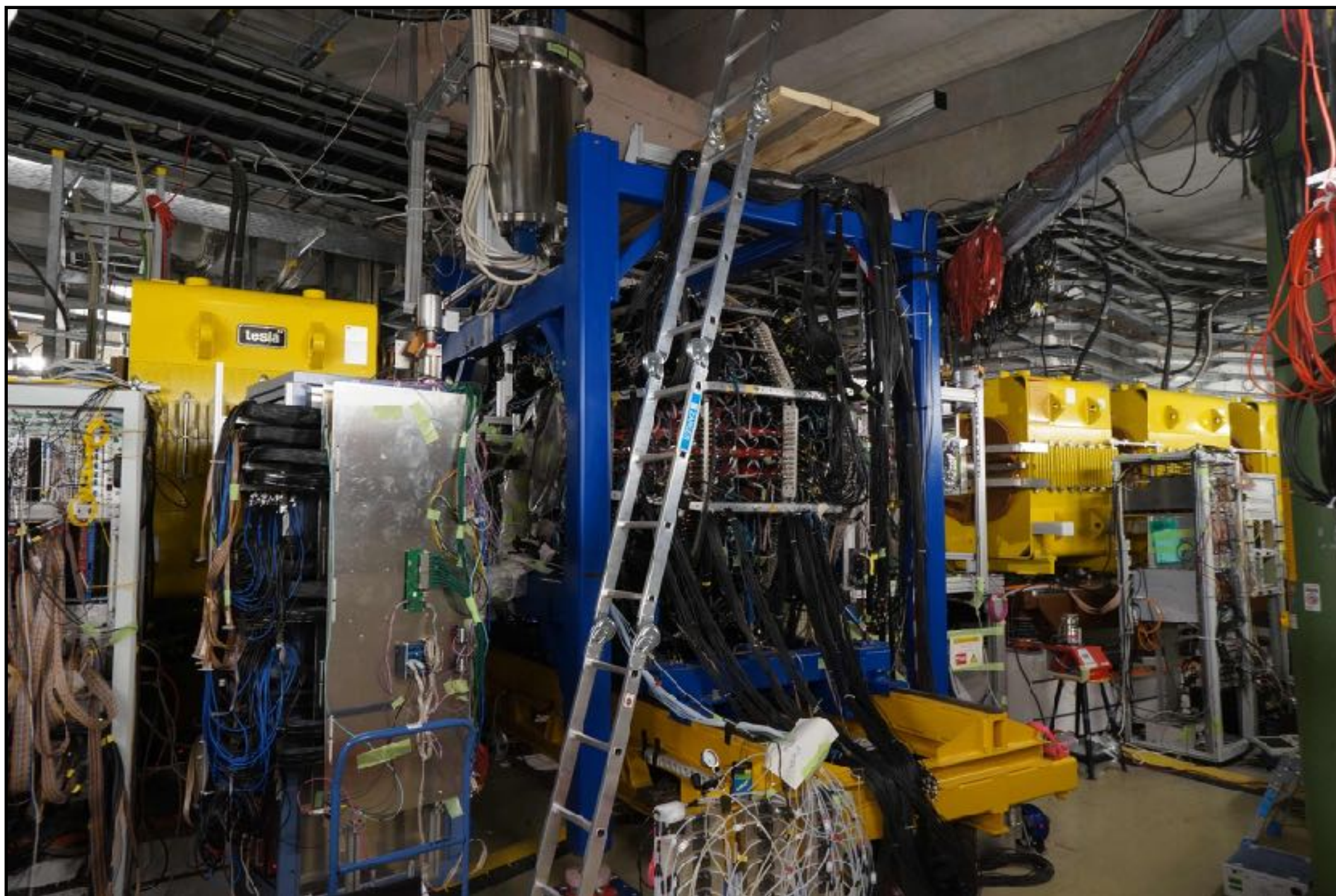


MDC+PSB+miniFiber were integrated to the MDC structure and these were installed as one unit

WASA Installation at GSI-FRS F2

December, 2021 (last week)

WASA detector was closed for final tests



Beam Time is scheduled in 2022

FEB	Tue	Wed	Thu	Fri	Sat	Sun	Mon	Tue	Wed	Thu	Fri	Sat	Sun	Mon	Tue	Wed	Thu	Fri	Sat	Sun	Mon	Tue	Wed	Thu	Fri	Sat	Sun	Mon
2022 v026	1	2	3	4	5	6	7	8	9	10	11	12	13	14	15	16	17	18	19	20	21	22	23	24	25	26	27	28
SIS	S518 Stroth 1-H; HAD																											
SIS	WASA; 1-H; HFS		S483 Nociforo; 1-H; HFS					S488 Winkler; 1-H; HHT																				
SIS	Test Beam																											
ESR																												
CRY								LOC-CRY																				

MAR	Tue	Wed	Thu	Fri	Sat	Sun	Mon	Tue	Wed	Thu	Fri	Sat	Sun	Mon	Tue	Wed	Thu	Fri	Sat	Sun	Mon	Tue	Wed	Thu							
2022 v026	1	2	3	4	5	6	7	8	9	10	11	12	13	14	15	16	17	18	19	20	21	22	23	24	25	26	27	28	29	30	31
SIS	S518 Stroth 1-H; HAD	S490 Itahashi; 1-H; HFS					S447 Saito; 6-Li; HFS							OP Training						U514 Sturm; 238-U; HTD	S506 Palit; HFS; 238-U										
SIS			S488 Winkler; 1-H; HHT					S483 Nociforo; 12-C; HTP			RSB Simon; 12-C; HTP		SMAT Bender; 12-C; HTP							E137 Bräuning-Demian; 238-U;											
SIS	Main Beam Time (S490 + S447)																														
ESR																															
CRY								E149 Brandau; 20-Ne; LOC-CRY																							

**4 weeks
to remove inner
detectors**

Summary

- Spectroscopy of bound states in nucleus offers possibility to directly study in-medium properties of hadrons.
- We performed first experimental search for η' mesic nuclei by missing-mass spectroscopy of the $^{12}\text{C}(p,d)$ reaction in 2014.
 - Excitation-energy spectrum of the $^{12}\text{C}(p,d)$ reaction has been obtained around the η' emission threshold, with a high statistical sensitivity and sufficiently small resolution.
 - As no distinct peak structure is observed, upper limits of formation cross section have been determined.
 - From comparison with theoretically-calculated formation spectra, large potential depth $|V_0| \sim 150$ MeV is excluded around $|W_0| < 25$ MeV.
- We plan a new experiment to search for η' mesic nuclei by combination of missing-mass spectroscopy and tagging decay particle.
The experiment will be performed with WASA+FRS setup in 2022 soon !